

University of Southern Queensland
Faculty of Engineering & Surveying

Development and Characterisation of an Anechoic Chamber

A dissertation submitted by

Andrew Woods

in fulfilment of the requirements of

ENG4112 Research Project

towards the degree of

Bachelor of Engineering (Electrical and Electronic)

and

Bachelor of Business (Logistics and Operations Management)

Submitted: June, 2006

Abstract

This project explores the testing procedures in which the anechoic chamber, located on level 2 of the Faculty of Engineering and Surveying building at the University of Southern Queensland, can be characterised in the way of its performance regarding electromagnetic compatibilities. This characterisation will help further users of the anechoic chamber better understand the results in which are obtained within the chamber as well as know the interference that could be caused by the leakage of signals coming from the chamber.

The performance characteristics that will be looked at are first of all the ability for the anechoic chamber to keep environmental noise from entering the chamber walls, creating false measurements, preventing harmful signals escaping and interfering with other commercial bandwidths.

Then the pyramidal absorbers themselves will be analysed and their capability of attenuating a wide range of frequencies over a set number of angles of incidences will be recorded. This is the first step in a bigger task of being able to explain the patterns of variation in the electromagnetic field in a two dimensional plane. The way in which the performance of the pyramidal absorbers varies with angle helps explain this, as it gives the magnitude of absorption when a wave is reflected off the wall and interferes with the direct path, This process of following the different paths around the enclosed area is called ray tracing which is touched on in this project, but due to time constraints only the theory of the technique is recalled.

From the results that were obtained, the anechoic chamber can now be utilised as to get a more accurate measurement by being able to configure the testing specifications to suit the chambers performance strengths and weaknesses. Even though some characterisation has been logged, there is still the potential for further work to be done to optimise the anechoic chambers useability and hopefully someday match the standards set for a commercial anechoic chamber.

Certification

I certify that the ideas, designs and experimental work, results, analyses and conclusions set out in this dissertation are entirely my own effort, except where otherwise indicated and acknowledged.

I further certify that the work is original and has not been previously submitted for assessment in any other course or institution, except where specifically stated.

Andrew Woods

00111220823

Signature

Date

University of Southern Queensland
Faculty of Engineering and Surveying

ENG4111/2 Research Project

Limitations of Use

The Council of the University of Southern Queensland, its Faculty of Engineering and Surveying, and the staff of the University of Southern Queensland, do not accept any responsibility for the truth, accuracy or completeness of material contained within or associated with this dissertation.

Persons using all or any part of this material do so at their own risk, and not at the risk of the Council of the University of Southern Queensland, its Faculty of Engineering and Surveying or the staff of the University of Southern Queensland.

This dissertation reports an educational exercise and has no purpose or validity beyond this exercise. The sole purpose of the course pair entitled “Research Project” is to contribute to the overall education within the student’s chosen degree program. This document, the associated hardware, software, drawings, and other material set out in the associated appendices should not be used for any other purpose: if they are so used, it is entirely at the risk of the user.

Prof G Baker

Dean

Faculty of Engineering and Surveying

Acknowledgments

I would first of all like to thank my supervisor David Parson for giving me guidance in achieving my key goals in this project. He also assisted in developing the apparatus need for the numerous tests that were performed. Glen Bartkouski also needs to be commended for constructing the apparatus that was used. USQ deserves a thankyou for providing the adequate equipment needed for the project to be completed.

Thankyou to my fellow student Dean Eckersley for assisting me during the long days of testing and transportation of equipment. Most of all, to my parents Wayne and Julie Woods goes the greatest thankyou for their endless support and encouragement to keep me going though out the years.

ANDREW WOODS

University of Southern Queensland
June 2006

Contents

Abstract	i
Acknowledgments	iv
List of Figures	vii
List of Tables	ix
Chapter 1 Introduction	1
1.1 Objectives	2
1.2 Anechoic Chamber	3
1.3 Radio Wave Absorbers	6
1.3.1 Broadband Pyramidal Absorbers	7
1.3.2 Ferrite Tiles	10
1.4 Antennas	12
1.4.1 Logarithmic Antenna	12
1.4.2 Bi-Conical Antenna	14
1.5 Hardware	14
1.5.1 Spectrum Analyser	14
1.5.2 Signal Generator	15
1.5.3 Emissions Reference Source	15
1.6 Overview of Dissertation	15
Chapter 2 Anechoic Chamber Attenuation	17
2.1 Methodology	17
2.2 Results	20

Chapter 3 Pyramidal Wall Absorber	30
3.1 Methodology	31
3.2 Testing Process	36
3.3 Results	38
Chapter 4 2-D Planar Variation	46
4.1 Methodology	48
4.2 Results	50
Chapter 5 Ray Tracing Techniques	55
Chapter 6 Conclusion	57
References	59
Appendix A Project Specification	62
Appendix B Spectrum Analyser Outputs	63
B.1 Anechoic Chamber Attenuation	63
B.2 Pyramidal Absorber Performance	68
B.3 2-D Field Performance	71

List of Figures

- 1.1 Cross-sectional Side View of Anechoic Chamber
- 1.2 Plan View of Anechoic Chamber
- 1.3 Inside of Anechoic Chamber with Receiving Antenna
- 1.4 Behaviour of Planar Electromagnetic Absorber
- 1.5 Variations in Reflectivity of Absorbers with Carbon Loading Variations
- 1.6 AEP -12 Broadband Pyramidal Absorber
- 1.7 Use of Dielectric for Increased Bandwidth
- 1.8 Loss of Varying Dielectric Spacer
- 1.9 Typical Radiation Patterns for Ultra-Log Hybrid Antenna
- 1.10 Bi-Conical Antenna

- 2.1 Automated Spectrum Analyser
- 2.2 Vertical Polarisation of Ultra-Log Antenna
- 2.3 True Emissions Reference Source
- 2.4 Output of Spectrum Analyser – Door Open
- 2.5 Output of Spectrum Analyser – Door Closed (500 mm)
- 2.6 Output of Spectrum Analyser – Door Closed (120 mm)
- 2.7 Attenuation of Anechoic Chamber
- 2.8 Output of Spectrum Analyser – Door Opened (Amplified)
- 2.9 Output of Spectrum Analyser – Door Closed (Amplified)
- 2.10 Attenuation of Amplified Emissions Reference Source
- 2.11 Attenuation of Anechoic Chamber from Combined Results

- 3.1 Layout of Open-Area Test Site
- 3.2 Transmitting Antenna Arrangement
- 3.3 Receiving Antenna Arrangement – Ultra-log
- 3.4 Receiving Antenna Arrangement – Trolley
- 3.5 True Emissions Reference Source

- 3.6 Spectrum Analyser Output – Angle Incidence of 15°
- 3.7 Spectrum Analyser Output – Angle Incidence of 45°
- 3.8 Spectrum Analyser Output – Angle Incidence of 75°
- 3.9 Spectrum Analyser Output – Emissions Reference Source
- 3.10 General Pyramidal Absorber Performance
- 3.11 AEP-12 Radio Wave Absorbing Performance
- 3.12 Spectrum Analyser Output – Reflective Barrier

- 4.1 5x5 Matrix Receiving Antenna Stand
- 4.2 Receiving Dipole Antenna
- 4.3 2D Planar Output – Node (2,0)
- 4.4 2D Planar Output – Node (2,1)
- 4.5 2D Planar Output – Node (3,3)

- 5.1 Graphical Representation of Ray Tracing inside Anechoic Chamber

List of Tables

- 1.1 General Pyramidal Absorber Performance
- 1.2 AEP-12 Radio Wave Absorbing Performance

- 2.1 Resonant Frequencies of Anechoic Chamber

- 3.1 Absorption of Reflected Signal (-dB)

- 4.1 Frequency Wavelengths vs. Dipole Length

Chapter 1

Introduction

When testing a component with regard to electro-magnetic compatibility (EMC), an open-test site is what is nominally sought after as there is little ambient noise about to interfere with the measurements being taken, except from the surrounding test equipment such as computers, frequency generators, spectrum analysers and mobile phones. However, an ideal open-test site is not always available, so this is what gave engineers a task of creating a shielded room which would give the same minimal ambient interference as would an open-test site. These special shielded rooms came to be called anechoic chambers and are now commonly used for EMC testing for various standards testing and research and design.

The overall purpose of this project is to evaluate the anechoic chamber that has been built in the Faculty of Engineering building, by the University of Southern Queensland, to a standard where future users of the chamber can rely on the results gathered for their EMC testing. The evaluation of such a chamber will be achieved through numerous radio frequency through to microwave frequency testing.

Such tests will include the attenuation of the anechoic chamber as a whole, the absorption of the radio wave absorbers at a range of angles and using ray-tracing techniques to evaluate the chamber.

With no restrictions on the viewing of the final dissertation, other organizations that are interested in building their own anechoic chamber can analyse the results that are documented. Through this analysis, they can decide on whether the much cheaper alternative of this anechoic chamber constructed by the University is a feasible option to commercially available ones.

1.1 Objectives

This research project's aim as mentioned before is to record the performance of the anechoic chamber located in level two of the Faculty of Engineering and Surveying building. For this main task to be completed, specific aspects of the anechoic chamber's performance needed to be identified as most important as to gather only relevant information.

For the majority of the tests that the anechoic chamber will be used for, the most important characteristics of the chamber that will be sought will be concerning the quality of the radio frequency absorbing materials which line the inner walls, roof and floor.

The specific objectives that have been finalised to see the completion of this research project are as follows and a copy of the official agreement can be viewed in Appendix A.

- Research the background information of anechoic chambers and radio frequency absorbing linings, including their use and theoretical performance
- Characterise the testing equipment for initial environment activity. This will include calibrating the antennas and corresponding equipment using the emissions references source.
- Measure the attenuation of known signals over a range of frequencies as they travel through the anechoic chamber walls.
- Measure the absorption of radio signals by both the floor tiles and wall pyramidal absorbers through a range of frequencies and angles of incidence.

- Measure the variation, if any, in signal strength when the receiving antenna is moved within the anechoic chamber, relative to the transmitting antenna. Attempt to relate and detected pattern to theory using ray-tracing techniques

1.2 Anechoic Chamber

An anechoic or anti-echo chamber can be defined as a test chamber designed to reduce unwanted reflected energy, so that free-space electromagnetic measurements can be simulated to an acceptable degree and be repeated giving results with little deviation.

An anechoic chamber is a special room used for a variety of indoor antenna measurements, electromagnetic interference (EMI) measurements, and electromagnetic compatibility (EMC) measurements, where there is minimal interference from external sources. As well as preventing most destructive signals from the surrounding environment interfering with these EMC tests, the walls of the anechoic chamber minimise any radio signals produced inside the chamber from being noisy to other radio signals. This absorption of radio waves is achieved through the application of pyramidal absorbers to the walls and roof of the chamber and ferrite tiles are laid on the floor (Hemming 2002).

One of the major requirements is the presence of an emitting source. This can be in the form of an antenna, device under test (DUT) or characterised transmitters such as an emissions reference source (ERS). These transmitters generate microwave signals within the chamber walls and a receiving antenna samples the field strength which can then be used for evaluating desired results.

From the testing of EMI and EMC in electrical components such as computer hardware, TVs, etc. within an anechoic chamber, the compliance with standards can be analysed with minimal interference from external source such as radio and television stations, radios and mobile phones that are continually transmitting at sometimes higher signal strengths than the emission source.

The attenuation of external, unwanted signals that enter the chamber is achieved by having the outside of the chamber being metal so that signals are reflected. If signals do however enter the chamber through small gaps in the walls or door gaskets, the lining of radio wave absorbing materials to the inner walls, roof and floors is used to attenuate these signals to an acceptable level.

A typical anechoic chamber and the one that is going to be used throughout the duration of this paper is shown in cross-sectional side view in Figure 1. A device under test (transmitting source) and accompanying receiving antenna is shown as well as the radio wave absorbers lining the inner walls.

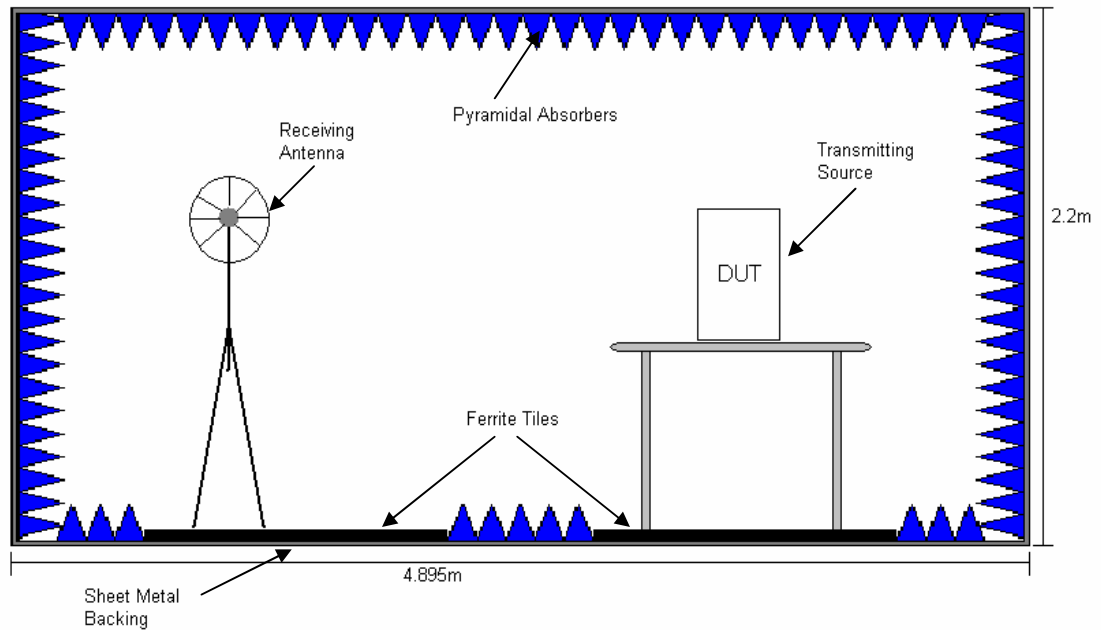


Figure 1.1 Cross-sectional Side View of Anechoic Chamber

As can be seen, the ferrite tiles are only laid on the floor of the chamber so that antennas and other equipment can be placed without damaging the pyramidal absorbers. Therefore there is some restriction of where the equipment can be placed. A plan view is also shown below which shows the doors that gives access to both sides of the chamber and the input/output connectors that allow the co-axial cables to pass through the walls without allowing unwanted signals in or out.

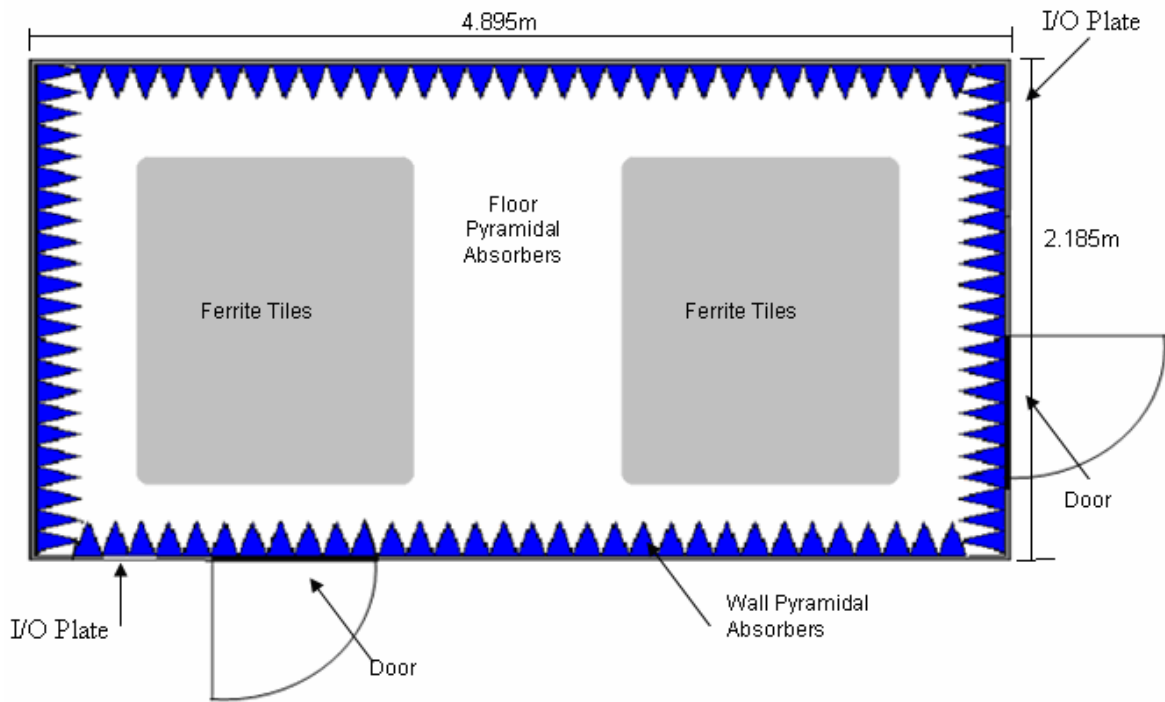


Figure 1.2 Plan View of Anechoic Chamber

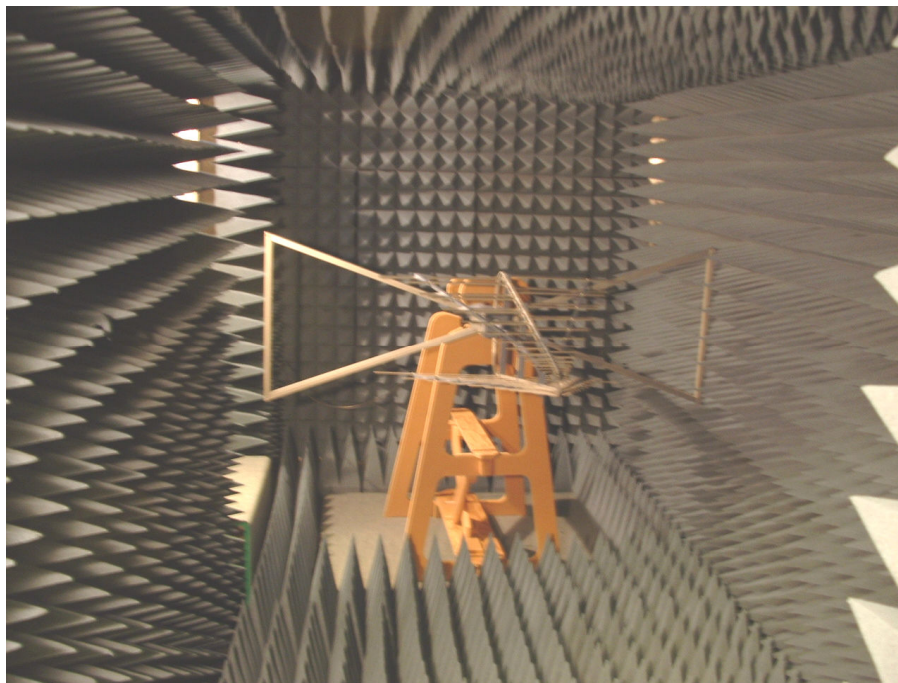


Figure 1.3 Inside of Anechoic Chamber with Receiving Antenna

1.3 Radio Wave Absorbers

There are a range of radio wave absorbers that are available to assist in the absorption of radio waves that try to enter or exit an anechoic chamber. The two types of absorbers that are used in this particular anechoic chamber are the broadband pyramidal foam absorbers and floor ferrite tiles.

The basic concept of how any planar electromagnetic absorber involves the variable quantities shown in the figure below. When a radio wave is travelling through free space and encounters a different medium (at $z=0$), the wave will have one of three different reactions. It will be reflected, transmitted, and/or absorbed.

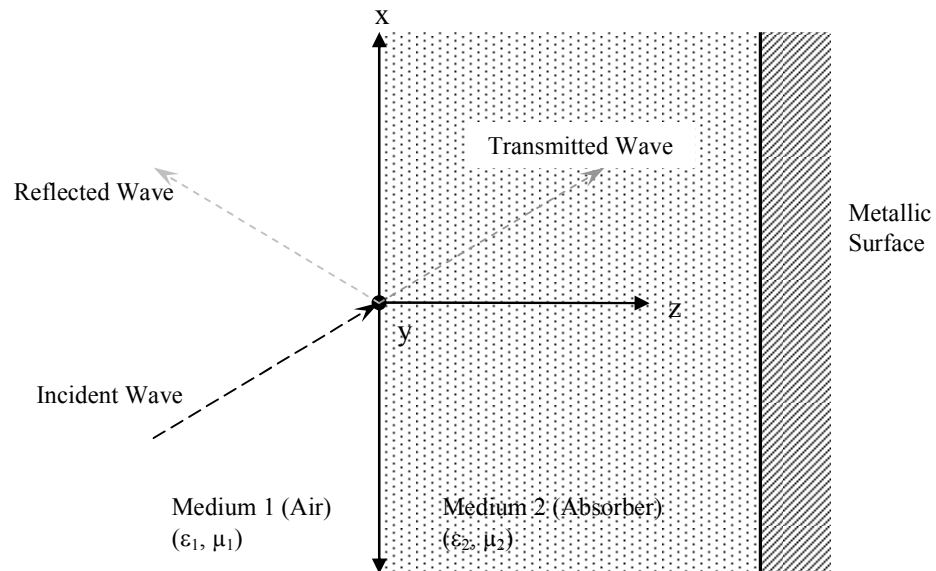


Figure 1.4 Behaviour of Planar Electromagnetic Absorber

Where:

μ_1 = relative permeability of medium 1 (air)

ϵ_1 = relative permittivity of medium 1 (air)

μ_2 = relative permeability of medium 2 (absorber)

ϵ_2 = relative permittivity of medium 2 (absorber)

From this diagram the main quantity that is of interest is the reflected wave from the absorber. Any reflections from the absorbing material constitute constructive or

destructive interference at the receiving antenna. Therefore a smaller reflection is wanted to minimise error in measurements taken. The reflection coefficient of a metal backed absorber (Γ), absorber's impedance (Z) and Return Loss (RL) can be calculated by the following equations:

$$Z_f = \sqrt{\frac{\mu_r}{\epsilon_r}} \cdot \tanh \left[\left(\frac{2\pi d}{\lambda} \right) \left(\sqrt{\mu_r \epsilon_r} \right) \right] \quad (\text{ohm})$$

$$\Gamma = \frac{Z_f - Z_0}{Z_f + Z_0}$$

$$\text{RL} = 20 \log_{10} (\Gamma) \quad (\text{dB})$$

Where:

$\mu_r = \mu' - j\mu''$ = complex relative permeability of medium (absorber)

$\epsilon_r = \epsilon' - j\epsilon''$ = complex relative permittivity of medium (absorber)

Z_0 = impedance of free space (air)

d = thickness of absorber

1.3.1 Broadband Pyramidal Absorber

Pyramidal Absorbers are made up of a majority of urethane foam which has been treated and loaded with carbon. As a safety standard, the carbon-loaded urethane foam is treated with fire-retardant chemicals either when the carbon is applied to the foam or as a second treatment (Hemming 2002). The primary use for pyramidal absorbers is to reduce the forward scattering of electromagnetic wave but can also be used for its back scattering capabilities also.

The degree of carbon loading in the urethane foam is an important factor when producing these absorbers. The reflectivity can be greatly varied depending on the amount of carbon introduced into the foam. These variations can be seen in the graph below and where the reflectivity is measured versus the thickness of the carbon coating in the foam in relation to the frequency being used in the test.

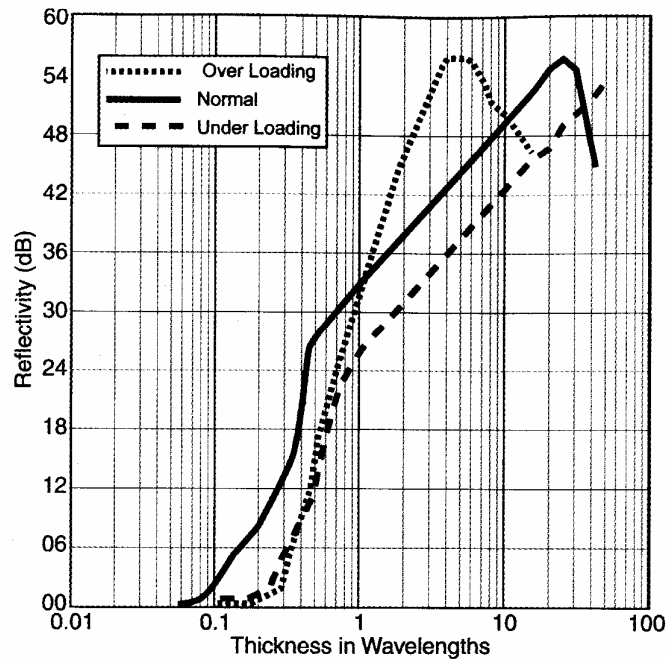


Figure 1.5 Variations in Reflectivity of Absorbers with Carbon Loading Variations [1]

As can be seen in the above graph, the optimal amount of carbon introduced onto the foam is shown by the solid black line. As the amount of carbon applied is decreased, the reflectivity curve shifts to the right implying that it takes a lot more carbon to achieve the same reflectivity characteristics.

The absorbers such as the ones used in this particular chamber are painted with a blue latex based paint which reduces the requirements for lighting within the chamber as the paint provides a good light reflectance from the external lighting. However as a rule of thumb, the tips of the pyramidal absorbers are not painted as to allow some ‘give’ due to possible traffic knocking them around. Common figures also gives the latex based blue paint a degradation of absorber reflectivity of approximately 5dB at 95GHz, although this frequency will not be encountered in the following set of testing.

The electromagnetic performance of pyramidal absorbers are generally specified as the reflectivity at normal incidence and is stated in –dB. This performance is commonly displayed in tables of absorber thickness versus frequency as shown below (Cumming Microwave 2006)

Type	Height (cm)	Weight (kg)	Tips per piece	Normal Incidence Reflectivity, GHz									
				0.12	0.3	0.5	1.0	3.0	6.0	10.0	18.0	36	50
P-4	10.9	1.4	144					30	35	42	50	50	50
P-6	15.2	1.6	100					32	40	45	50	50	50
P-8	20.3	2	64				30	37	45	50	50	50	50
P-12	30.5	2.7	36				35	40	45	50	50	50	50
P-18	45.7	5.4	16			30	37	40	45	50	50	50	>45
P-24	61	7.7	9		30	35	40	45	50	50	50	50	>45
P-36	91.4	10.9	4		35	37	42	50	50	50	50	50	>45
P-48	121.9	17	2	28	35	40	50	50	50	50	50	50	>45
P-72	182.9	23	1	33	40	45	50	50	50	50	50	50	>45

Note: Base dimensions are 2ft x 2ft

Table 1.1 General Pyramidal Absorber Performances

The pyramidal absorbers that are used in this anechoic chamber are manufactured by Advanced Electromagnetics, Inc. which is a division of Orbit/FR. The model which was chosen from the range is the AEP-12 which is a twelve inch absorber and is designed to have a useful performance over the range 500 MHz to 30 GHz.

The material is made up of a foam which has been chemically coated. The pyramids are on a square base of twenty-four inches in length. The pyramids including the square base are twelve inches tall and each base contains thirty-six pyramids. One square base is shown below including some of the dimensions just mentioned.

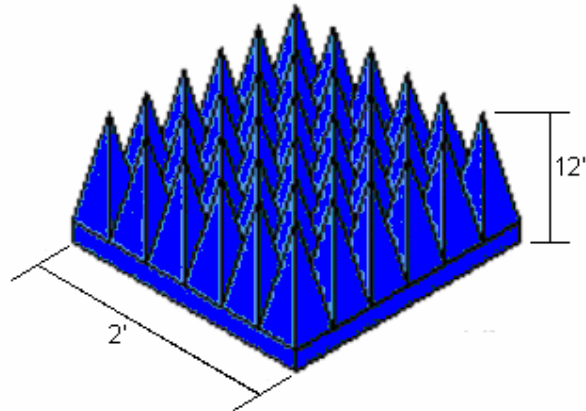


Figure 1.6. AEP -12 Broadband Pyramidal Absorber

The radio wave absorbing properties for the AEP-12 were given by Advanced Electromagnetics, Inc. in a crude form. However future comparisons can be made with this data. The absorbing material was tested under high power conditions and it was shown to be able to dissipate power densities of 0.5 watts per square inch over the frequency range shown in the table below.

FREQ (GHz)	0.25	0.5	1.0	3.0	6.0	10.0	18.0	30.0
LOSS (dB)	-22	-28	-35	-40	-45	-50	-50	-50

Table 1.2 AEP-12 Radio Wave Absorbing Performance [3]

This manufacturer's table matches the general table of performances stated earlier in this section apart from the extra figures at lower frequencies (<1.0GHz) which cannot be generalised due to the dependence of the absorber's density which varies between manufacturer's.

1.3.2 Ferrite Tiles

The ferrite tiles that were purchased for the anechoic chamber being tested were from Fair-Rite Products Corp. These tiles provide an attractive alternative to the bulkier foam walk-way tile usually used. These walk-way tiles are specially moulded twisted pyramidal absorbers that come in pairs as to inert one tile onto the top of another as to give a flat surface to walk on. These walk-way absorbers are more often used in much larger anechoic chambers as the one under test. The thickness of the ferrite tiles is only 6mm, where as equivalent foam walk-way tiles with a similar electromagnetic reflective performance are approximately 2400mm thick (Advanced ElectroMagnetics Inc. 2006).

The theory of operation of ferrite tiles is the thickness of the tiles is tuned so that the incident wave and reflected waves' relative phases cancel to form a resonant condition. This resonant condition can be noticed when the return loss is plotted against a range of frequencies (Fair-Rite Products Corp. 2005).

Not only could the thickness of the tiles be tuned to produce a certain resonant condition, the responsive bandwidth can be increased by installing the ferrite tiles on top of a dielectric spacer. This dielectric space is typically made of wood and varying the thickness of the wood can vary the maximum responsiveness of the tiles. Once his thickness is optimised, the maximum responsiveness of the tiles can be increased from 600 MHz to 1500 MHz. Any further increase in bandwidth needs a specially engineered hybrid absorber using matched pyramid and wedge shaped dielectric absorbers such as walk-way absorbers discussed earlier in this section. This increase in bandwidth with

varying thickness of a dielectric can be seen in the figure below which was provided by Fair-Rite Products Corp.

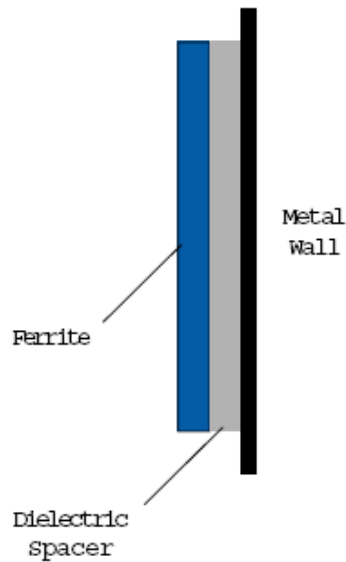


Figure 1.7 Use of Dielectric for Increased Bandwidth

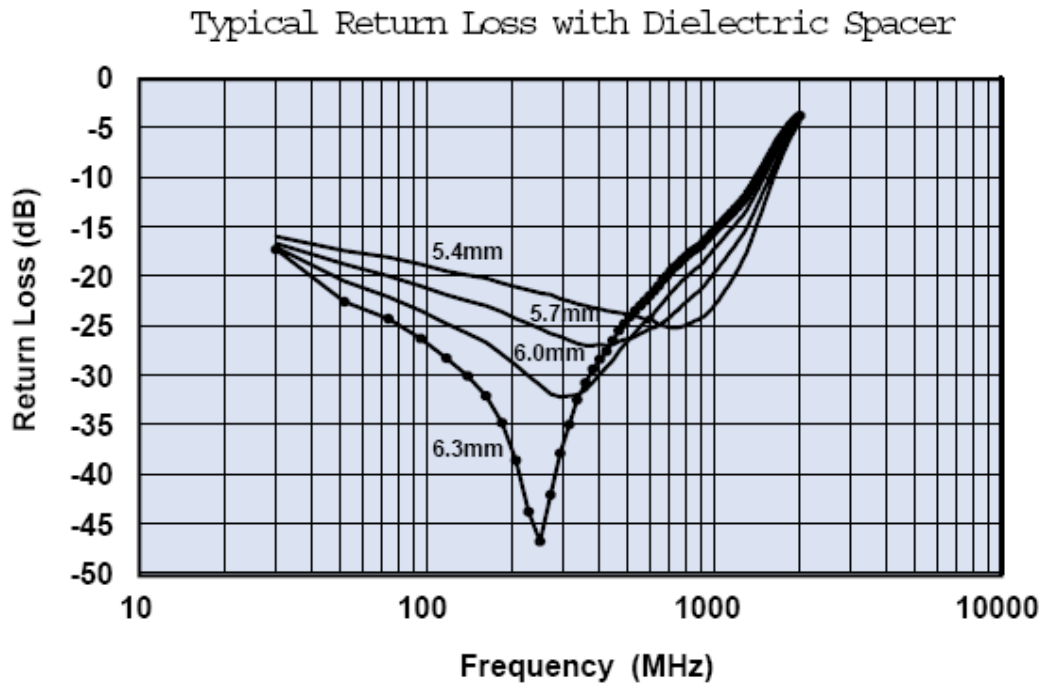


Figure 1.8 Return Loss of Varying Dielectric Spacer (Fair-Rite Products Corp. 2005)

When placing multiple tiles next to each other, care must be taken as to leave very minimal gap between each tile as the return loss can be derived to relate to these gaps. The amount of possible gaps amplifies as the need for ferrite tile absorbers for

walkways and device under test (DUT) pads increase. Therefore some manufacturers are now producing ferrite tiles in 200mm² instead of the normal 100mm² which reduces the amount of possible gaps significantly (Hemming 2002).

1.4 Antennas

Through the duration of this project there were only limited antennas available for use. The main two antennas that were used during the testing were a logarithmic or ultra-log which was used for receiving, and a bi-conical for transmitting.

These two antennas were chosen as they had already been calibrated by previous students that had used the testing equipment. The calibration that was performed was in the form of manually entering the varying antenna gain over the desired frequency range into the automatic testing spectrum analyser which will be discussed a later chapter. Even though there were other calibrated antennas available, these two proved to also have the best directivity which is important when using them inside an anechoic chamber as to minimise any potential reflection of radio waves off the radio wave absorbers (EMCO 2005).

A handmade half-dipole antenna was also used in one of the tests performed as a small sized antenna was needed and none were available for use. This antenna however was not characterised but the results were all relative making this discrepancy irrelevant.

1.4.1 Logarithmic Antenna

The Logarithmic/Ultra-log antenna which is classified as a hybrid antenna and is made up of a mix of a bi-conical and log periodic antennas to give a frequency range of generally 30MHz to 3GHz. The radiators are V-shaped to achieve gain and rotationally symmetrical patterns at frequencies above 200 MHz. This gives uniform illumination in the field of coverage. To comply with CISPR 16-1 for measuring apparatus for radio disturbance and immunity measuring apparatus, the antenna has >20-dB polarization isolation (Rohde & Schwarz 2006)(IEC 2003).

The typical radiation patterns as given by Rohde & Schwarz is shown below in Figure 1.9 which shows the directivity at the lower and upper limits of its frequency response range (30 MHz and 3000MHz respectfully) (Rohde & Schwarz 2006).

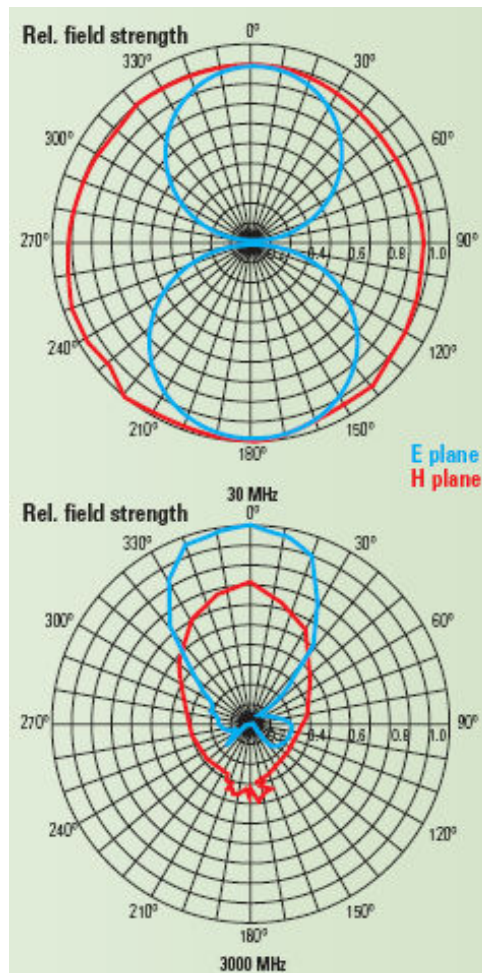


Figure 1.9 Typical Radiation Patterns for Ultra-Log Hybrid Antenna

From the above radiation patterns, E plane refers to the electrical component of the radiated signal, the signal of primary concern in EMC tests. H plane deals with the magnetic component of the antenna's radiation, which is perpendicular to the E plane (White 1999). This is important in the lower end of the EMC spectrum but seldom used above 50 MHz. Near field is an area near the antenna where the E plane characterization is quite complex and the angular distribution of radiated signal changes with the distance from the antenna. Generally, a near field exists for transmitting antennas below 300 MHz. Far field relates to points at which the E plane signal decreases in a well-defined manner as you move farther away and angular distribution of the signal is independent of the distance.

This was used primarily for the reception of the signal source as it had the greatest sensitivity. Not only was the sensitivity desirable, but this antenna proved to be able to transmit over a wide frequency range, the polarisation was easily selectable and has high gain at higher frequencies.

1.4.2 Bi-Conical Antenna

A bi-conical antenna consists of an arrangement of two conical conductors, which is driven by an alternating magnetic field and the coupled alternating electric current at the vertex. The conductors have a common axis and vertex. The two cones face in opposite directions as shown below in Figure 1.10. Bi-conical antennas are broadband dipole antennas transceiving signals from 30 MHz to 300 MHz.

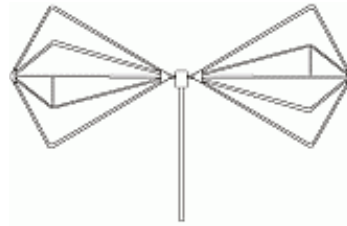


Figure 1.10 Bi-Conical Antenna

1.5 Hardware

The main equipment that was also needed to complete this project will be explained briefly.

1.5.1 Spectrum Analyser

Rohde and Schwarz, Test Receiver 9 kHz - 3 GHz [8]

The spectrum analyser was used to graphically display and determine the shielding effectiveness of the anechoic chamber by examining the graphs produced. The spectrum analyser connected to an accompanying computer using a GPIB connection so that the computer can be used to control the spectrum analyser and can store the graphs and data electronically for examination on a later date through the use of Microsoft Excel spreadsheeting.

1.5.2 Signal Generator

Rohde and Schwarz, Signal Generator 9 kHz - 1.1 GHz (Rohde & Schwarz 2006)

The signal generator was used mainly for testing of specific frequencies where the shielding effectiveness of the anechoic chamber appeared to be insufficient. By using the spectrum analyzer, the attenuation could be determine more practically by scanning the region to see how much of a decrease there was or if there was any actual decrease in attenuation.

1.5.3 Emissions Reference Source (ERS)

The emissions reference source was used, as it produces signals at even intervals of 1MHz or 5MHz over a transmitting range of 30MHz to 1.5GHz. This proved to be useful because the signal generator did not have a tracking function that would allow the spectrum analyser and the signal generator to work together. The emissions reference source was used with its built-in antenna which is vertically polarised. If greater directivity was needed, then the built-in antenna was replaced with the bi-conical antenna to provide better direction and the possibility of amplification of the signal.

1.6 Overview of Dissertation

This dissertation is organised as follows:

Chapter 2 reveals the first set of testing, which treats the anechoic chamber as a whole. The overall attenuation of the anechoic chamber will be sought after using relative testing in which the method will be detailed and results discussed.

Chapter 3 is the next test as defined in the project specifications of singling out the pyramidal radio wave absorbers and determining their performance. This will be under numerous different orientations of incident angles and frequencies.

Chapter 4 will be looking at the anechoic chamber as a whole again but this time looking at the variations in the vertical field strength. This is using a vertical two dimensional testing matrix perpendicular to the transmitting antenna

Chapter 5 uses the results from chapter 3 and chapter 4 to analyse the consistency between the two through the use of ray tracing techniques.

Chapter 6 discusses the results obtained from the past chapters and draws conclusions on the overall performance of the anechoic chamber. Flaws will be pointed out and any improvements that may increase the chamber's performance noted.

Chapter 2

Anechoic Chamber Attenuation

The first set of testing as specified by the objectives laid out in an earlier chapter is to measure the attenuation of known signals over a range of frequencies as they travel through the anechoic chamber walls. This was chosen to be the first test, as it investigates the chamber's interaction with the external electromagnetic environment. The effectiveness of the chamber's shielding is an important factor in determining how much unwanted external noise will get through the walls and create errors in a test. As well as discovering the attenuation of entering noise, the results will be able to show the magnitude of any signals generated inside the chamber interfering with the external environment.

Before this first lot of testing was conducted the characterization of the antennas and testing equipment had to be confirmed as per the project specification. A previous student of the university, Shayne Wright, had completed a project the previous year (2004), which involved the use of the anechoic chamber. This meant that the antennas were already calibrated and the calibration of the testing equipment was checked against the antennas.

2.1 Methodology

The initial setup of the testing apparatus was thought about thoroughly. The ultra-log antenna was used for receiving which was connected through the I/O ports on the

chamber walls with matched coaxial cables. The exterior coaxial cable connects to a spectrum analyser which in turn is connected via a specialised parallel port to one of the university's computers. This computer has matching software to the spectrum analyser so that test runs can be customised and controlled. The ultra-log was positioned at the far end of the chamber as seen in figure 1.3. The only difference compared to this figure was that the antenna was in vertical polarisation to match the emissions reference source as shown in Figure 2.2.

Not only is it a requirement of both the MIL STD 285 standard and the IEC TS 61587-3 standard that the antennas are polarised in the same direction but it is stated that antennas need to be both polarized the same, as the loss from transmitting and receiving the signal is much less than if they were polarised differently to one and other (Morgan 1994).

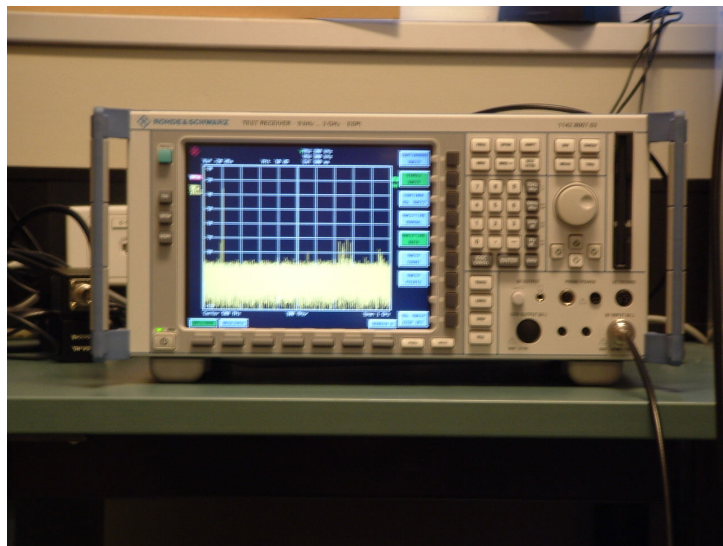


Figure 2.1 Automated Spectrum Analyser



Figure 2.2 Vertical Polarisation of Ultra-Log Antenna

The emissions reference source (ERS) was used as the transmitter and was positioned outside the chamber on a stool as to be level with the receiving antenna. A spacing of 5 MHz between each frequency generated was chosen as to achieve the best ratio between signal strength and data points. Initial problems were encountered with no sign of the emissions reference source on the spectrum analyser. With the help of some of the technical staff at the university, the problem was found to be a flat battery in the ERS, so a recharger had to be developed and this problem was alleviated.

Since these tests are all relative then the signal strength of the transmitted radio waves are not important. For the attenuation of the anechoic chamber as a whole to be discovered, a test was conducted with the end chamber door open as to have a direct line of sight between the source and receiver. Once the results were gathered, the test was re-run with the door closed as record how much of the source got through the walls.

The test parameters were as follows:

- Minimum Frequency: 30 MHz
- Maximum Frequency: 1500 GHz
- Resolution Bandwidth: 120 Hz
- Units of Measurement: dB μ V/m

The results from both the tests are then extracted from the software that was used to control the spectrum analyser and imported into Microsoft Excel. From there a

subtraction of the two lots of data can be performed to discover the difference or attenuation of the chamber.

2.2 Results

For a direct comparison of future results, a plot of the emissions reference source as taken by the ultra-log antenna with no obstacles in the path of the two antennas is given below in Figure 2.3.

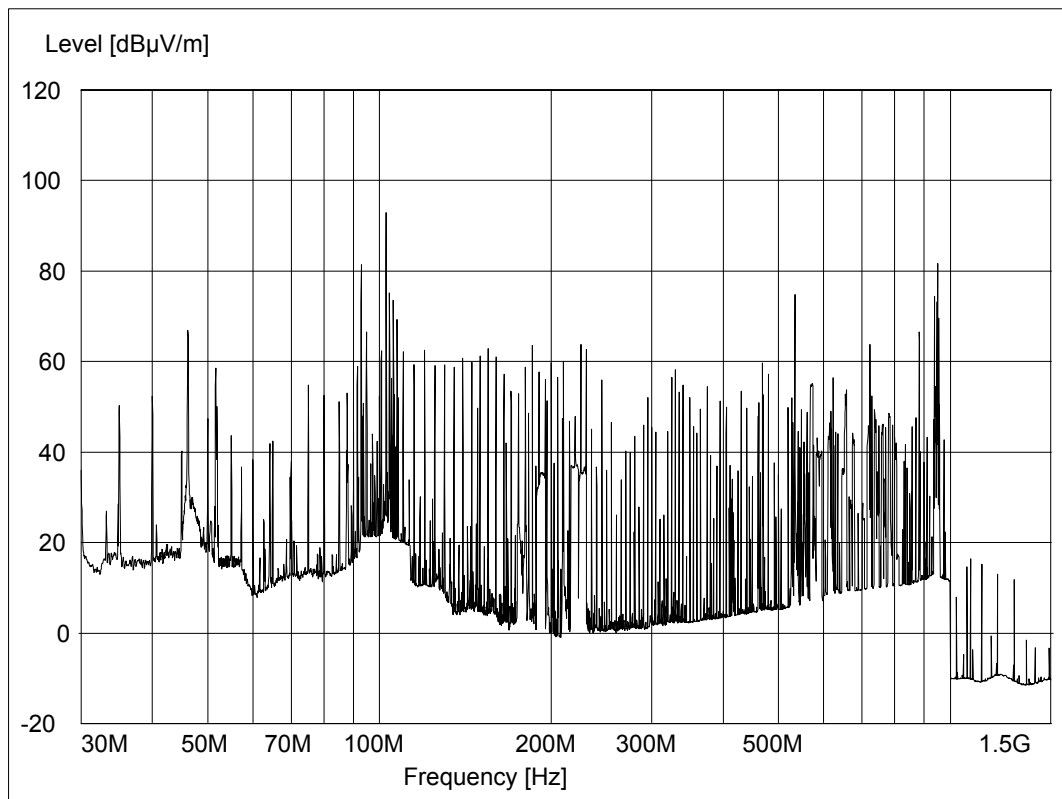


Figure 2.3 True Emissions Reference Source

Since this is the first of many outputs from the spectrum analyser, it is thought that an explanation of the sharp drop in signal strength at 1GHz should be given. Although the recorded data above gives values of negative signal strength, it is thought to be still valid as all conclusions are derived from a relative perspective. After a more detailed look at the large list of recorded data and characterised information, the conclusion was come to that the sign of the entered data in the calibration table is used as a negative

gain and if used as a positive initial value would line up neatly with the flow of data before the 1GHz mark.

The initial testing of the anechoic chamber with the doors open allowing line of sight from the ERS (outside chamber) to the receiving antenna (inside chamber) was conducted with the initial setup of the computer software taking longer than expected due to no prior knowledge of the functions that were needed to be used. Below is the output from the spectrum analyser of the initial test.

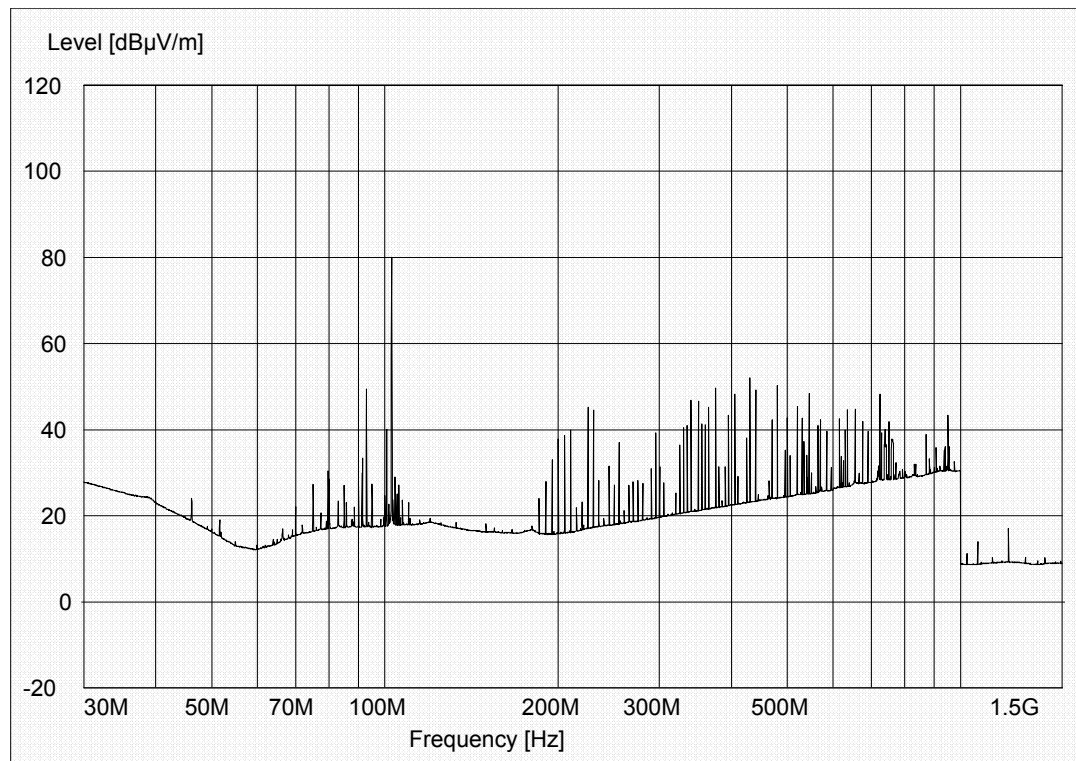


Figure 2.4 Output of Spectrum Analyser – Door Open

From this graph, the 5 MHz spacing generated by the emissions reference source can be seen. Even though both the antennas have direct line of sight through the end doorway of the chamber, it can be seen by comparing Figures 2.3 and 2.4 that there is still a drastic drop in signal strength over the whole range of frequencies. Over the whole range, there is a drop of approximately 20dB between the two configurations, with a large null being present between 100MHz and 200MHz. This could be due to the resonance inside the chamber and will be looked at later in this chapter.

From an initial environmental ambience reading which was taken, some of these reading can be ignored due to local radio and television transmissions. These readings are tall spikes around 100 MHz and the clustered spikes between 400 MHz and 800 MHz.

The testing of the anechoic chamber with the doors closed giving no line of sight between source and receiving antenna was conducted next to discover the overall attenuation. Placing the emissions reference source far enough away from the door as to allow the free swinging of the door proved to be a problem when recording the readings. The distance directly perpendicular from the left hand side of the doorway to the transmitting antenna was 500mm which was initially the same distance for the door-open test. The readings that were taken were very small and amongst the noise. The output from the spectrum analyser was as follows.

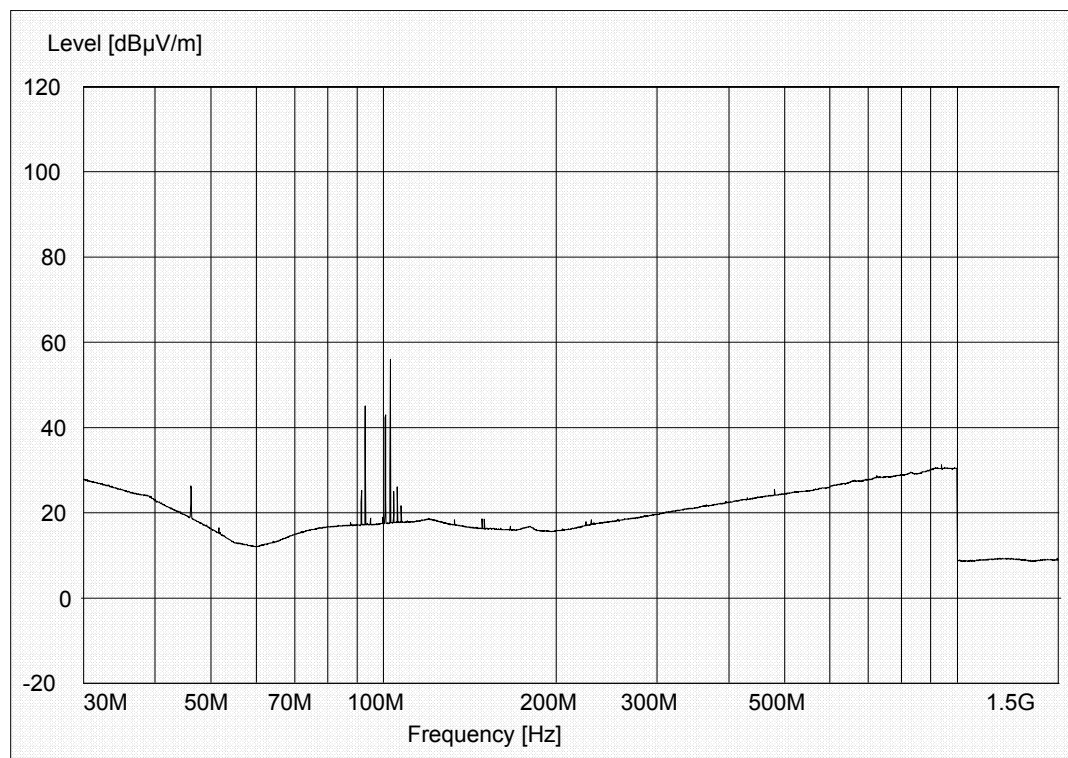


Figure 2.5 Output of Spectrum Analyser – Door Closed (500 mm from door)

As can be seen above, it looks as if the anechoic chamber walls are working very efficiently but by looking closer it was noticed that the ultra-log was not picking up any signal from the emissions reference source due to the low signal strength being transmitted. To alleviate this problem, reducing the distance from the anechoic chamber

door to the emissions reference source was one of the solutions that was thought of. Instead of the original 500mm from the door, distance of 120mm away from the doorway was considered optimal taking into consideration the close proximity of the door gaskets which could allow clear passage of transmitted higher frequencies, and the recorded results.

The test was re-run and the response was recorded giving an output from the spectrum analyser shown below. The open door test was also redone at the new distance to ensure that there was no change in those results, but it was found that this small change made no difference.

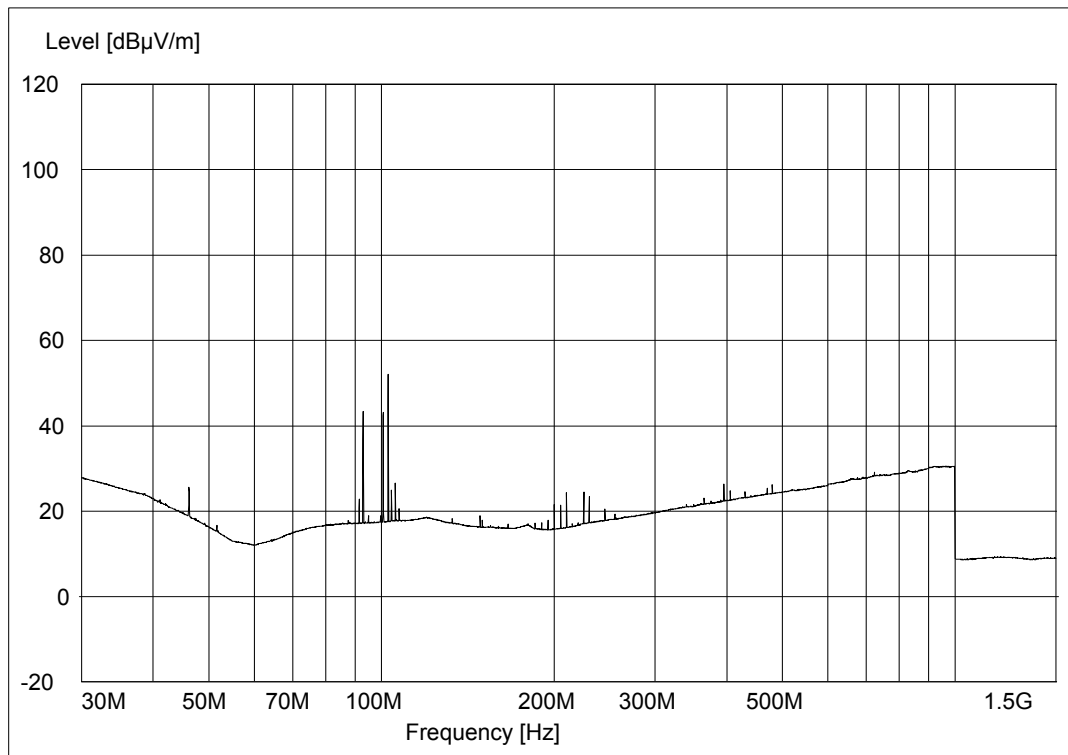


Figure 2.6 Output of Spectrum Analyser – Door Closed (120 mm from door)

This shows that there is an average attenuation of 15dB over the whole range. At first glance, it can be said that these results are very similar to the test done at 500 mm but by magnifying this it was seen that all data points were consistently above the noise level.

With both tests successfully producing data, the calculation of the attenuation can be accomplished. This attenuation was calculated by importing both sets of data into Microsoft Excel and subtracting the data series from having the door open away from

the data series of having the door closed at 120 mm. This plot of the attenuations at each frequency can be seen below in Figure 2.7

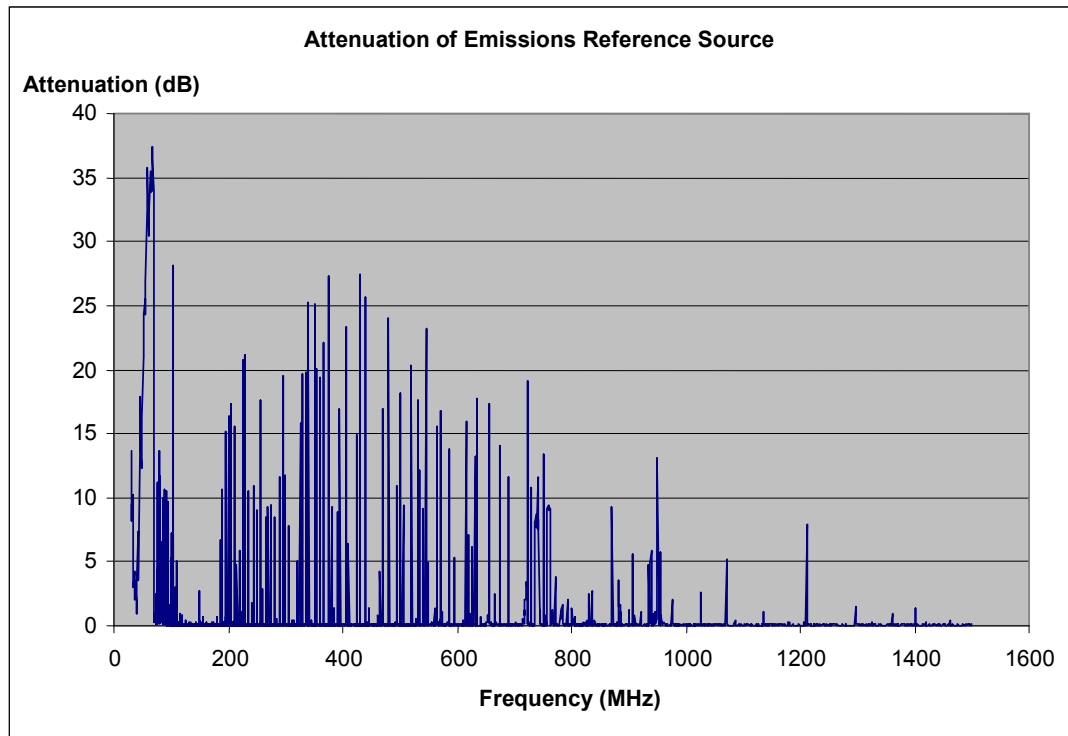


Figure 2.7 Attenuation of Anechoic Chamber

From this plot it can be seen that the anechoic chamber is very effective at attenuating signals from an external source giving a maximum attenuation of around 25dB which peaks about 400MHz. This effectiveness is only as high as 800 MHz however, meaning there is little to no attenuation at higher frequencies. This can be due to the smaller wave lengths of those at higher frequencies sneaking though the gaps in the wall joins or through the door gaskets.

Another abnormality that was noticed and was thought to be of more importance was the absence of recorded data from 100 MHz to 200 MHz. From Figure 2.7, it is quite deceiving because it can be taken that there is just no attenuation in this particular frequency range, however, this due to the fact that there was no actual recordable data in both the open and closed door test to evaluate the attenuation. This could be due to the placement or size of the receiving antenna in relation to the resonant frequencies in the chamber. After some investigation into the resonant frequencies of the anechoic chamber it was noticed that a larger cluster of calculated frequencies lay within the 'gap' that was present.

The formula that was used to calculate the resonant frequencies is as follows:

$$\text{Resonant Frequency} = 150 \times \sqrt{\left(\frac{k}{l}\right)^2 + \left(\frac{m}{w}\right)^2 + \left(\frac{n}{h}\right)^2} \text{ (MHz)}$$

Where:

l - length of the anechoic chamber (4.895m)

w - width of the anechoic chamber (2.185m)

h - height of the anechoic chamber (2.2m)

k,m,n – constants (1, 2...)

The resonant frequencies that were calculated where m or n could be zero (but not both) are:

k	m	n	Resonant Frequency (MHz)
1	0	1	74.75149007
1	1	0	75.17866538
1	1	1	101.4918325
1	1	2	155.7140747
1	2	1	156.3298194
1	2	2	195.9216512
2	1	1	114.5323835
2	1	2	164.5112393
2	2	1	165.0941769
2	2	2	202.9836649
3	2	2	214.2370018

Table 2.1 Resonant Frequencies of Anechoic Chamber

It was decided that the emissions reference source could be amplified to a level where reading could be seen for every frequency in the ‘gap’. This amplification was achieved by using a coaxial cable to route the output from the emissions reference source through a 36dB amplifier to the ultra-log antenna. The amount of amplifying that was needed to receive recordable data was 20dB. This was this reason why it was felt that the test had to be performed in a timely manner as to not interfere with external transmissions. The ultra-log antenna was placed in the same position as the emissions reference source and the bi-conical antenna was used as the receiving antenna and was placed in the same location as ultra-log was originally located.

Swapping the ultra-log antenna to be used as a transmitter was decided upon by the fact that it has greater directivity and since this test will be only done at lower frequencies, the bi-conical is noticeably more efficient at these frequencies.

The frequency responses of the open and closed door tests with the source being amplified, is shown below in separate figures.

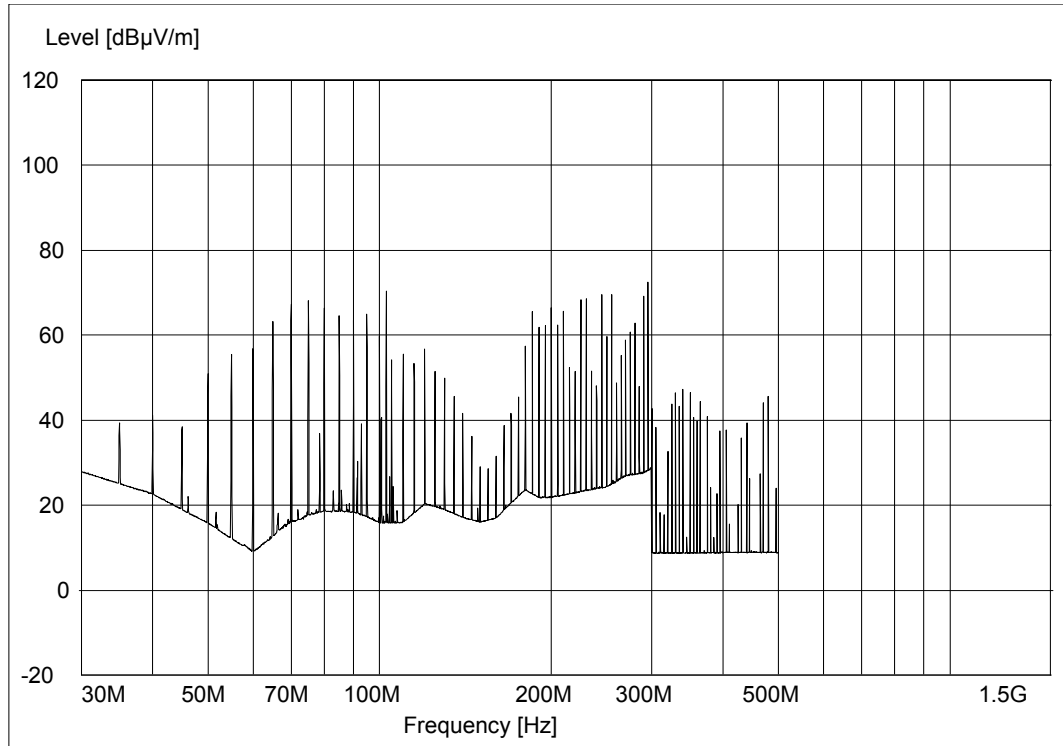


Figure 2.8 Output of Spectrum Analyser – Door Opened (Amplified)

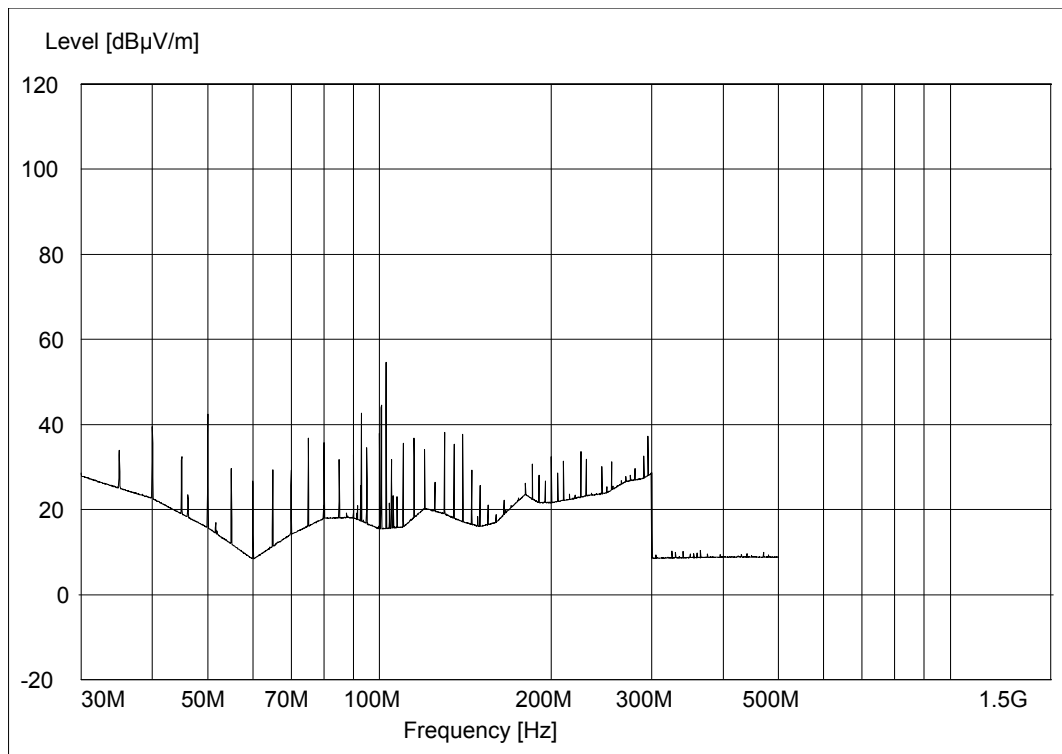


Figure 2.9 Output of Spectrum Analyser – Door Closed (Amplified)

By comparing the two previous outputs from the spectrum analyser, a significant drop in the signal strength can be seen for the whole frequency range. The ultra-log antenna, which was used as the receiving antenna is only characterised to 300 MHz which was not an issue because the amplified tests were only conducted at lower frequencies. Also the calculations that will be performed to find the attenuation are all relative which also alleviates this issue.

The attenuation of the amplified signal by the anechoic chamber is shown below in Figure 2.10.

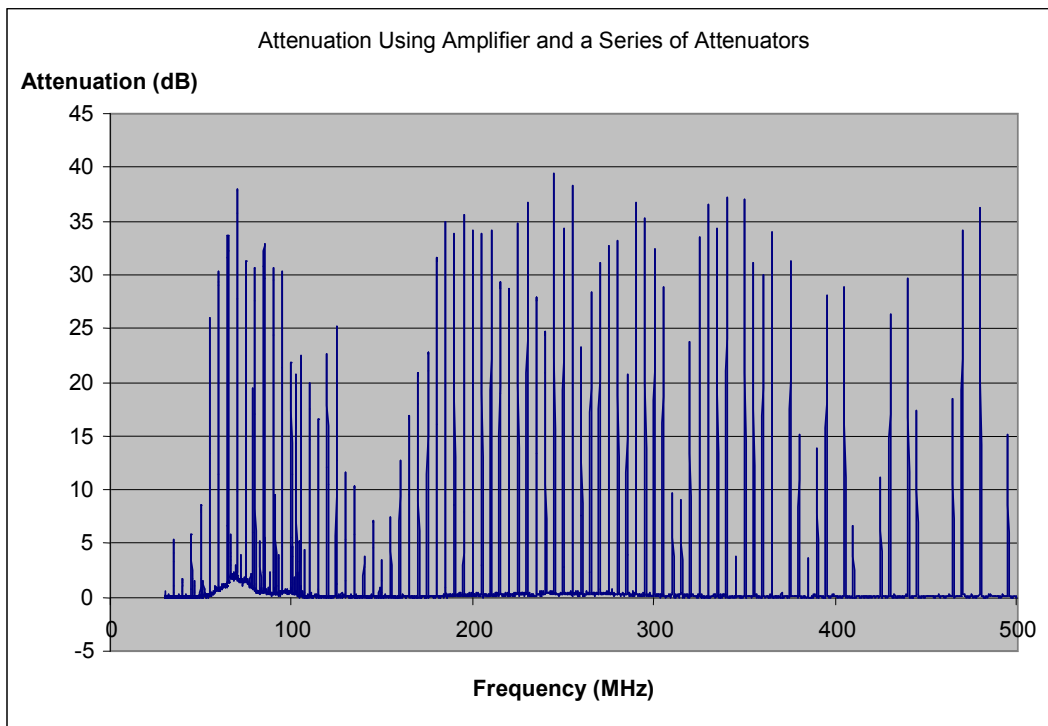


Figure 2.10 Attenuation of Amplified Emissions Reference Source

The tests points that were taken for frequencies that were measurable in both the first lot of testing and the amplified testing showed that there was consistent attenuation between the two. This led to the conclusion that these attenuation calculations could be used in conjunction with the original data to produce an overall attenuation characteristic display.

Using Microsoft Excel this combined attenuation can be seen below in Figure 2.11. The measurements from the first lot of testing were removed from the list of measurements and the new amplified set was introduced.

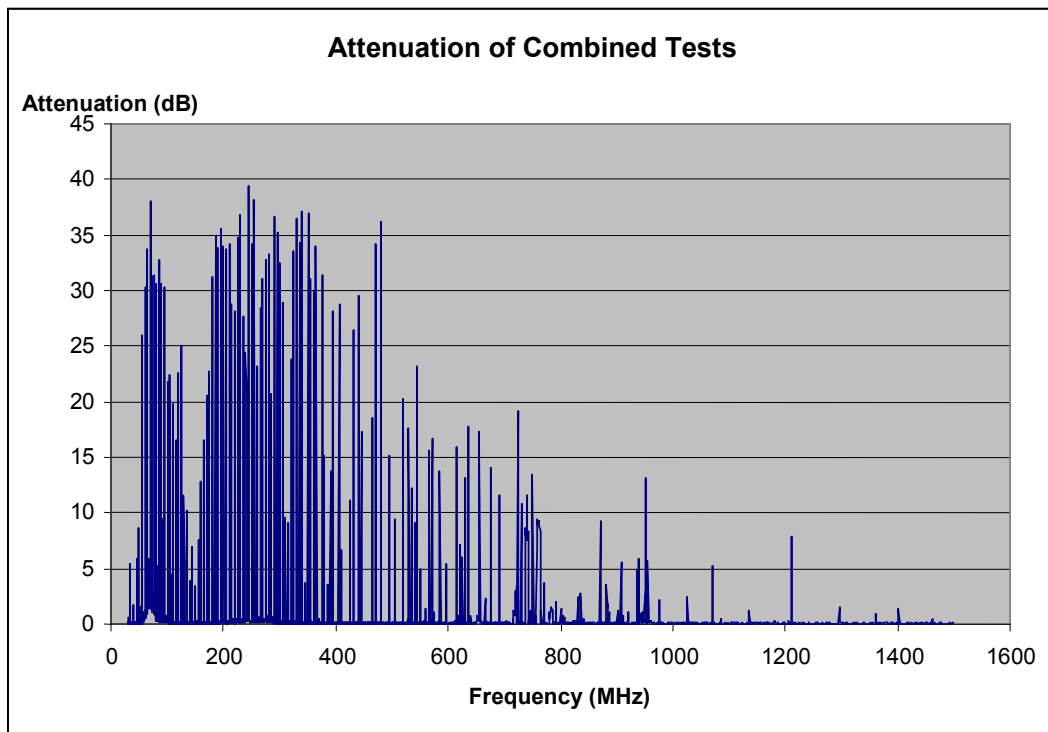


Figure 2.11 Attenuation of Anechoic Chamber from Combined Results

From this combined results graphical representation, it can be seen that the anechoic chamber walls are more effective at attenuating at the lower frequency band than at higher frequencies. Attention should be drawn to the null that occurs above the 800MHz mark. One explanation for this null could be that due to the large physical size of the receiving antenna. At the higher frequencies such as above 800MHz, the antenna would span both the maxima and minima of the transmitted standing wave pattern, which will result on the antenna not recording much of a signal. Any future testing that will be performed during this paper, care should be taken as to not use a high frequency transmitting signal so that minimal interference is done to external transmissions.

Chapter 3

Pyramidal Wall Absorber

From initial thoughts of testing the anechoic chamber as a whole, emphasis was made to evaluate the pyramidal absorbers by themselves to define their performance under a wide array of variations to the transmitting source. The variations that were deemed to be most relevant to the overall characterization of the chamber were in the frequency and angle of incidence. These variations reflect the real life situations that are present when tests are being performed inside the anechoic chamber. The ranges of frequencies represent the diverse tests that will be conducted throughout its use, and the different angles of incidence correspond to the varying distances between the source and receiving equipment that will occur.

During the initial thoughts of how this second series of tests were to be performed, it was obvious that there was not any room at all to move the bulky antennas within the anechoic chamber to vary the angles of incidence. Also there would be too many reflections to take into account from the other surrounding walls and floor. With this being an obvious obstacle to overcome, this was the main focus of this series of testing before any test runs could take place. The solution was to acquire an open-area test site that could accommodate all the testing equipment needed as well as the physical space that is needed, that will be discussed later.

Considerations or criteria when determining an ideal position for an open-area test site can be listed as follows were control must be taken of (Hemming 2002):

1. Inductive coupling between antennas
2. Phase curvature of the illuminating wave front
3. Amplitude taper of the illuminating wave front
4. Spatial periodic variations in the illuminating wave front caused by reflections
5. Interference from spurious radiating sources

Criterion 1 through to 4 are quantifiable considerations as to determine the initial dimensions of the open-area test site. Point 5 can only be considered as to minimise the amount to external noise that will be recorded by the receiving antenna.

Instead of taking the first four points into great consideration, it was thought to only allow the main lobe of the transmitting antenna to be able to reach the receiving antenna by blocking all other possible paths of the transmitted signals. A distance between the both the transmitting and receiving antenna to the wall of absorbers was decided to be three metres as to comply with the recommendations outlined in the ‘Standard for Methods of Measurement of Radio Noise Emissions from Low-Voltage Electrical and Electronic Equipment in the Range of 9kHz to 40GHz’ by the ANSI (2000).

3.1 Methodology

As just discussed, the first hurdle in this task was to determine a satisfactory open-area test site which can supply power to the receiving spectrum analyser and computer. Also the physical size of the test area was an issue as from the initial design, the total area need would be approximately a semi-circle of 4m radius. This initial plan ended up being what was used in the final series of testing. The general overview of the test area is shown in the plan below.

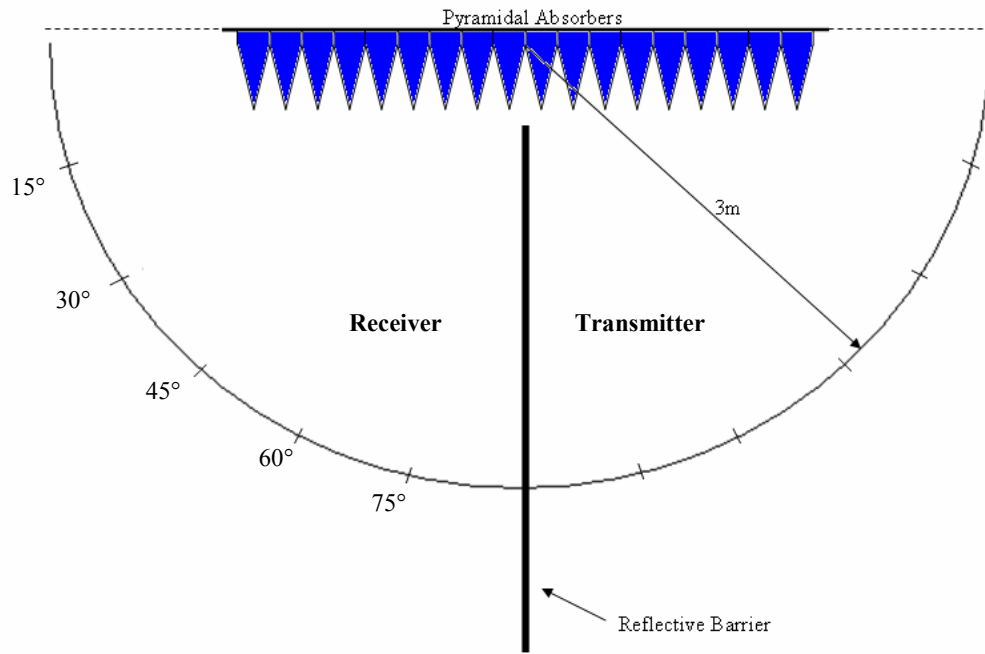


Figure 3.1 Layout of Open-Area Test Site

The plan shows that there is cluster of pyramidal absorbers that were used to represent a section of wall of the anechoic chamber. This temporary wall was constructed by the skilful tech support staff that used spare tiles of the absorbers. These were fastened to a self supporting wall which was lined with sheet metal to act as backing for the absorbers.

Perpendicular to the wall of pyramidal absorbers was a temporary reflective shield which was constructed from the same type of wall as just explained. However only the sheet metal was screwed onto these two wall sections as to act as a reflective barrier to stop the source antenna achieving a direct path to the receiving equipment. The reflective barrier was tested for its effectiveness and is shown in the following sections. These walls proved to become a bother when testing as the slightest wind would tip them over. Guide ropes were used to guard against this but one incident occurred when a sudden gust of wind blew over one of the walls knocking the sheets of metal from their restraints.

The area which was chosen for this testing to occur was on the roof platform on top the Faculty of Engineering and Surveying building. This proved to be one of the best options as it could accommodate the large area needed for the rotating antennas and the numerous pieces of apparatus needed for each antenna. Easy access to power was

present via the use of the antenna hut which was also used for the storage of the absorber wall and reflective barriers. The railings around the platform served as more than adequate anchors for all the barriers, the tie-downs that were used proved to be inferior and had to be reinforced to prevent a repeat of the first incident.

The angle of incidence of the antennas was chosen to be at intervals of 15° which gave a good basis on which to evaluate the absorber's performance. The way in which it was ensured that the antennas were on the mark for each test was by using their phase centres on each. The ultra-log antenna had its phase centre mark on the main boom which was put there by the manufacturer. The bi-conical antenna didn't have a phase centre designated on it so it was decided that a constant reference point in the middle of the antenna would be designated. The phase centre of the antenna proved to be the point where the two cones of the antenna meet in the middle which is where the stand is also attached. The vertical shaft of the stand was then used as a plum line to line up the antenna for reference with the angles of incidence.

The arrangement of equipment that was used for transmitting onto the wall of absorbers was the bi-conical antenna being powered by the emissions reference source. This was possible by detaching the default gold rod from the box and attaching a coaxial cable between the two. This arrangement in actual testing conditions on level 5 is shown below in figure 3.2.



Figure 3.2 Transmitting Antenna Arrangement

The receiving antenna arrangement required a slightly more complex setup in the way of its logistics. The ultra-log antenna as used as the receiving antenna as it had the greater directivity of the two and could be concentrated on the signals being reflected off the absorbers. The trolley that was chosen to carry the computer and spectrum analyser had to have enough room to fit all the equipment on without the risk of anything falling off while being moved around. Having enough room did have its trade-offs as the trolley couldn't be too big otherwise it could not be taken up to level 5 and moved around when it was up there. A larger length of coaxial cable was used to connect the spectrum analyser and ultra-log antenna to ease the positioning requirements of the trolley. A picture of the ultra-log antenna and the trolley is shown below in figure 3.3 and 3.4.



Figure 3.3 Receiving Antenna Arrangement – Ultra-log



Figure 3.4 Receiving Antenna Arrangement – Trolley

3.2 Testing Process

Setting up of the testing area was a task in itself. The days that the testing could be performed were limited to days that weren't windy or raining. Help from a fellow student was needed to carry all the necessary equipment up to level 5. Once the computer trolley and antennas were set up in the far corners, the middle barrier was then constructed. A guide rope either side of each wall piece was then anchored down to the surrounding railings and were adjusted so the whole wall was vertical. The last step was to carefully carry out the wall of absorbers and place perpendicular to the reflective wall as shown previously in figure 3.1.

First of all when setting up the equipment, the reflective barrier was made sure that it was dividing the wall of absorbers in half as to get an even distribution on both sides. This was done by counting how many spikes were along the width of the wall and moving the absorber wall accordingly. Once the middle was established, a 3m arc was drawn using a pre-measured length of string and some chalk. The chalked out semi circle could then be marked into 15° increments. The way in which these angles were found was by determining the circumference of a circle of 3m radius and dividing that figure by 24. This result gave the distance between each 15° increment along the chalked out arc.

The ultra-log antenna and measuring equipment was setup on the receiving side (left) as per figure 3.1. An extension cord that ran from the antenna hut, behind the wall of absorbers and around behind the receiving arc was used to power the computer and spectrum analyser. Enough extension cord and coaxial cable was used as to not have the requirement to move the trolley with the ultra-log every time it needed to be moved to the next testing increment. A temporary plum line was constructed off the antenna from spare guide rope as to be able to accurately position the antenna over the marks on the arc as can be seen in Figure 3.3 and 3.4.

Once the receiving side was completed, the easier, transmitting arrangement was started. The bi-conical antenna was just placed over each test point according to the vertical shaft of the stand. The emissions reference source was connected by a coaxial cable of shortest possible length as it was no hassle in moving the box along with the antenna.

An initial run to see what was being received by the ultra-log was done at an angle of incidence of 45°. The normal range of 'spikes' received from the emissions reference source in previous tasks was seen and was then assumed to be working correctly. Once this test run was completed another run of the exact same specifications was performed except the emissions reference source was turned off as to get an ambient noise reading for later analysis.

Now that it was known that everything was working, the antennas were placed at an angle of incidence of 75° and then a test run performed. The antennas were then stepped through each test increment until all the angles of incidence was completed. Care had to be taken at every increment as to ensure measurements were being recorded as the computer monitor and spectrum analyser were very difficult to read due to being outside in the sun. This checking proved to be useful as a couple of increments proved to be an ineffective run as the emissions referenced source was not turned on in one instance and also the wrong specification were chosen at the beginning of another.

Once the all the test points had been stepped through, it was then decided that the reflective dividers themselves should be tested to record their effectiveness. This would then be on record to answer any queries that could be raised about the effectiveness of this arrangement and whether the barrier prevented the antennas from have a direct line on communication.

The wall of absorbers were carried inside before this test was performed as to ensure that it would not blow over since this piece of wall was not needed or being focused on. Both the ultra-log and bi-conical antennas were placed 3m apart giving a distance of 1.5m from the wall and each antenna. This distance was referred to the points on the antennas as explained before for positioning them on the test points. The antennas were faced in the middle of one of the reflective barriers as to minimise the amount of possible gaps that could occur such as the wooden gap with the adjoining barrier.

Once the first test run was completed, then the barriers were removed and stored away in the antenna hut. Another test was performed with just the antennas facing each other as to compare to the last assessment.

3.3 Results

First of all looking at the Emissions Reference Source (ERS) initial plot done in the previous chapter as a base for comparison should be displayed.

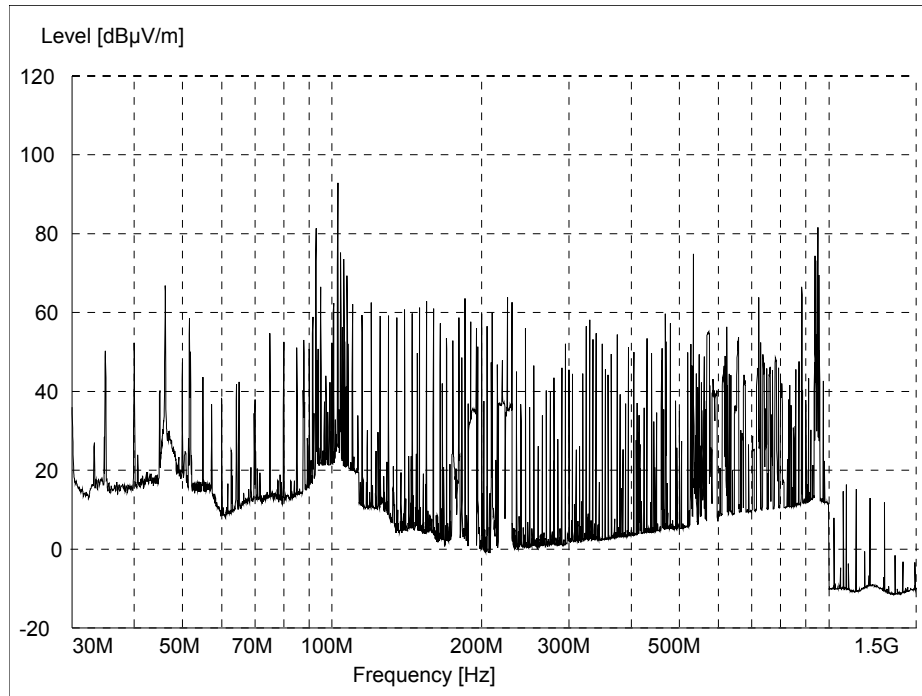


Figure 3.5 True Emissions Reference Source

The first thought about the expected results was that the greater the angle of incidence, the more attenuation to the reflected signal will result. This trend is evident all the way through from an angle of incidence of 15° to 75° . The attenuation of the absorbers through the method of testing used was not able to be obtained due to the equipment size restraints.

As shown below in figure 3.5, the angle of incidence is at 15° . The definite 5MHz spacings of the emissions reference source can be seen throughout the whole frequency range of the test. The deteriorated signal strengths between 100MHz and 200MHz is no longer present giving evidence that the main resonant frequencies (100MHz to 200MHz) of the anechoic chamber are of correct calculations and is now be justified. The larger signal spikes can be attributed to the surrounding environmental noise that is being generated by radio stations (~ 100 MHz) and television stations (500MHz-1GHz).

Comparing the incidence angle of 15° to the true emissions reference source plot in Figure 3.5, it can be seen that there is little to no attenuation of the transmitted signal across the whole frequency range. Making over-head transparency copies of the plots enabled the direct overlay of the two outputs which gave a closer comparison. The only difference between the two was that each spike was not as thick in the 15° incidence as to the true ERS plot. It is thought that the absorbers could have attenuated the side lobes of the transmitted spikes and given a sharper range of spikes in the recorded graph.

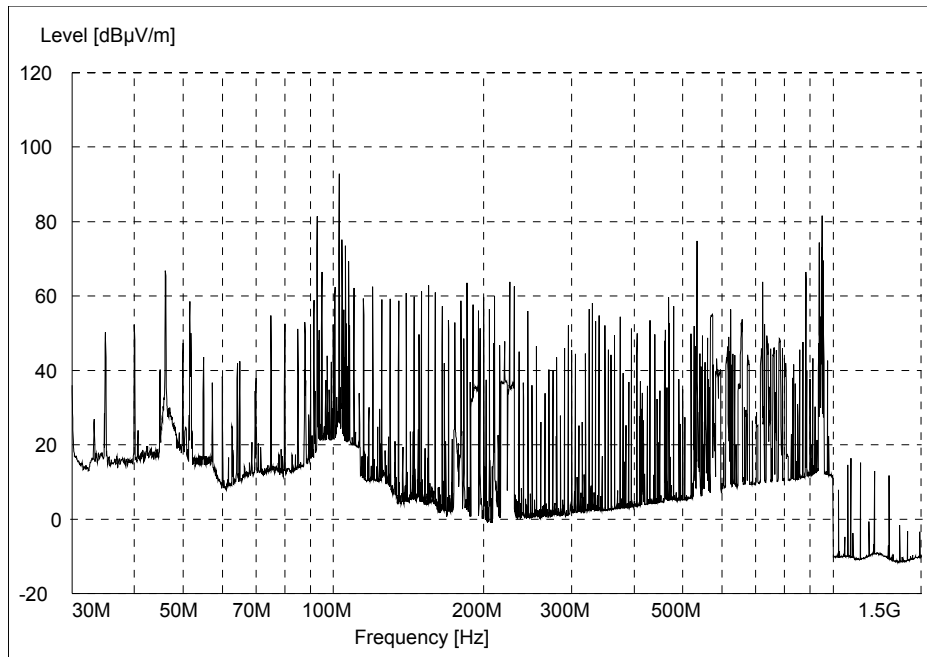


Figure 3.6 Spectrum Analyser Output – Angle Incidence of 15°

Now comparing to the spectrum analyser output for 45° shown in Figure 3.7, it can be seen that there is an overall reduction in the strength of the reflected signal of 10dB. Notice how the large signal spikes are still present in this next graph. Even though there is a reduction in signal strength compared to the previous output these signals are continuously varying due to changing information being transmitted. There is an average reduction of signal across the frequency of approximately 10dB from 100MHz to 500MHz. However, after careful analysis of the lower end of the frequency range of both graphs it was noticed that the signal strength actually increased slightly from the first angle of incidence. This trend of both an increase and decrease in reflected signal strength will now be studied in relation to the other spectrum analyser outputs and try to conclude on whether these are common occurrences.

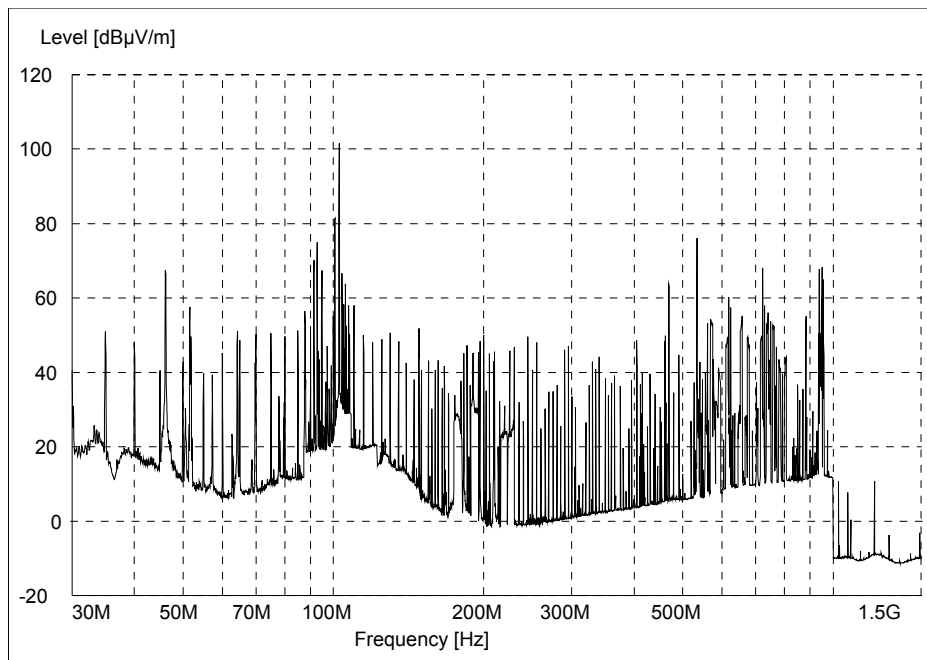


Figure 3.7 Spectrum Analyser Output – Angle Incidence of 45°

This trend of a reduction in signal strength in the mid to high frequencies and slight increase at lower frequencies stands when looking at the spectrum analyser output for an angle of incidence of 75°. However, the decrease of signal strength is of greater magnitude to the extent that none of the signals are being reflected giving an attenuation of 40dB to the transmitted source. Also when looking at the lower end of the frequency range, the measured points do increase, but there are fewer of them compared to the output at 45°. The external signals are even more noticeable now with most of the transmitted signal being attenuated.

Even though the performance of the pyramidal absorbers at an incidence of 75° is very good once the ambient environmental noise is discarded, in most situations when receiving a signal within the anechoic chamber, an angle of incidence of this size is rarely come across which will contribute to destructive or constructive interference at the receiver. The only time that this angle would occur would be when the transmitted signal will be reflected off the end walls.

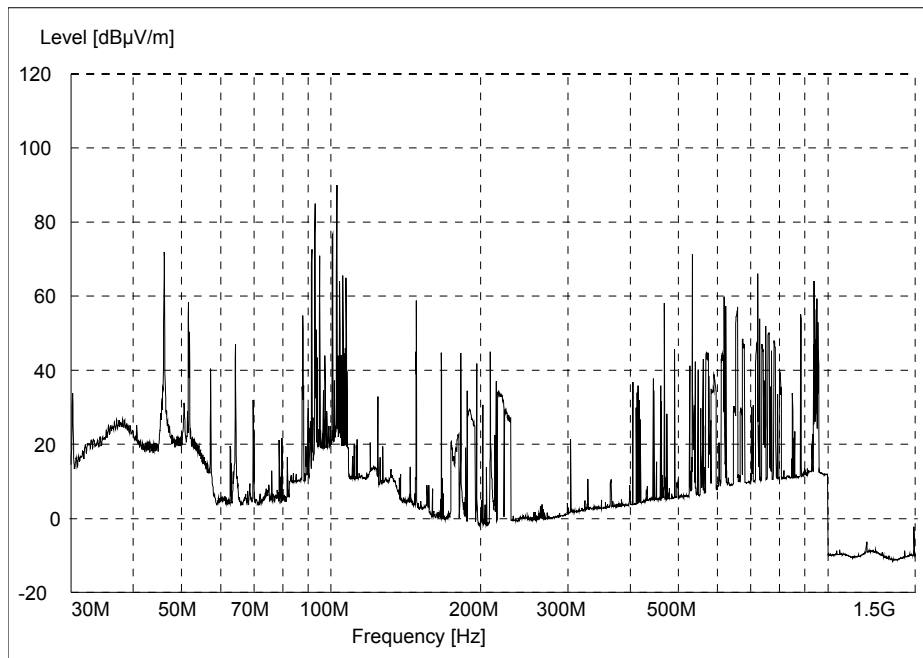


Figure 3.8 Spectrum Analyser Output – Angle Incidence of 75°

The average distance between the transmitting and receiving antennas taking into account the possibilities of variations of position on the ferrite tiles, the smallest angle of incidence that will occur when being reflected off the side wall absorbers is approximately 30°. This means that the performance at 15° can be omitted from the overall performance of the absorbers when being referenced to the anechoic chamber.

So far the analysis had been a comparative one, explaining the trend in which the absorbers perform when subjected to different angles of incidence. Now the actual magnitude of absorption of the reflected signal will be looked a relative to the signal strength of the direct path from the source to the receiver.

The normal, direct line of sight signal strength of the emissions reference source is shown below in Figure 3.9 and this will be the reference to which the other graphs will be compared to.

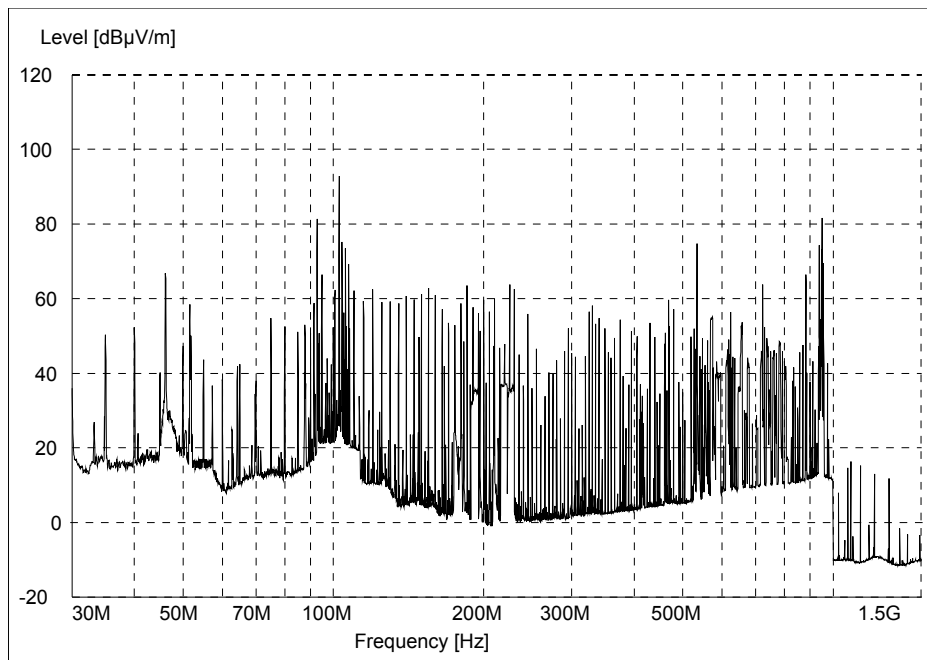


Figure 3.9 Spectrum Analyser Output – Emissions Reference Source

It was first of all thought that this output had been misnamed and been the output of the angle of incidence of 15° . However this was not true. Comparing the two outputs just mentioned, it can be concluded that at an angle of 15° , the pyramidal absorbers offer little, if not, no absorption of the signal when being reflected.

The idea that the reflective barriers were too far away from the absorber wall was raised, so therefore the barriers were moved closer to the absorber wall, between two columns of pyramids. The new gap was only 50mm from edge of wooden frame of the reflective barrier to the base of the pyramid on the absorbers. This change in distance proved to be a waste of time, with the output of the spectrum analyser producing the same as before.

When comparing the rest of the incidence angles, a table was produced to summarize the absorbers performance at designated frequencies. From this, further assumptions can be made and will be discussed in later chapters regarding the figures in the table below. The way in which this table is constructed is by taking average difference of the surrounding signal strengths instead of exactly the designated frequency as the spectrum analyser samples did not always sample on each specific mark. For example, for a frequency of 100 MHz, five sample either side were compared to their corresponding reference and then those differences were averaged.

Angle of Incidence	Frequency (MHz)								
	30	50	70	100	200	500	800	1000	1500
15°	- Too Small To Measure -								
30°	0	3	-5	-5	7	15	5	0	0
45°	0	6	-2	-1	10	20	5	10	0
60°	0	8	1	2	14	22	10	15	0
75°	0	10	5	22	25	30	10	32	35

Table 3.1 Attenuation of ERS Signal (-dB)

Looking back at the two published table listing the various performances of pyramidal absorbers, will give an idea of how justifiable the method of testing was. The typical performances of a pyramidal absorber is show below in Figure 3.10, which is followed by the manufacturer's data specific to the absorbers which are used in the anechoic chamber (Figure 3.11).

Type	Height (cm)	Weight (kg)	Tips per piece	Normal Incidence Reflectivity, GHz									
				0.12	0.3	0.5	1.0	3.0	6.0	10.0	18.0	36	50
P-4	10.9	1.4	144					30	35	42	50	50	50
P-6	15.2	1.6	100					32	40	45	50	50	50
P-8	20.3	2	64				30	37	45	50	50	50	50
P-12	30.5	2.7	36				35	40	45	50	50	50	50
P-18	45.7	5.4	16			30	37	40	45	50	50	50	>45
P-24	61	7.7	9		30	35	40	45	50	50	50	50	>45
P-36	91.4	10.9	4		35	37	42	50	50	50	50	50	>45
P-48	121.9	17	2	28	35	40	50	50	50	50	50	50	>45
P-72	182.9	23	1	33	40	45	50	50	50	50	50	50	>45

Note: Base dimensions are 2ft x 2ft

Table 3.10 General Pyramidal Absorber Performance (Cumming Microwave 2006)

FREQ (GHz)	0.25	0.5	1.0	3.0	6.0	10.0	18.0	30.0
LOSS (dB)	-22	-28	-35	-40	-45	-50	-50	-50

Table 3.11 AEP-12 Radio Wave Absorbing Performance (Advanced ElectroMagnetics Inc. 2006)

As these two published graphs are only giving data for normal incidence, there is no ability for a direct comparison. However, the largest incidence angle taken in the testing phase was 75°. Following the trend from the smallest angle of incidence up the range of tests, it can be seen that the reflection if a larger angle of incidence could have been tested, the recorded data would have been very close if not the same as the published

figures. The results for 75° @ 1GHz is very similar to the figures for the generalized performances (-32dB and -3dB respectfully) which is also the result obtained by the manufacturer.

The lower frequency reflections are already very close to the manufacturer's data however the high frequency reflections need to improve to correspond to the whole range of published results. It is felt that this would happen as the angle of incidence increased in practice. The trend of the recorded data leading towards the figures of the manufacturer's published results and familiarity of the generalised data gives substance to the method of testing and the results obtained.

Finally the effectiveness of the reflective barrier is to be evaluated. The results were as wanted. The results were that the reflective barrier proved to be very efficient in stopping any transmitting waves from the side lobes of the antenna pattern to be picked up by the receiving antenna and corrupt the results. The output from the spectrum analyser of the reflective barriers performance is now shown in Figure 3.10.

The attenuation of the antennas facing each other through the reflective barrier gives a value of 40db. This is more than sufficient as the antenna pattern of the transmitting source gives a much less transmitting signal strength than the main directional lobe. This gives no concern of interfering data being recorded from a direct path between the two antennas of the series of test just performed.

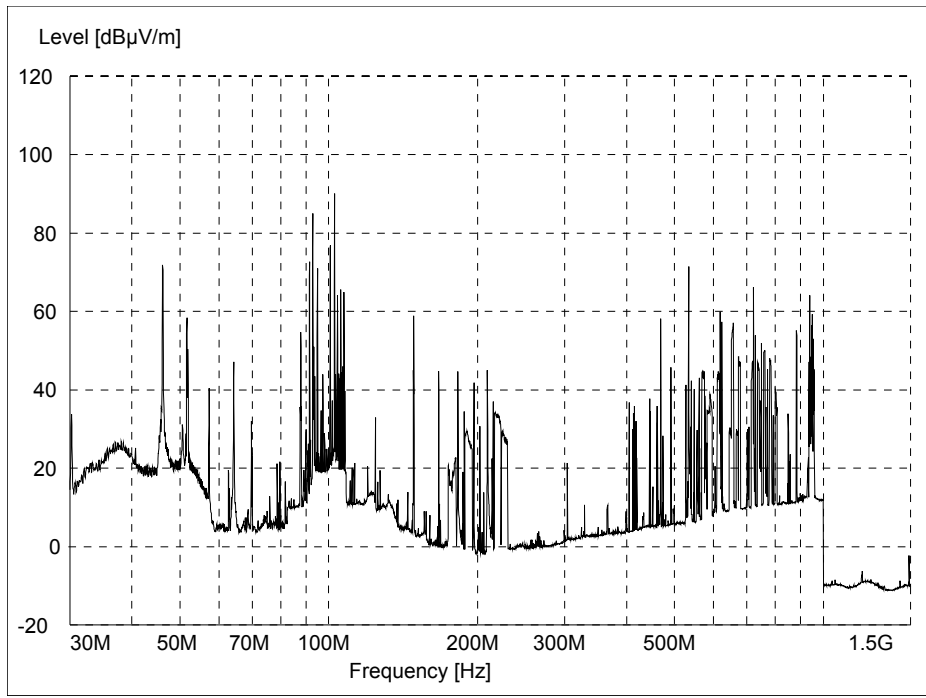


Figure 3.12 Spectrum Analyser Output – Reflective Barrier

Chapter 4

2-D Planar Variation

Now that the behaviour of the wall absorbers has been tested and evaluated, the field performance inside the chamber can be analysed and then hopefully related back to the pyramidal absorbers' characteristics. From the chapter title, it can be known that the variation of the testing field in a 2 dimensional plane will be looked at. The section or plane in which will be evaluated is that of where the average position of the receiving antenna is placed when the anechoic chamber is being used. The plane is a cross-section, cutting the anechoic chamber across its length and it extends out to cover most of the space not used up by the pyramidal absorbers.

The way in which the plane could be tested was to design a simple, non-conductive stand that could be sturdy enough to hold evenly distributed points across the whole test area. The stand was chosen to be made out of wood and be of simple enough design as to be easily made by the technical staff in the Faculty of Engineering and Surveying building. It was decided that an adjustable 'cross' would be made as to represent a matrix through the test plane. Everything would be held together by wooden pegs as to provide no interference with the tests being conducted. The plane consists of 25 data plots over the already specified frequency range, which meant that the stand gave a 5x5 matrix once all test points had been analysed. The distance between each node in the matrix in the horizontal and vertical direction was made equal at a distance of 200mm. Below is a basic schematic of how the stand was constructed in figure 4.1.

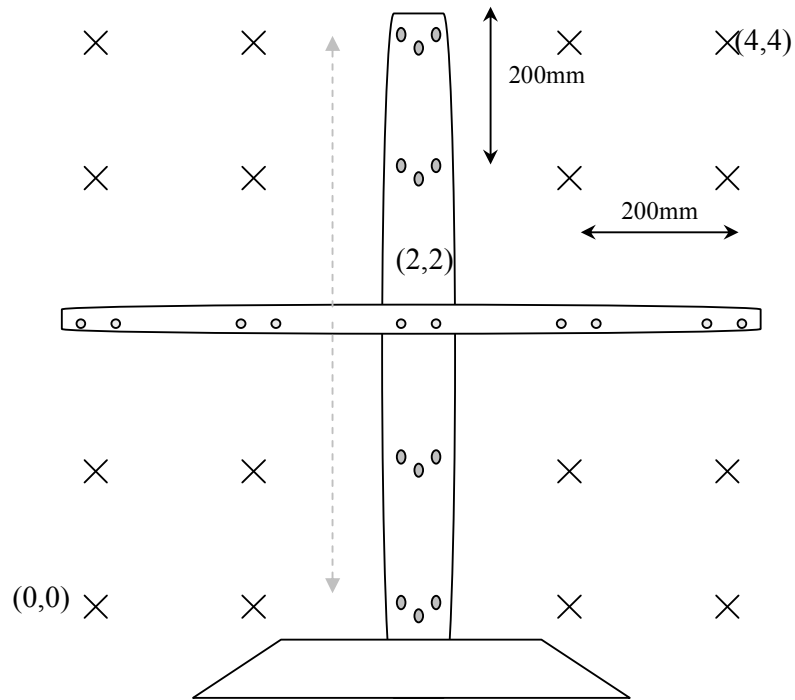


Figure 4.1 5x5 Matrix Receiving Antenna Stand

Since the difference in field strength is to be determined, the receiving antenna can not be too big as to blur the test nodes together. The choices for the antennas were very limited due to there being limited supply of small antennas on hand at the faculty's store. A small dipole which was constructed on a printed circuit board was chosen as it was of small size and had enough excess circuit board to have holes drilled in it to be held secure on the stand by wooden pegs. The stand was situated at the far end of the anechoic chamber as shown in figure 1.3, not only because the outlet of the chamber leads to the spectrum analyser at that end but the wall behind the stand is a continuous surface with no door gaskets separating the absorbers like the transmitting end. Once both the stand and transmitting, ultra-log antenna was in place, a standard distance of three metres (3m) was created between the reference points of the equipment. The dimensions of the dipole are as follows as shown in the below schematic.

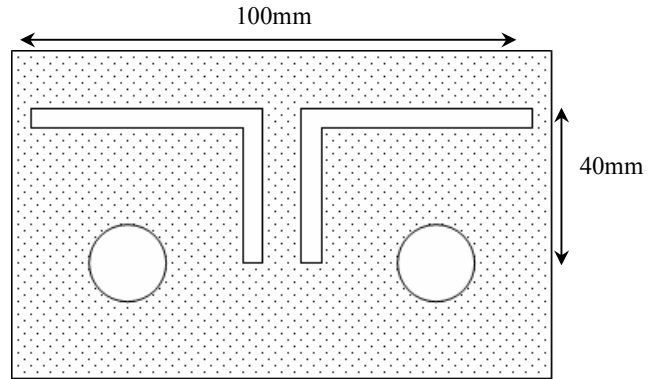


Figure 4.2 Receiving Dipole Antenna

Before this dipole that was chosen could be used, it must be calculated that the dipole is much shorter than the wave lengths of the frequencies used in the testing phase. In doing so, the wavelengths had to be calculated and are shown in the first part of the table shown below (Figure 4.1).

Frequency (MHz)	Wavelength (m)	Comparison to Dipole (100mm)
300	0.9993	$\ll 1/2$
500	0.5996	$\ll 1/2$
1000	0.2998	$< 1/2$
1500	0.1999	$1/2$

Figure 4.1 Frequency Wavelengths vs. Dipole Length

For the dipole to be considered short, the length of the dipole must be less than half of the wavelength as a general rule of thumb (Connelly 2004). As can be seen in the right column in the table above, the dipole easily passes the general test of a short dipole which clears this antenna for be included as the receiving antenna. The dipole is exactly half for a frequency of 1.5 GHz; however, since this frequency is the upper limit of the testing, frequencies will not be used where the rule of thumb is conflicted.

4.1 Methodology

Since this series of testing is situated solely in the anechoic chamber, there is minimal setting up required. The transmitting arrangement consisted of placing the ultra-log

antenna on the ferrite tiles at the transmitting end and connecting it with a coaxial cable to the designated wall connector. From the outside of the chamber, another coaxial cable was connected from the corresponding wall connector to the emissions reference source. This arrangement was decided to be tried first of all but other alternatives were thought of.

Such an alternative was just placing the emissions reference source on a wooden table on the ferrite tiles. After further thought, it was decided that this would not be used as the default gold antenna is very unidirectional. This lack of direction means that there are a lot of possible reflections of the surrounding walls to take into account measuring with the dipole.

The bi-conical antenna was also thought of but for a similar reason as just discussed for the stand alone reference source, the lack of direction would be hard to take into account when logging the measurements.

The setting up of the receiving configuration was completed by first of all choosing a starting position of the stand and fastening the dipole to the horizontal boom of the stand. The starting point was at the bottom left node (0,0) as seen in figure 4.1. Care was taken as to the length of the connecting coaxial cable from the dipole to the wall connector. It had to be long enough to reach the far test points but not too long as to act as a contributing antenna to the measured signal. Any spare length of coaxial cable was run along the ground in between the spikes of the surrounding pyramidal absorbers as to shield the cable as much as possible. When the coaxial cable did need to be exposed, it was exposed in a vertical position as to be opposite polarisation to the transmitting antenna and therefore minimising the interference on the wanted data. There is a coaxial connector on the back of the printed circuit board of the dipole in which the coaxial cable could be attached.

The distance between the transmitting ultra-log antenna and the vertical shaft of the stand was measured for the use of ray tracing techniques discussed in the following chapters as well as any other important positioning measurements.

Once the first test at node (0,0) was completed, the dipole was repositioned along the horizontal boom to node (0,1) and the testing process repeated until the whole row had

been logged. Then the horizontal boom was raised to the next row and the whole process was repeated again until all the rows had been recorded.

Once all the nodes of the planar matrix had been recorded for its varying signal strength over a range of frequencies, any noticeable changes between nodes were noted and could be hopefully theorised in the following sections.

It was only after the results of this task was completed and commented on that a balun was not used in company with the coaxial lead and dipole antenna. Due to time constraints, a repeat of this time consuming task was not conducted as the same coaxial cable was used for each position on the stand. Therefore any errors should be consistent and any patterns could still be discovered.

4.2 Results

Since the dipole antenna that was used for receiving the signal from the emissions reference source was not characterised, a set base level of 0dB was issued to the antennas characteristics as to make comparisons easier.

Since there are a total of 25 output displays of the received signal, it would be too time consuming and irrelevant to discuss each graph individually. Therefore the series of test nodes will be treated as a whole and any patterns or unusual occurrences will be noted and tried to be explained. Each individual output from the spectrum analyser is displayed in Appendix B for individual perusal.

The first real interesting pattern that formed as the testing proceeded through the rows of nodes was that the first (far left) and second nodes on each row gave nearly identical outputs. This phenomenon however did not occur on the right hand side of the individual rows which starts to give thought on how this could occur. The fact that the side entrance door is situated just to the side of these nodes could be affecting the received signal by giving unabsorbed reflections from the unshielded door gaskets. Another thought would be the excess coaxial cable that is left hanging in a loop in the absorbers when the antenna is on the left hand side due to less coaxial cable being needed to reach the stand. The coaxial could be receiving the transmitted signal to a

large enough degree that any variations would not be picked up because they would be less than the interfering signals.

An example of the first two columns of each row showing no variation between plots is displayed below with the outputs from the spectrum analyser from (2,0) and (2,1). Through out the whole frequency range there is no change in signal strength. The test process was repeated due to this very strange occurrence and it was found that there was no change in the first two columns.

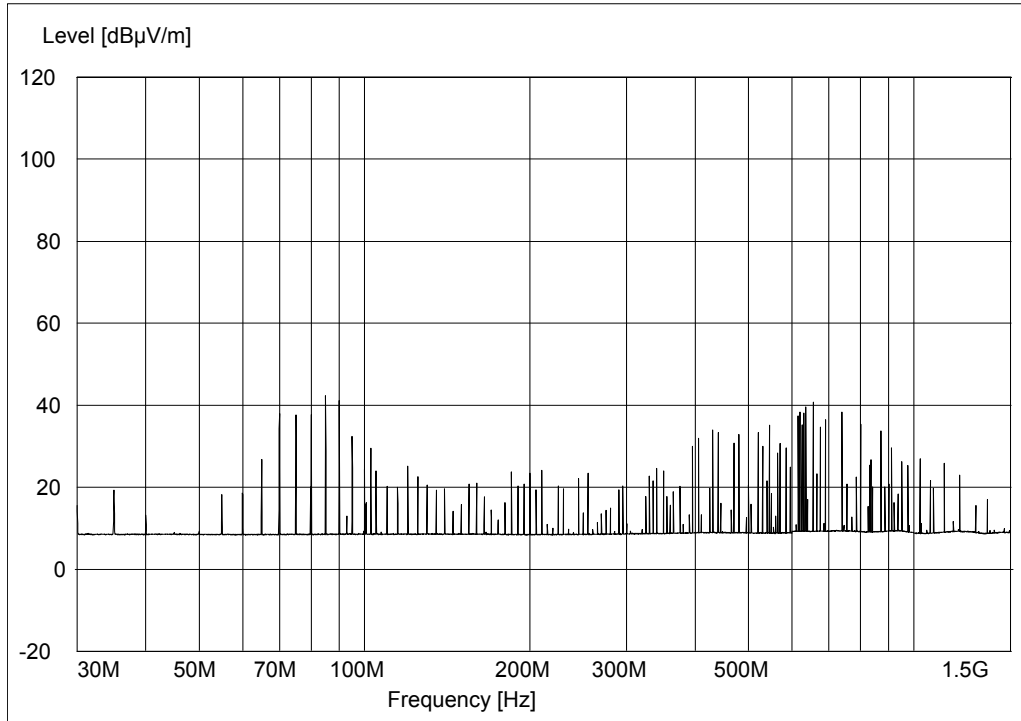


Figure 4.3 2D Planar Output – Node (2,0)

Another differentiation from the first two columns of each row and the rest of the nodes in the rows is that there is a consistent increase of 5dB in signal strength across the whole frequency range for all five rows. This gives the impression that there is a significant effect on the recorded data from the exposed seams of the door. The tests of the left two columns were repeated with the spare coaxial cable in different configurations. This proved to have no effect which makes the door gaskets appearing to be the main influence in the destructive interference. An example of the 5dB increase in signal strength is shown below in Figures 4.4 and 4.5.

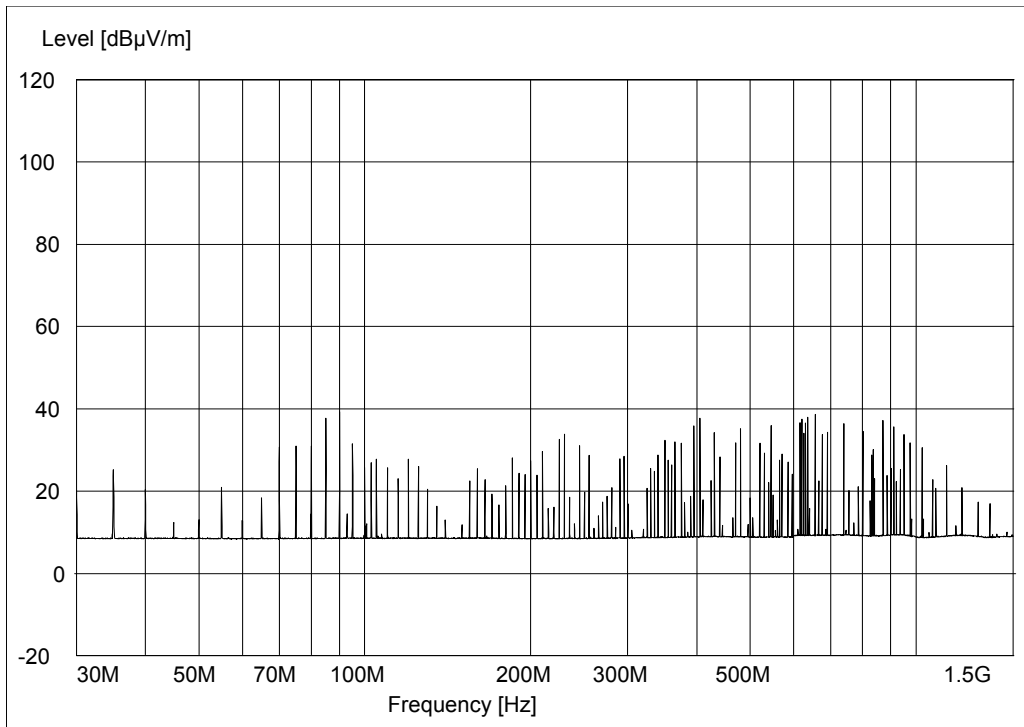


Figure 4.4 2D Planar Output – Node (4,1)

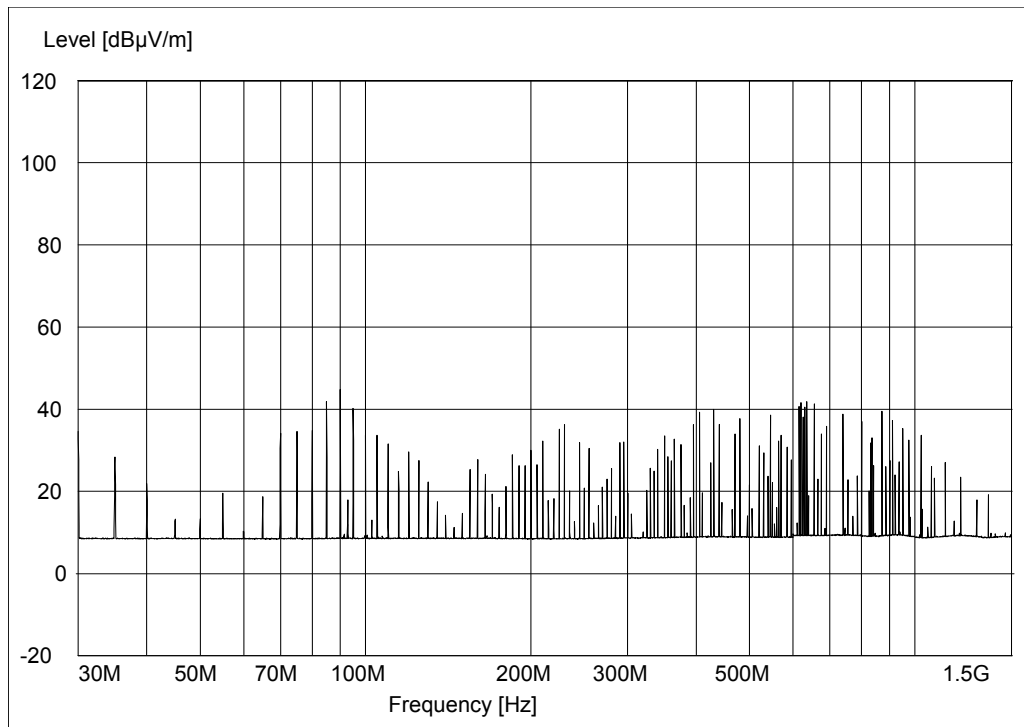


Figure 4.4 2D Planar Output – Node (4,2)

When looking at succeeding plots along the last three columns of each row, it was noticed that there were changes of 5dB constantly across the whole test range, however, the changes are not in any particular pattern or have no similarity in change between the other rows. There are just random changes in signal strengths across the whole frequency range by an average of 5dB.

Since the only initial observation are the ones just mentioned, the plots were exported and printed to file on the computer. Each plot was put in their corresponding rows and slide shows were made to change between each plot fast enough as to notice the smallest of changes.

When cycling through the rows, it was noticed there was a general increase in signal strength from column 0 to 2 and then it from column 2 to 4 the signal strengths decrease but at a lesser rate than that of the first columns. This gives the first impression that from the middle of the chamber to the right has a more stable testing plane in regards to repeatability. This is important when testing multiple DUTs for comparison purposes.

Changing the slideshows from showing the rows to comparing along the columns gave another interesting characteristic. All columns showed a shift in the lower frequencies, inversely proportional to the higher frequencies. The pivotal frequency in which this shift was occurring was 250 MHz.

All frequencies below this 250 MHz mark, increased by between 10dB and 20dB from row 1 through to row 4 with the greatest increases happening at the lower and upper limits of this segment. The greatest increase was between the frequencies of 30 MHz and 50 MHz with the signal strength increasing by up to 20dB.

The decreases on the upper of the 250 MHz mark was not as substantial but it appeared to be a more constant across the segmented range with most frequencies decreasing by 5dB. This shows a more stable frequency testing range at levels higher than 250 MHz. The changes in signal strength also appeared to be more aggressive in the first two rows in each column and eased through the third to the fifth row.

Now that the more definable variations and patterns in the matrix have been defined the search for the most stable area for testing can be underway. To accomplish this, all the

plots were looked at and a 'by-eye' judgment was made for the approximation of the most stable group of nodes. It was made sure that enough nodes were included from the initial approximation as to get the best possible sample.

The area of nodes that were chosen were, (2,2),(2,3),(2,4),(3,2),(3,3),(3,4),(4,2),(4,3) and (4,4). Placing all of the recorded data into a mass spreadsheet for all the nodes, gave a numerical representation of the changes through frequency of each node. Using multiple spreadsheets to centre different nodes, the average variation over the whole frequency range to the adjacent nodes was calculated. These spreadsheets could not be included in this report as they were excessively large.

After numerous miscalculations, it was discovered that the node with the smallest average variation between itself and the adjacent nodes was 3dB. The node that possesses this value is (3,3). This suggests that DUTs should be placed on a test bench inside the chamber that is at least 600mm high and 200mm right of centre when facing the back wall. Giving this exact positioning for the placement of objects in the anechoic chamber is sometimes unreasonable to achieve, so going back to the spreadsheets and taking note of the next best average variations gives a general area of a suitable place to position a DUT. This is shown in the Figure 4.5 below.

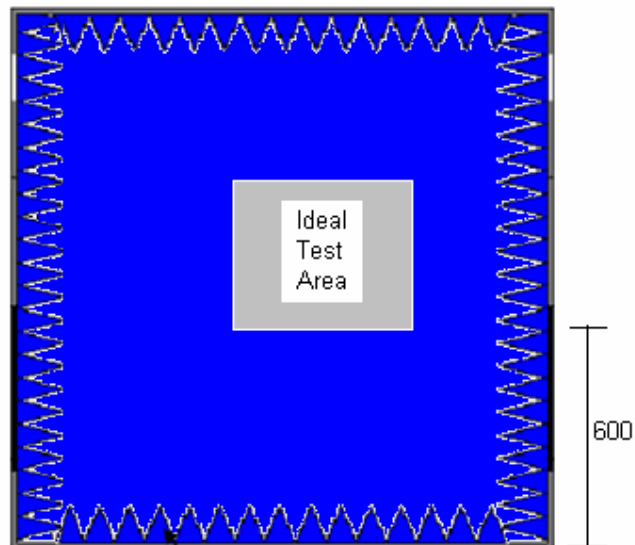


Figure 4.5 Ideal Test Area for Anechoic Chamber - 2D

Chapter 5

Ray Tracing Techniques

Ray tracing is a mathematical technique using vectors to theoretically trace rays of transmitted waves within a mathematically defined space, in this instance the anechoic chamber. The constructive and destructive components in a received signal can be discovered by drawing the paths that can be travelled by the transmitting antenna's signal and discovering the phase in which each non-direct ray will have and the reduced signal strength from being partially absorbed by the pyramidal absorbers. An example of how this can be graphically displayed is shown below in Figure 5.1.

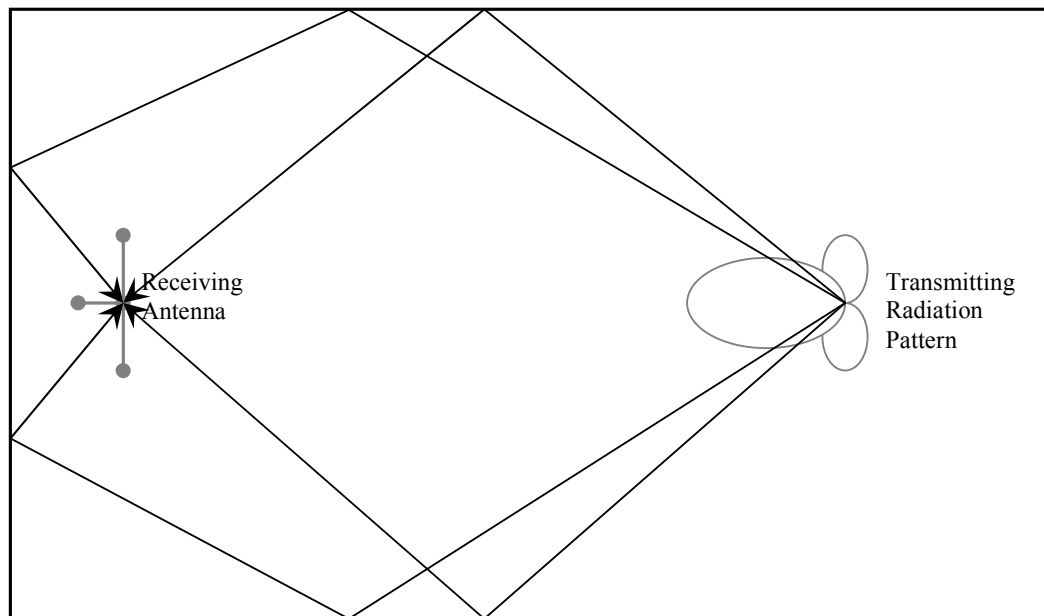
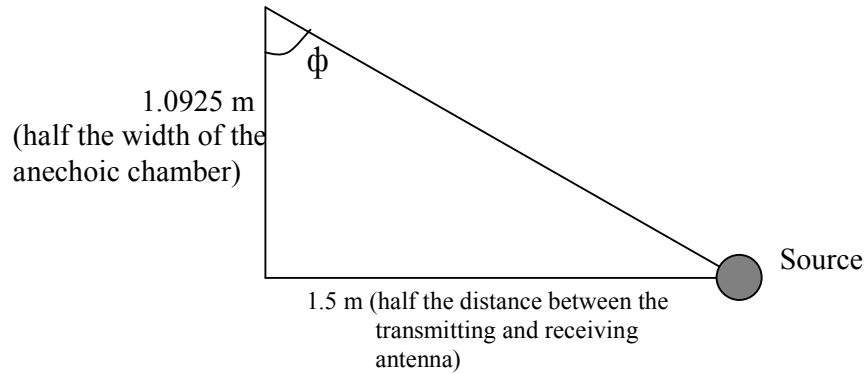


Figure 4.1 Graphical Representation of Ray Tracing inside Anechoic Chamber

This graphical representation shows only a select few of the possible paths in which the transmitting waves can take to reach the receiving antenna. However, from the

previously gathered data on the absorption levels of the pyramidal wall absorbers at different angles of incidence, the incidence rays will not achieve an angle on their first possible reflection of 33° where the transmitted ray will reach the receiving antenna after its first reflection. The calculation of this will now be stepped through.



$$\tan \phi = \frac{1.5}{1.0925}$$

$$\tan \phi = 1.373$$

$$\therefore \phi \approx 54^\circ$$

From this calculation it can be said that the minimum attenuation that a reflected signal will have will be approximately 15dB from Table 3.1. So it can be said that the signal strength from the reflected signal will not be strong, however, the phase differences of multiple reflected signals could still accumulate to give an unacceptable result.

Full understanding was not achieved in the method of ray tracing techniques as there were no sufficient sources of information than could be found to support earlier efforts. Even though several attempts were made, the end results did not show any relevance to the raw data received from the spectrum analyser so it was decided not to be included.

Chapter 6

Conclusion

The performance of the anechoic chamber was discovered to be quite effective and adhere to the published results of other test and manufacturer's specifications. However the presence of a large number of resonant frequencies very close together on the frequency scale, suggests that this certain area could be looked in to further. The mid-range of frequencies however can now be used when testing within the anechoic chamber with confidence in knowing the amount of interference that can escape from the chamber is minimal.

Since the overall performance of the anechoic chamber is known, breaking the chamber's components down for individual analysis was the next logical step. The pyramidal absorbers were tested and they were found to vary in a constant trend as the angles of incidence increased, so did the absorption. This trend was consistent with other references' tests as well which made these results relevant to the overall performance. This gives confidence to use actual site-specific data when attempting to further test the chamber as well as rate the chamber as a whole compared to commercially available ones.

Once the pyramidal absorbers were finalised, the results could be combined with the next series of tests which sought to discover patterns and behaviour of a two dimensional plane across the anechoic chambers free space. With the numerous tests performed and patterns noted, ray tracing techniques combined with the reflective performance of the pyramidal absorbers could of been used to discover the reasons for such a pattern if time permitted.

The big picture is characterising the Faculty of Engineering and Surveying's anechoic chamber located on level 2 needs to be looked at. With this in mind further work can now be suggested as to better the studies made and acquire different characteristics of the anechoic chamber that as not yet been discussed. The obvious one that would first of all come to hand would be to additionally study the theoretical process of ray tracing techniques and further explain the patterns present in the fields inside the chamber. When a full understanding is achieved of the environment inside the chamber, testing surfaces can be positioned as to optimise performance without acquiring too much interfering reflected waves etc.

Different arrangements of the pyramidal absorbers and ferrite tiles can be looked at as to optimise the best chamber characteristics for the desired range of frequencies being used. The different arrangements are defined by the thicknesses of the backing in which the ferrite tiles and pyramidal absorbers lay.

From the 2D planar testing, it is recommended that the door gaskets be looked at in the idea of reducing the possible full reflection of transmitted wave onto the DUT as they proved to be sufficient in preventing the passage of transmission through the door seals. A different way of travelling the coaxial cables from transmitters and receivers could be looked at also as to eliminate the possibility of the interfering with the reception of data, although this would prove difficult.

The anechoic chamber made and maintained by the University of Southern Queensland proves itself to be a very useful and adequate form of EMC and other testing as there is no known need for testing if equipment for complying with commercial standards. With further testing, this chamber could be assessed against the standards layout out for anechoic chambers and then could be commissioned as a justifiable chamber which would be of credit to the staff at the University who where involved in constructing it.

References

- Altman, Z, Fourestie, B & Kanda, M 1999, *Anechoic Chamber Evaluation Using the Matrix Pencil Method*, IEEE Press
- American National Standard Institute (ANSI), C63.4-2000: *Standard for Methods of Measurement of Radio Noise Emissions from Low-Voltage Electrical and Electronic Equipment in the Range of 9kHz to 40GHz*
- Anzai, H, Mizumoto, T, Naito, Y & Yamazaki, T 1996, *Criteria for Absorber's Reflectivity Lined in Semi-Anechoic Chambers Using Ray-Tracing Technique*, Tokyo Institute of Technology, Japan
- Connelly, M 2004, 'Wire Antennas', *Electrically-Short Dipole Antennas*, viewed 16 April 2006, < <http://www.hard-core-dx.com/nordicdx/antenna/wire/shortdipole.html>>
- Devor Jr., CL & German, RF 1999, *Comparison of Method to Evaluate Semi-Anechoic Chamber Performance*, Lehman Chambers
- EMCO 2005, *Antenna Catalogue – Essential Equipment for EMC Testing*, viewed 15 April 2006, < www.ets-lindgren.com >
- Fair-Rite Products Corp. 2005, *Ferrite Tile Absorbers for EMC Test Chamber Applications*, NY
- Hemming, LH 2002, *Electromagnetic Anechoic Chambers – A Fundamental Design and Specification Guide*, IEEE Press, NJ
- Hemming, LH 1991, *Architectural Electromagnetic Shielding Handbook – A Design and Specification Guide*, IEEE Press, NJ

- International Electrotechnical Commission (IEC) 2003, *Radio interference measurements and statistical methods: New CISPR 16 standards*, viewed 16 April, < <http://standards.org.sg/files/Vol11No1Art4.htm> >
- Johnk, RT, Medley, HW & Ondrejka 1998, *Low-Frequency RF Absorber Performance within SITU and Moveable Sample Techniques*, National Institute of Standards and Technology, USA
- Ko, CJ, Wu, BC & Yang, CF 1998, *A Ray-Tracing Method for Modelling Indoor Propagation and Penetration*, IEEE Press
- Morgan, D 1994, *A Handbook for EMC Testing and Measurement*, Peter Peregrinus Ltd. On behalf of the Institution of Electrical Engineers, Stevenage, UK
- Rohde & Schwarz 2006, Rohde & Schwarz, viewed 16 April 2006, < <http://www.rohde-schwarz.com/>>
- Summers, J & Smith, B 2004, *Communication Skills Handbook: How to Succeed in Written and Oral Communication*, John Wiley & Sons, Milton, QLD.
- Stutzman, WL, Thiele, GA 1998, *Antenna Theory and Design*, Second Edition, John Wiley & Sons, Inc.
- Technical Data Sheet, *Broadband Pyramidal Absorbers*, Advanced ElectroMagnetics Inc., viewed 16 April 2006, < <http://www.ce-mag.com/> >
- Technical Data Sheet, *Microwave Absorbers*, Rantec 2005, viewed 16 April 2006, <<http://www.rantecmdm.com/> >
- Technical Data Sheet, *Pyramidal Absorber*, Cumming Microwave, viewed 16 April 2006, < http://www.cummingmw.com/micro_rf_pc_310.html >
- Technical Data Sheet, *RF Absorbers – Technical Data for AEP Series*, AEMI 2005, viewed 16 April 2006, < <http://www.aemi-inc.com/>>

Technical Data Sheet, Fair-Rite Corporation, viewed 16 April 2006,
< http://www.fair-rite.com/newfair/pdf/15th_Edition_Fair-Rite_Catalog.pdf#page=1 >

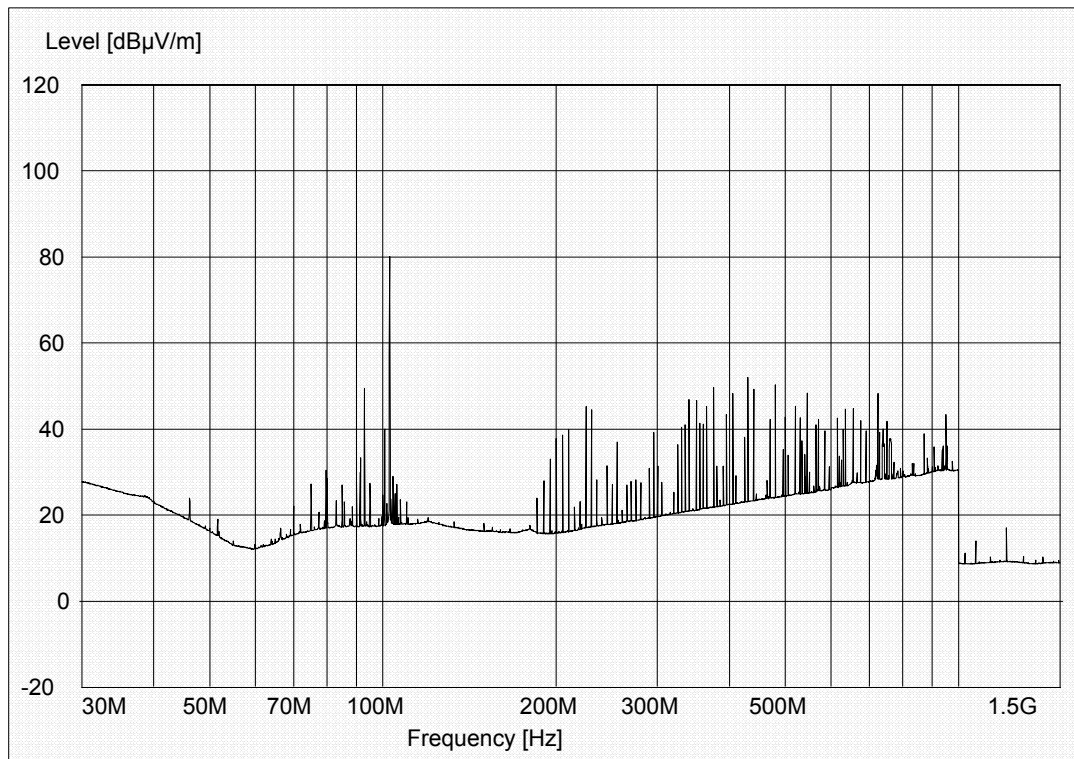
White, D 1999, *The EMC, Telecom, and Computer Encyclopaedia Handbook*, Third Edition, Emi-Rfi Control

White, DRJ 1986, *Shielding Design – Methodology and Design*, Interference Control Technologies, Virginia

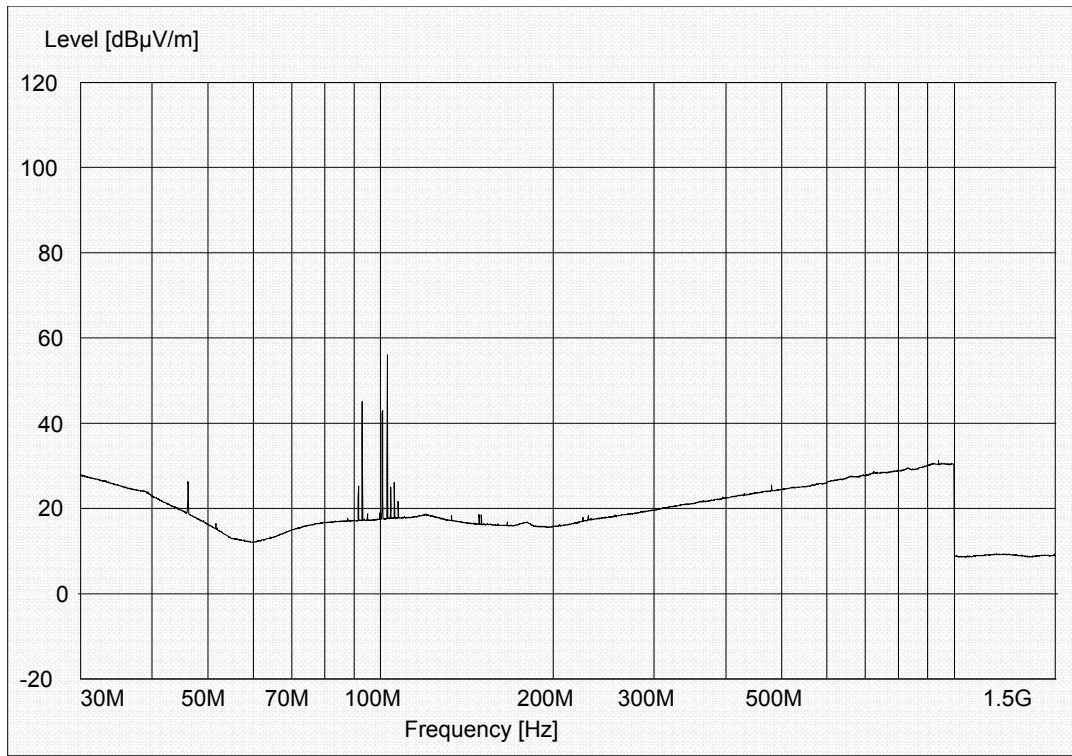
Appendix B

Spectrum Analyser Outputs

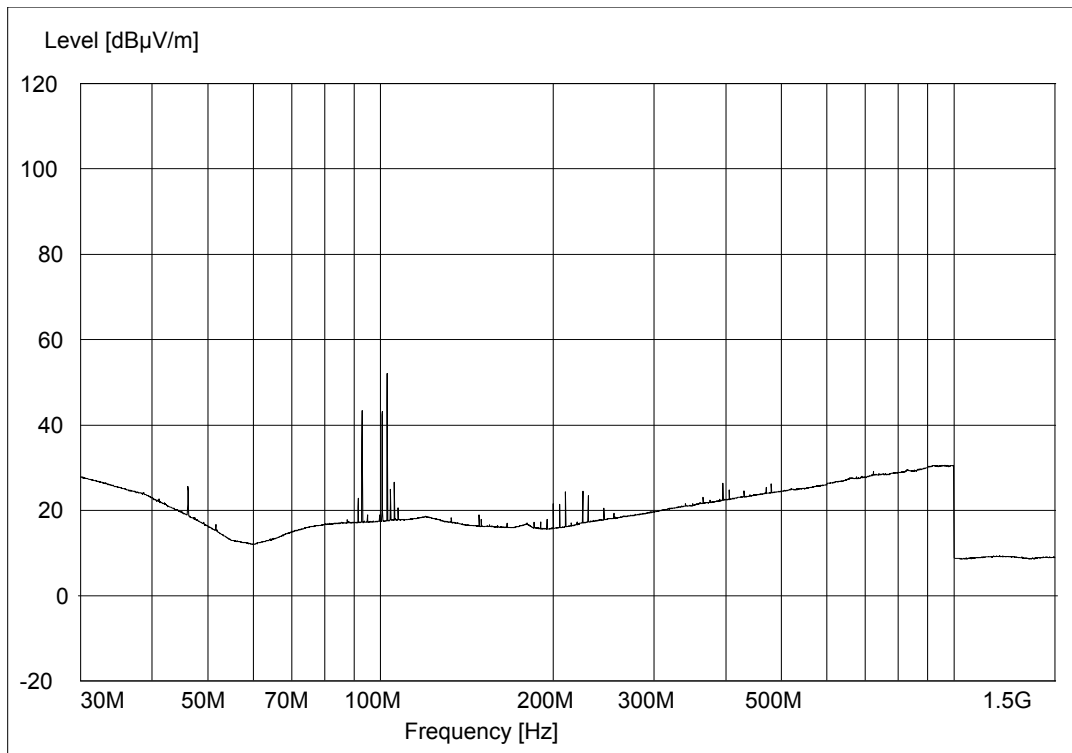
B.1 Anechoic Chamber Attenuation



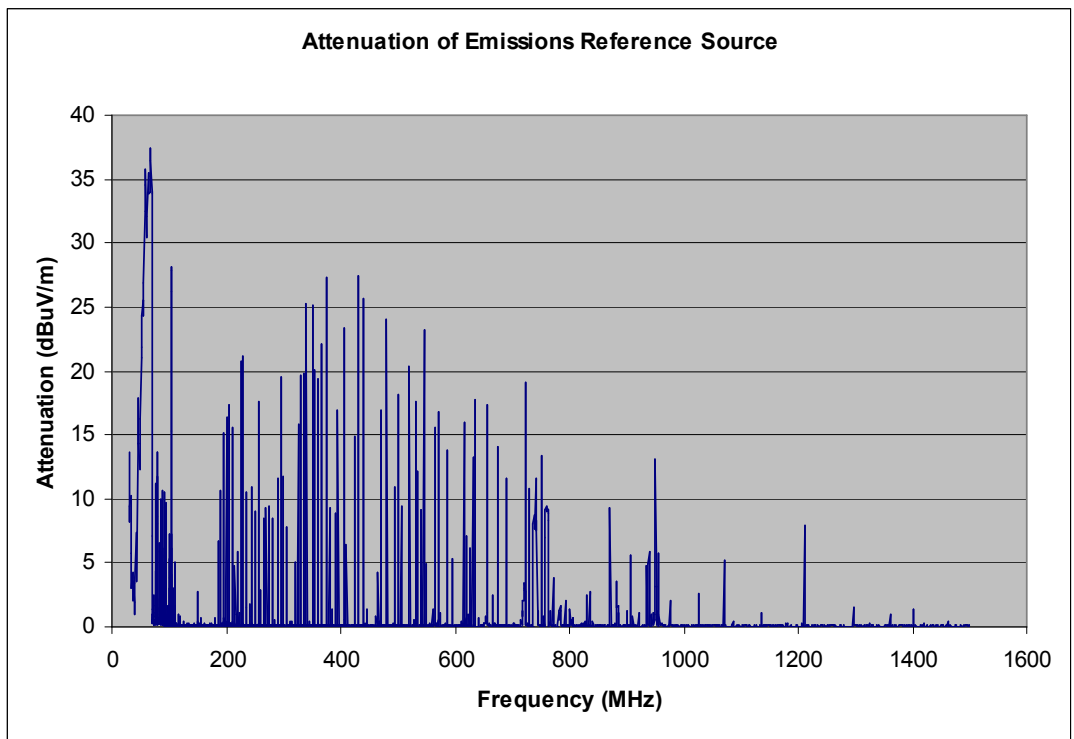
Output of Spectrum Analyser – Door Open



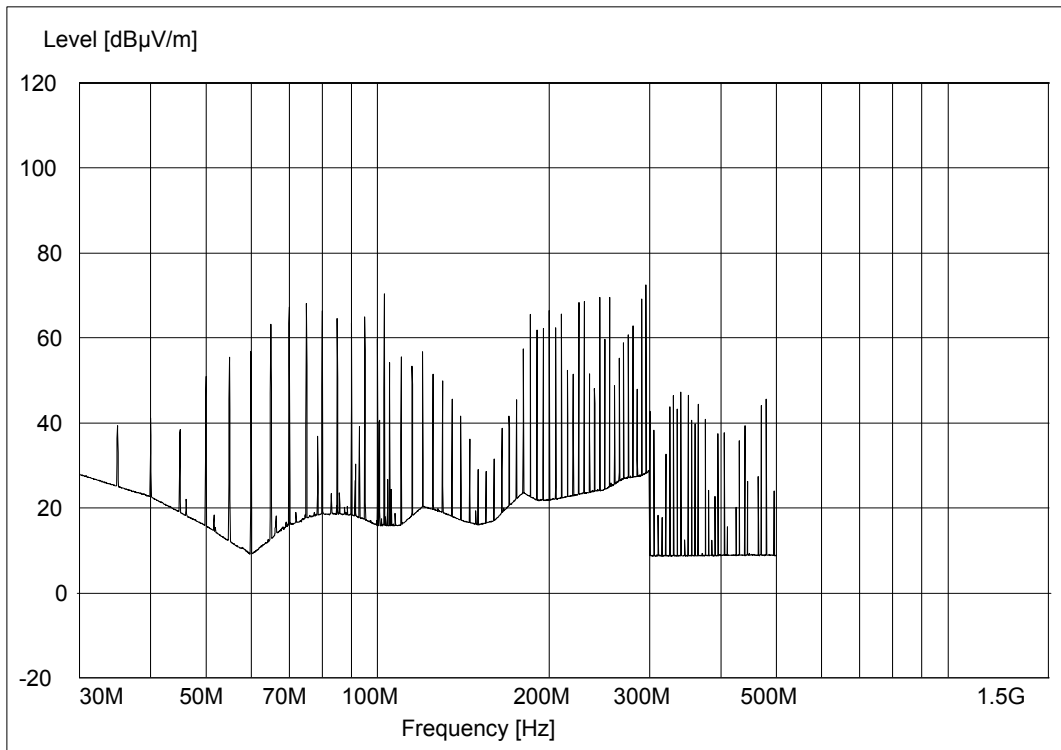
Output of Spectrum Analyser – Door Closed (500 mm)



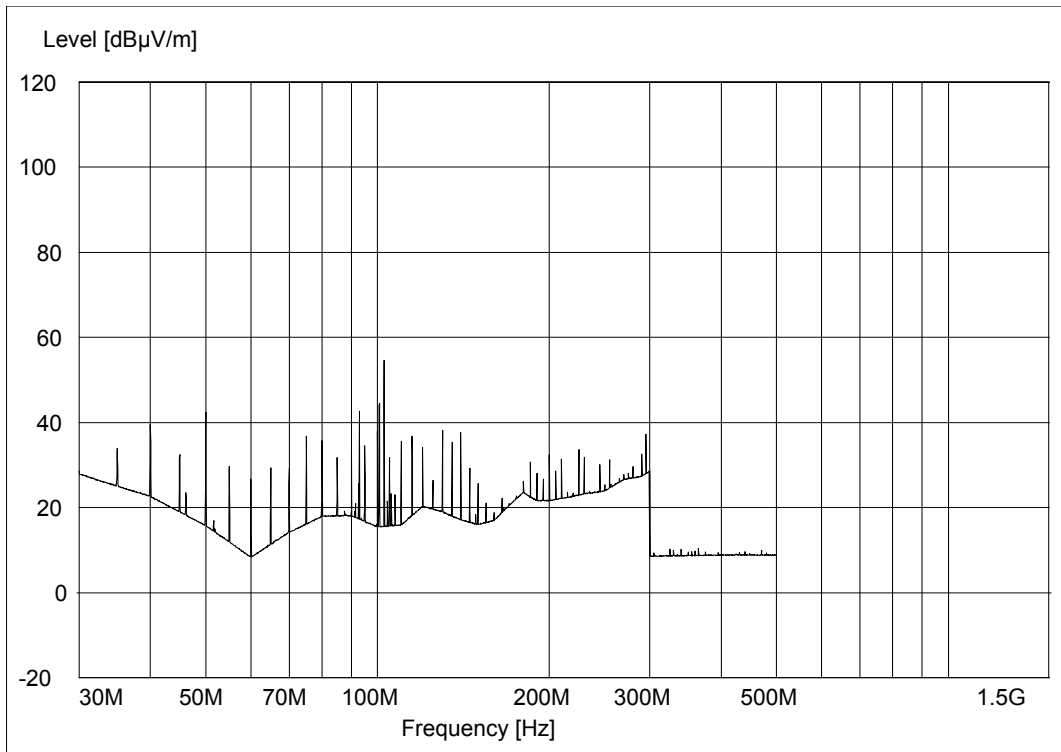
Output of Spectrum Analyser – Door Closed (120 mm)



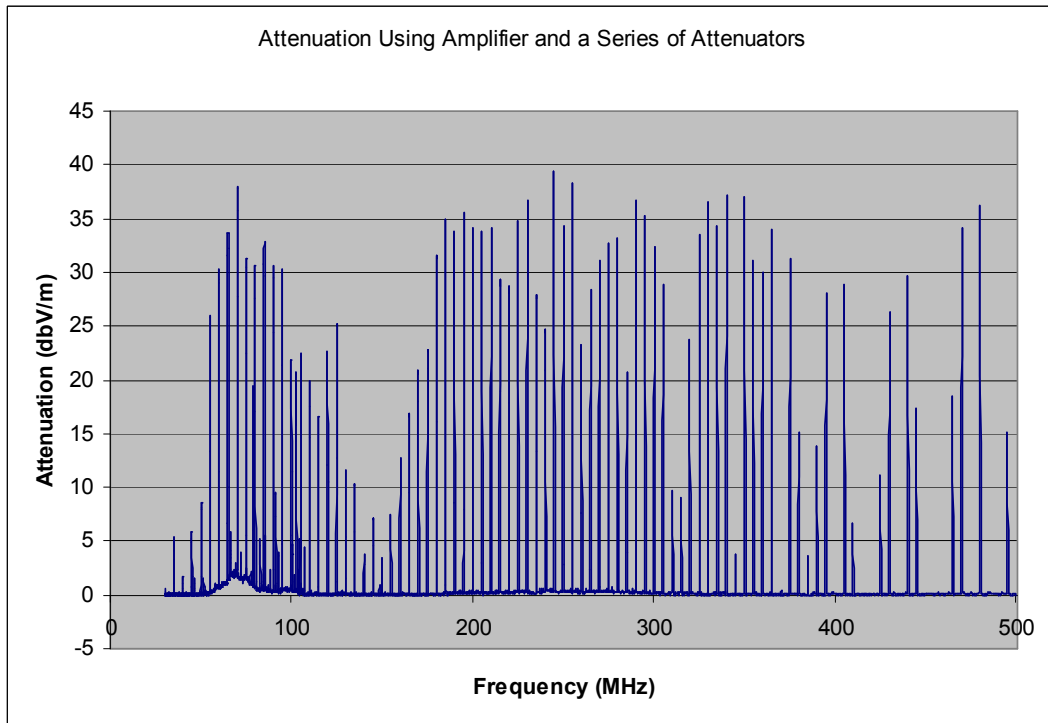
Attenuation of Anechoic Chamber



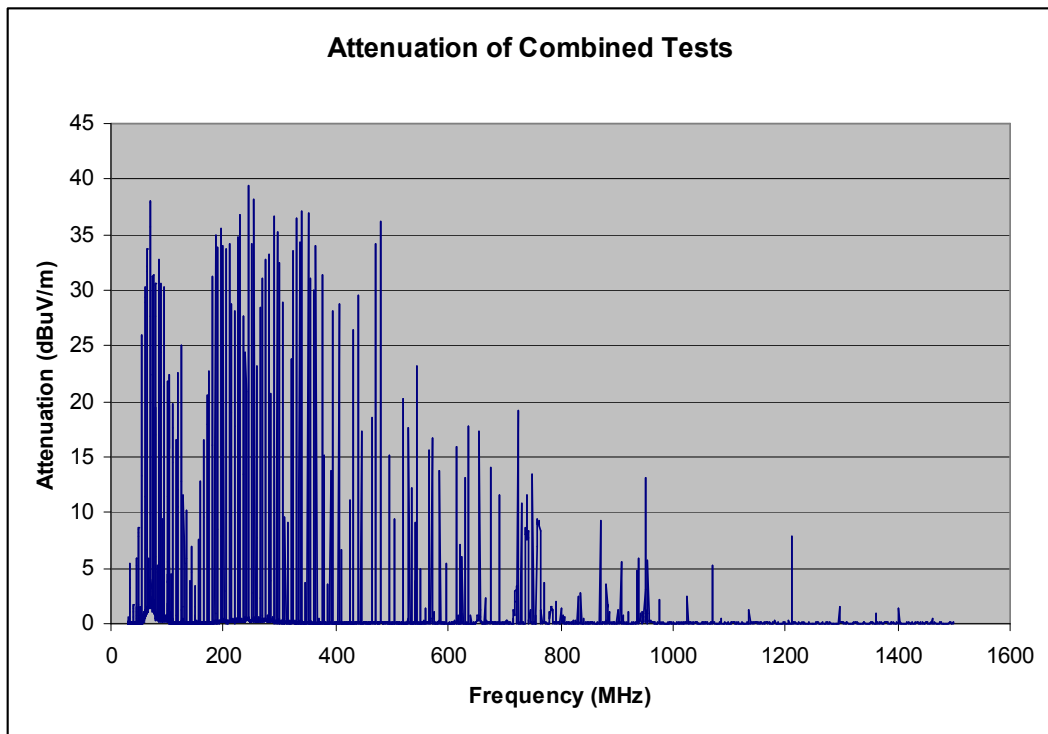
Output of Spectrum Analyser – Door Opened (Amplified)



Output of Spectrum Analyser – Door Closed (Amplified)

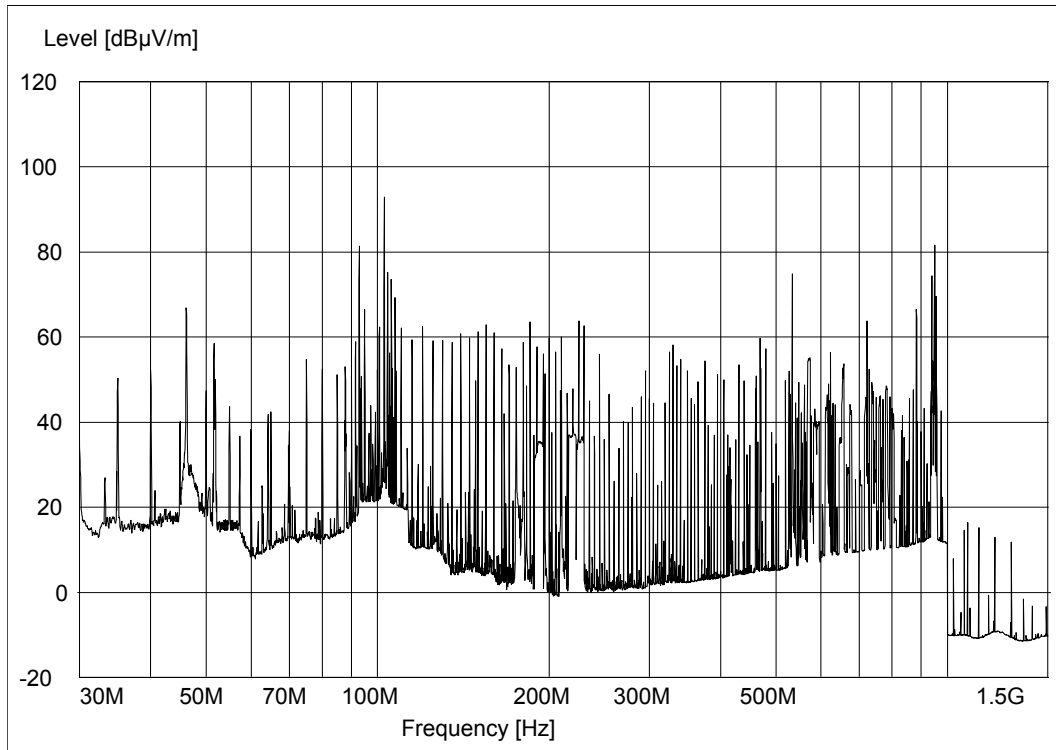


Attenuation of Amplified Emissions Reference Source

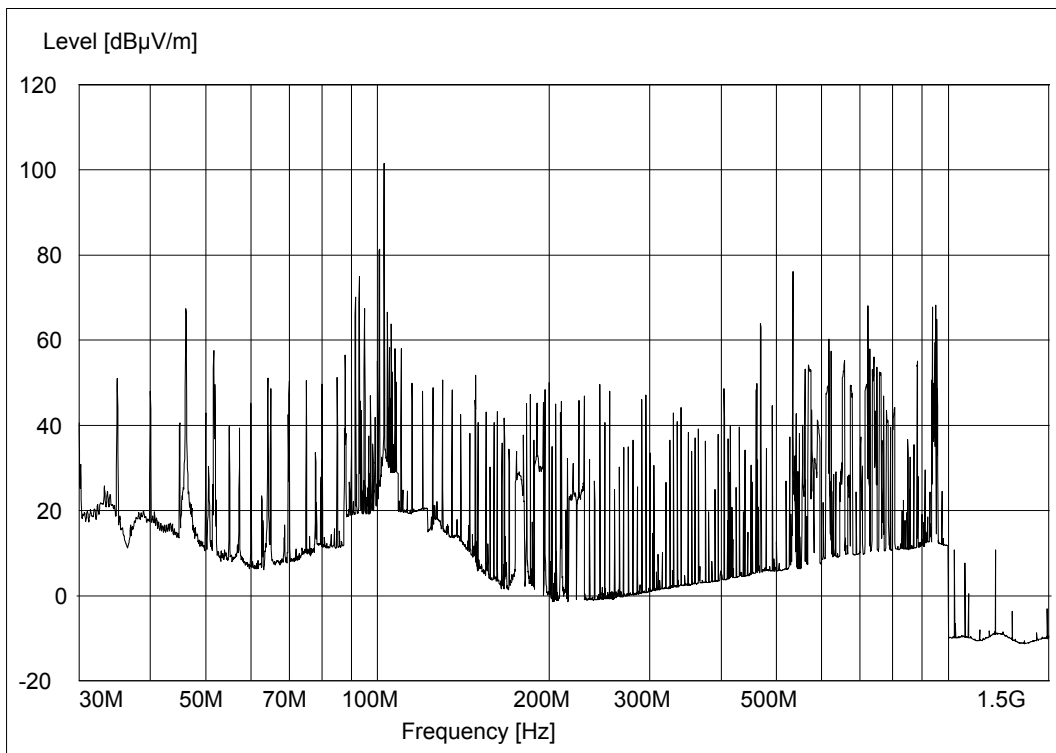


Attenuation of Anechoic Chamber from Combined Results

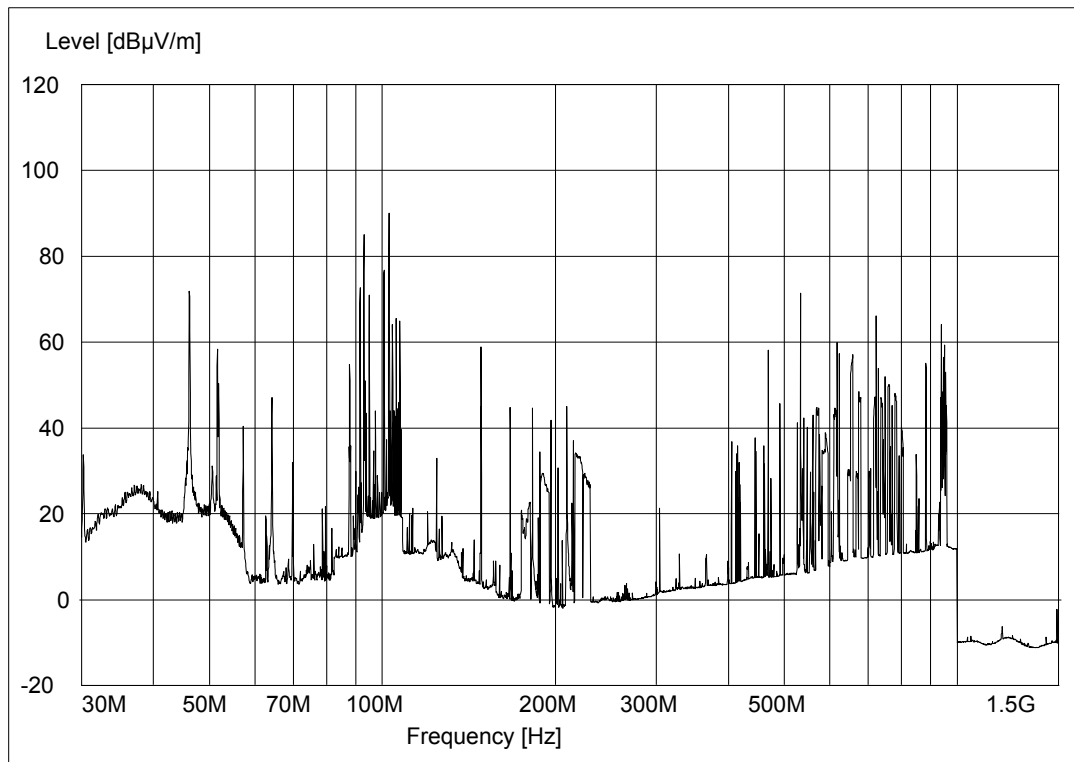
B.2 Pyramidal Absorber Performance



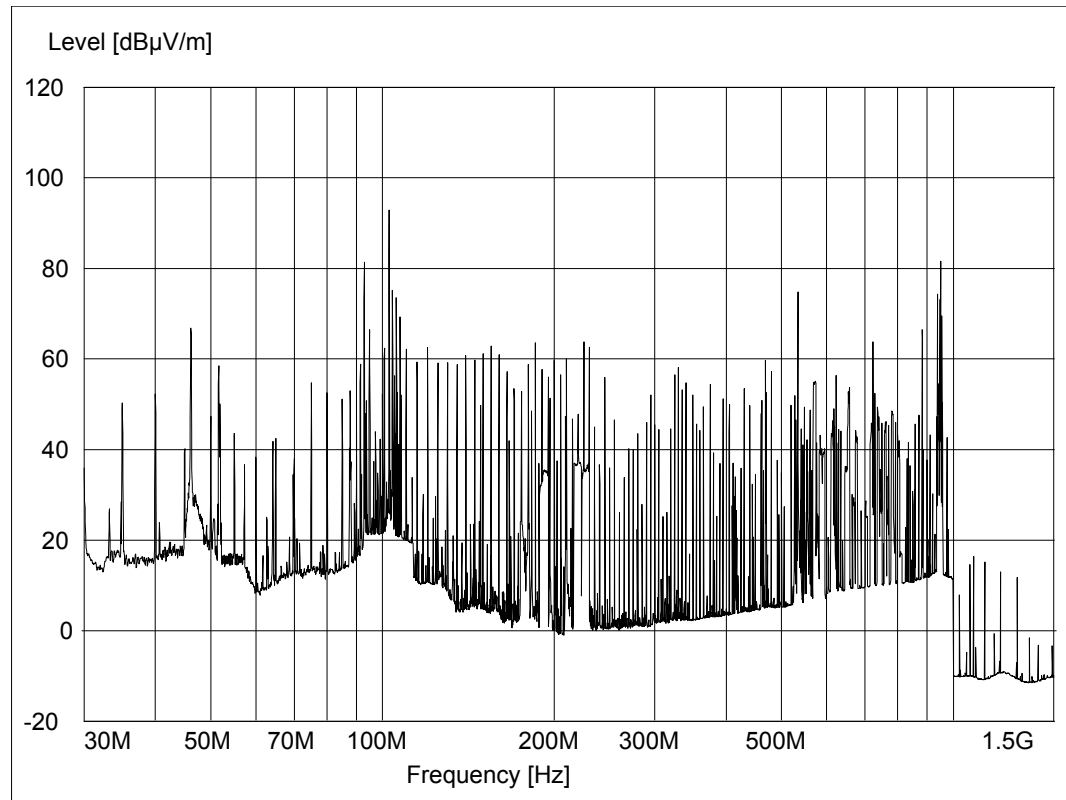
Spectrum Analyser Output – Angle Incidence of 15°



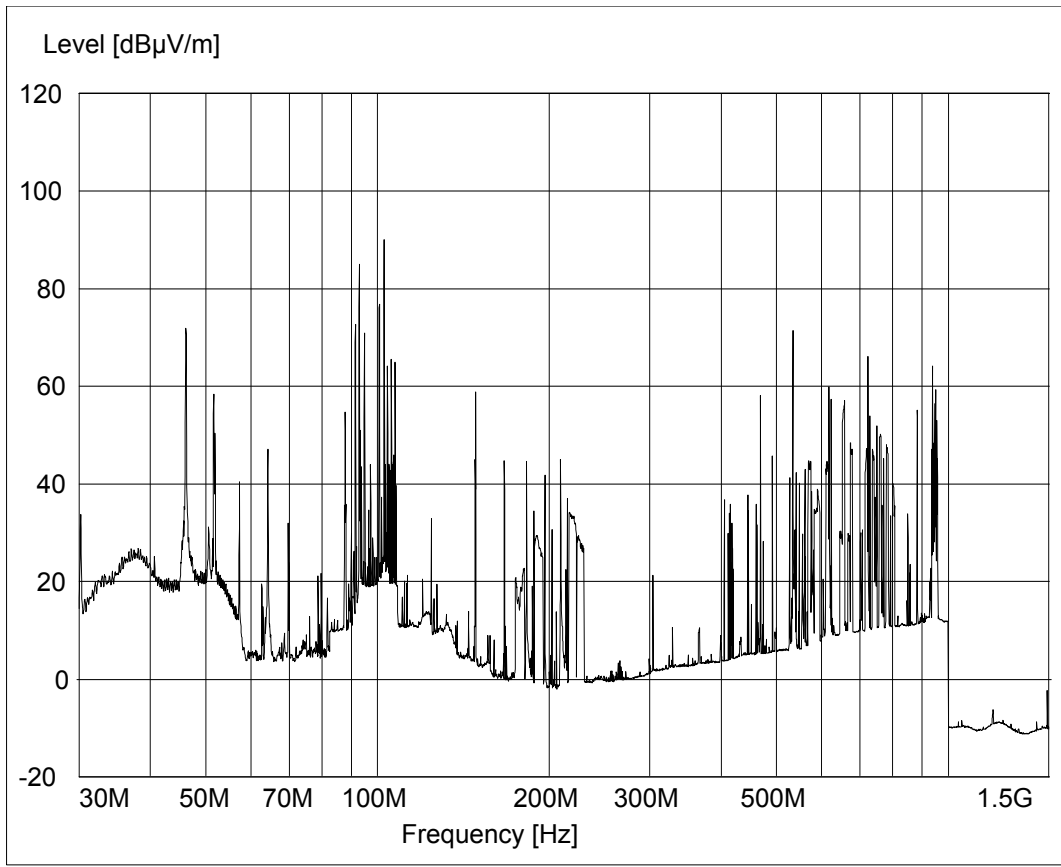
Spectrum Analyser Output – Angle Incidence of 45°



Spectrum Analyser Output – Angle Incidence of 75°



Spectrum Analyser Output – Emissions Reference Source (Direct)



Spectrum Analyser Output – Reflective Barrier

B.3 2-D Field Performance

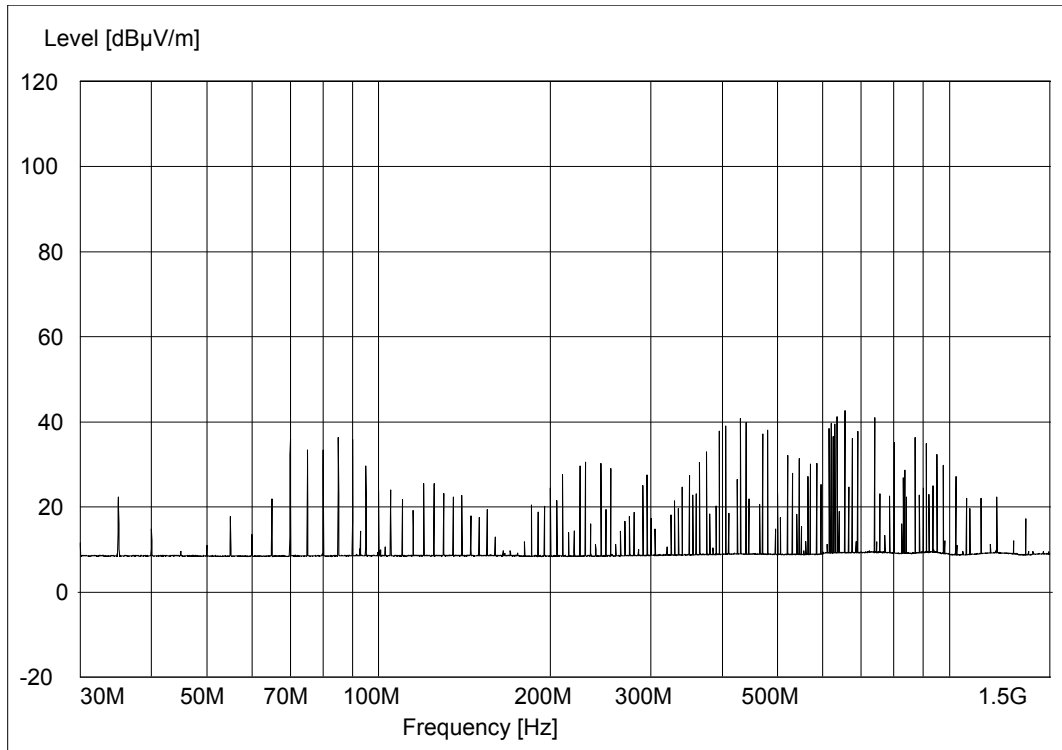


Figure 4.3 2D Planar Output – Node (0,0)

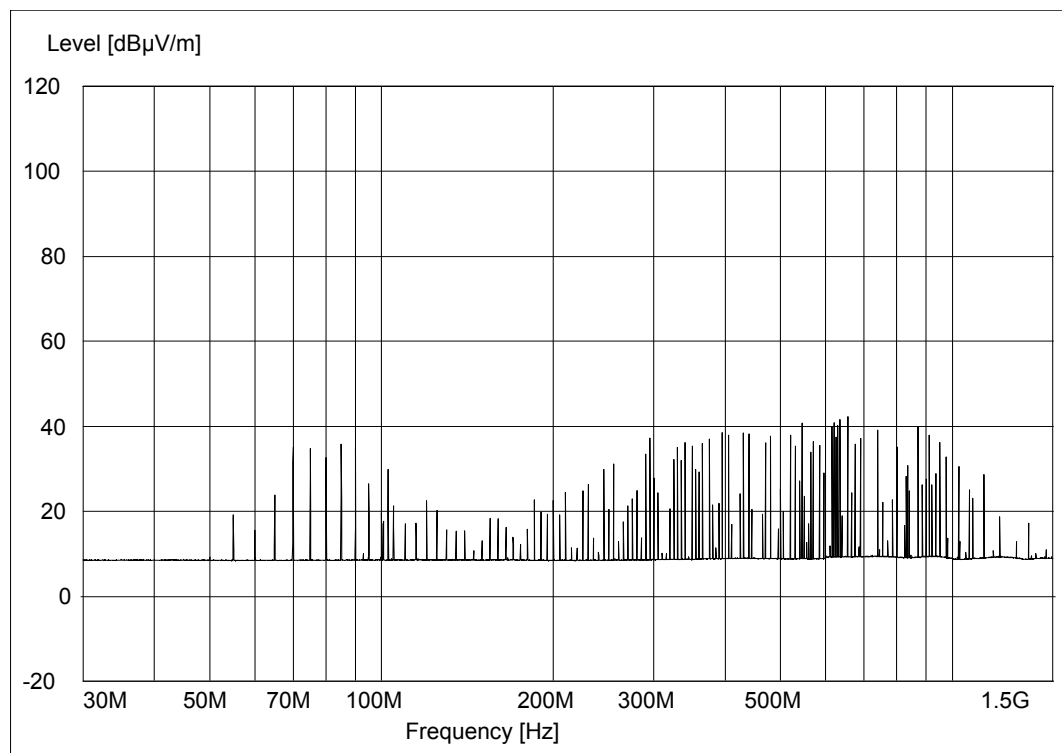


Figure 4.3 2D Planar Output – Node (0,1)

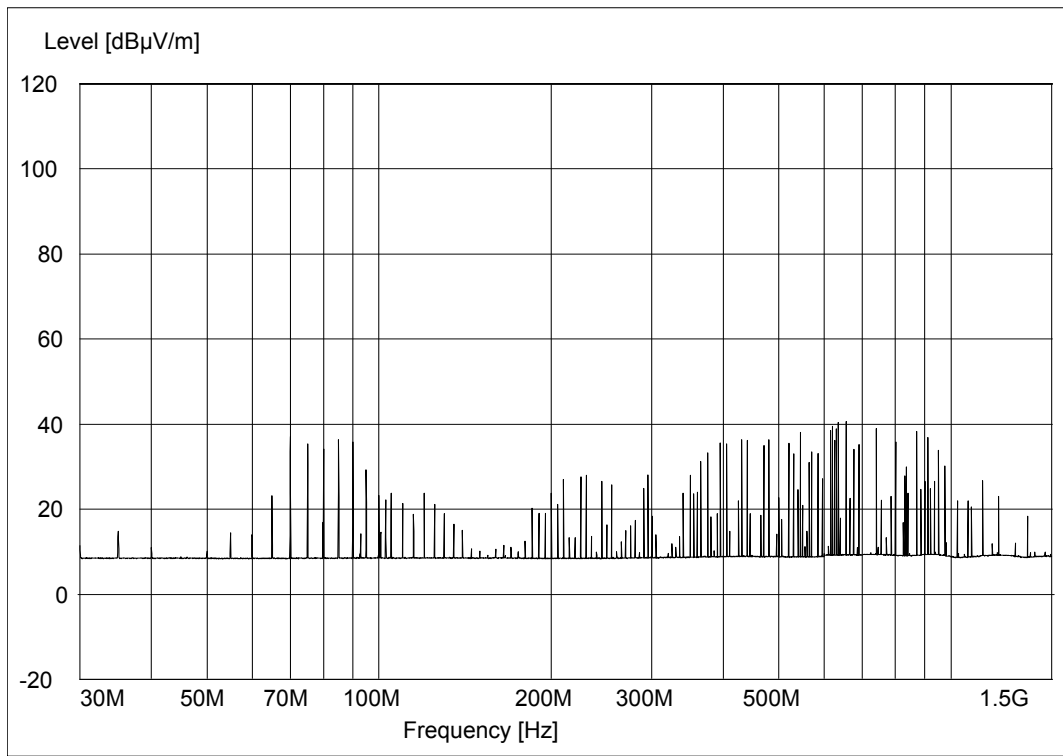


Figure 4.3 2D Planar Output – Node (0,2)

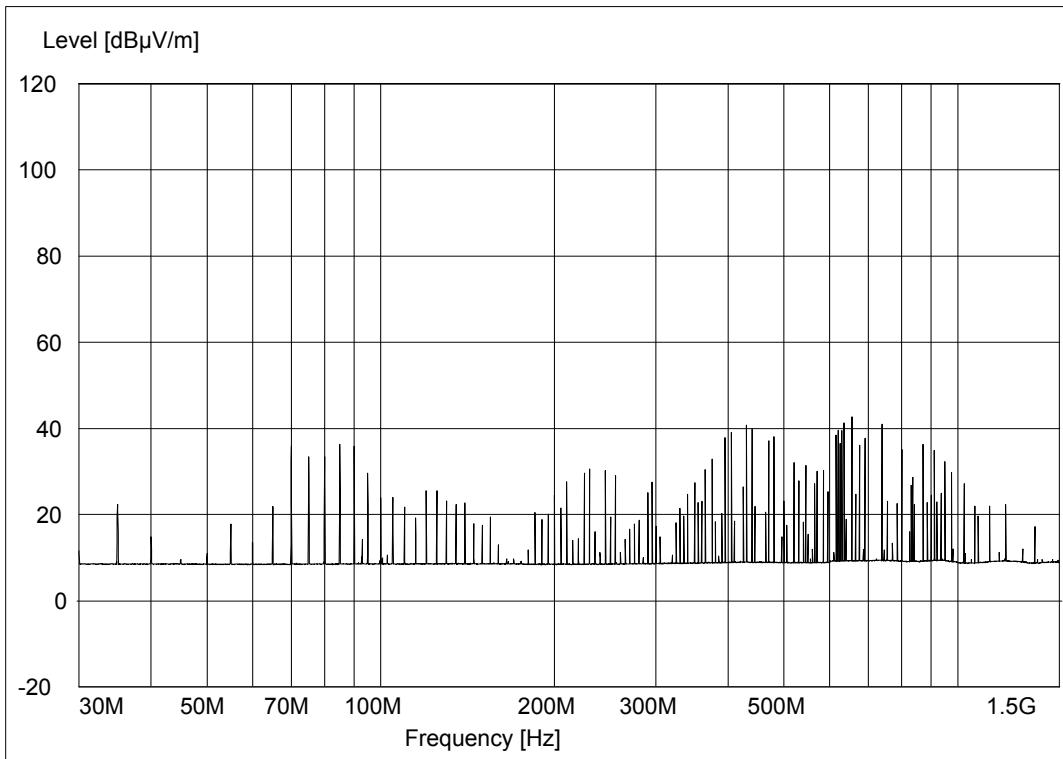


Figure 4.3 2D Planar Output – Node (0,3)

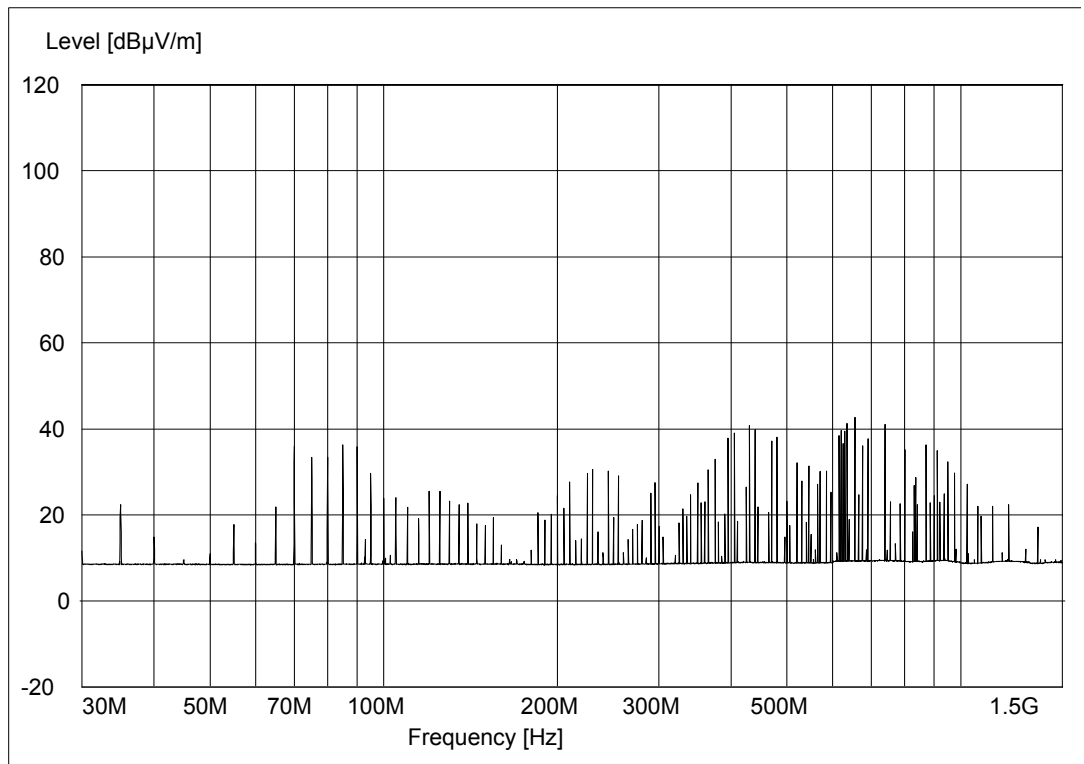


Figure 4.3 2D Planar Output – Node (0,4)

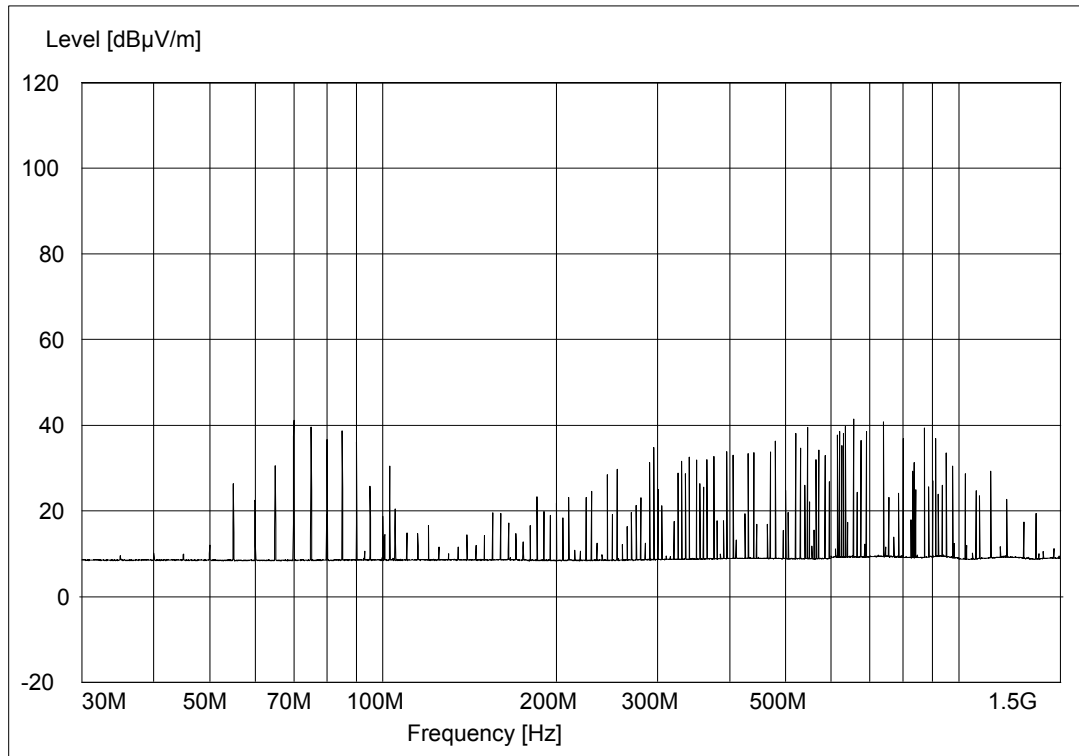


Figure 4.3 2D Planar Output – Node (1,0)

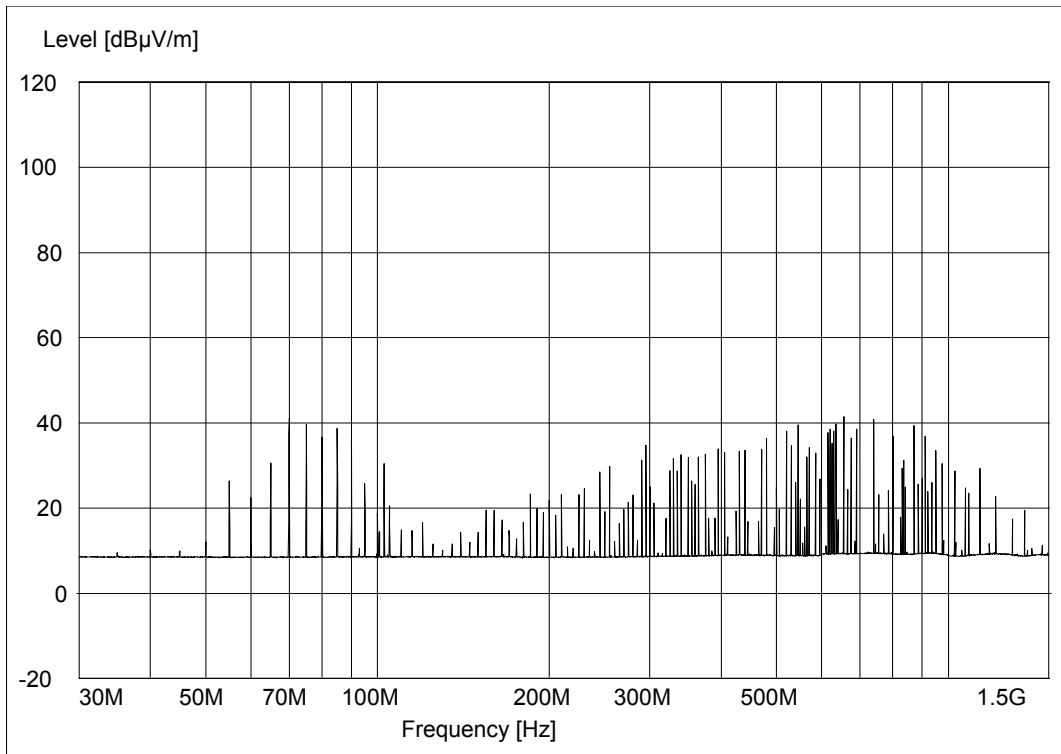


Figure 4.3 2D Planar Output – Node (1,1)

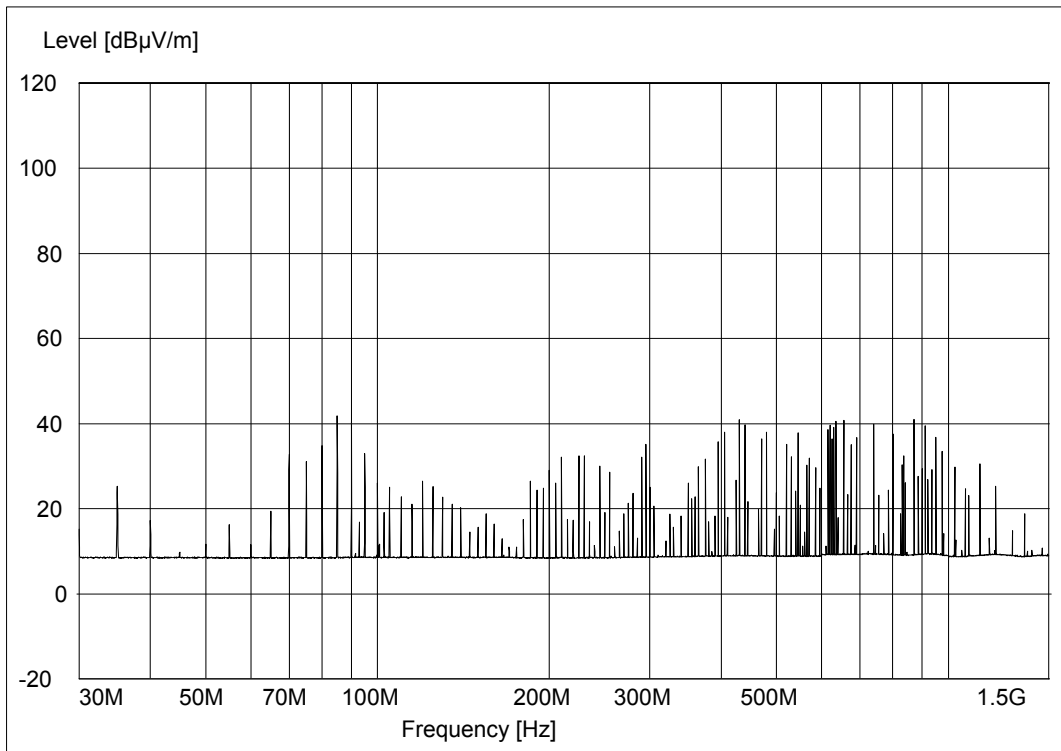


Figure 4.3 2D Planar Output – Node (1,2)

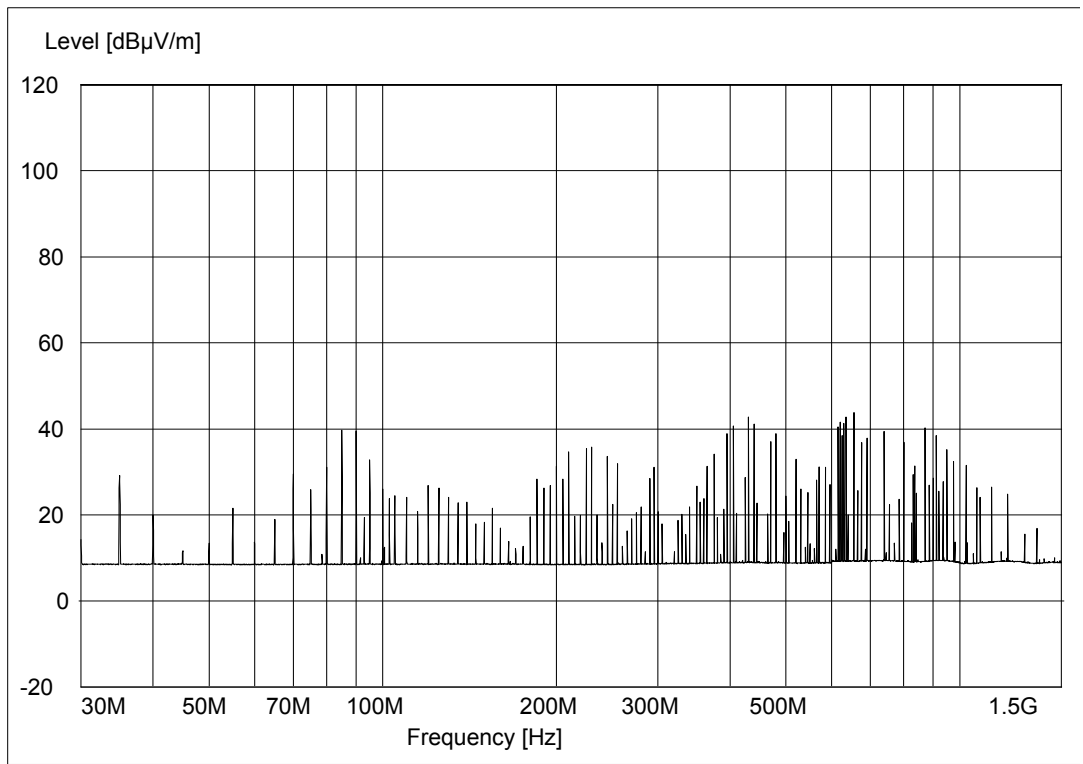


Figure 4.3 2D Planar Output – Node (1,3)

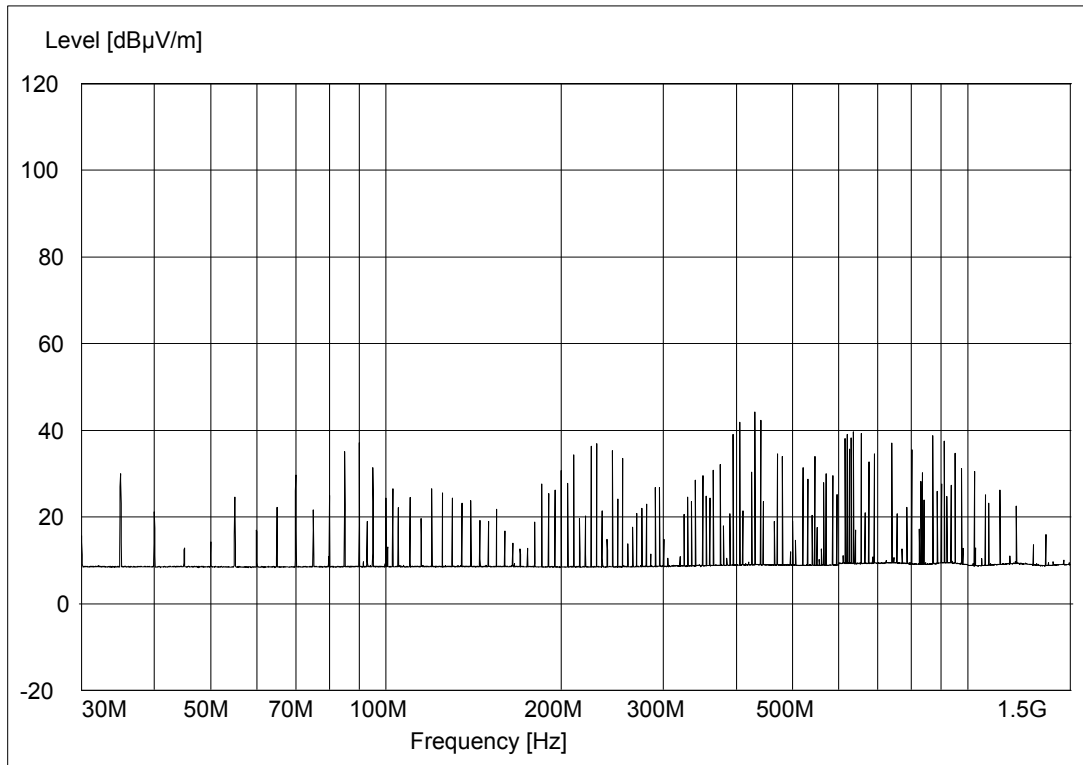


Figure 4.3 2D Planar Output – Node (1,4)

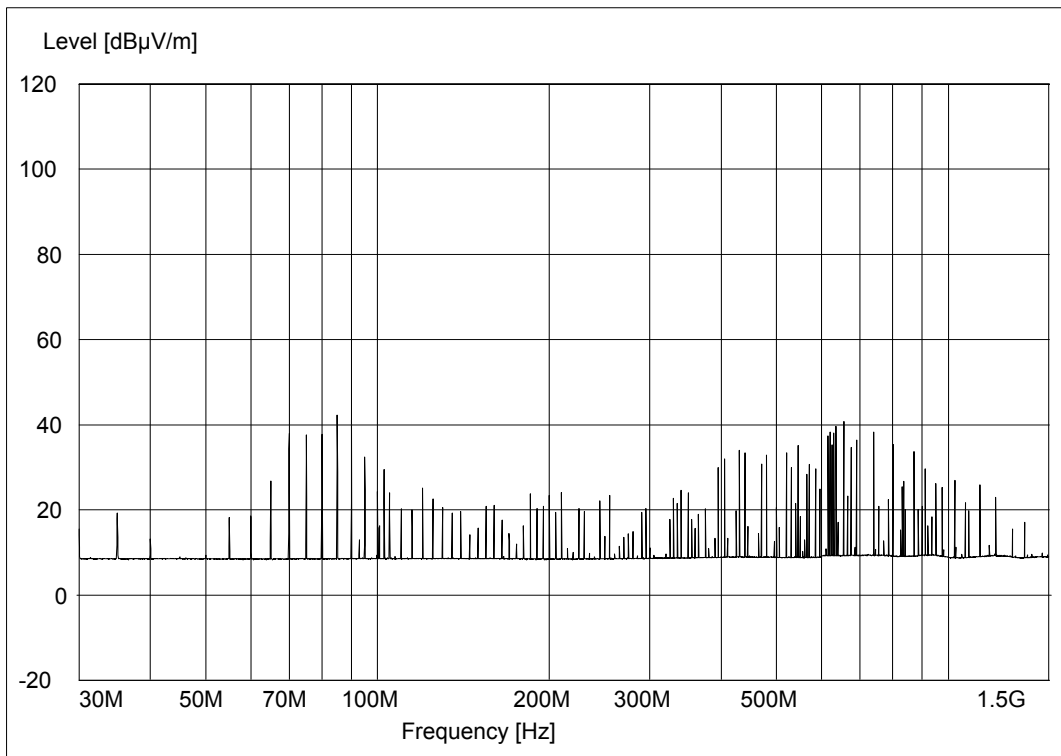


Figure 4.3 2D Planar Output – Node (2,0)

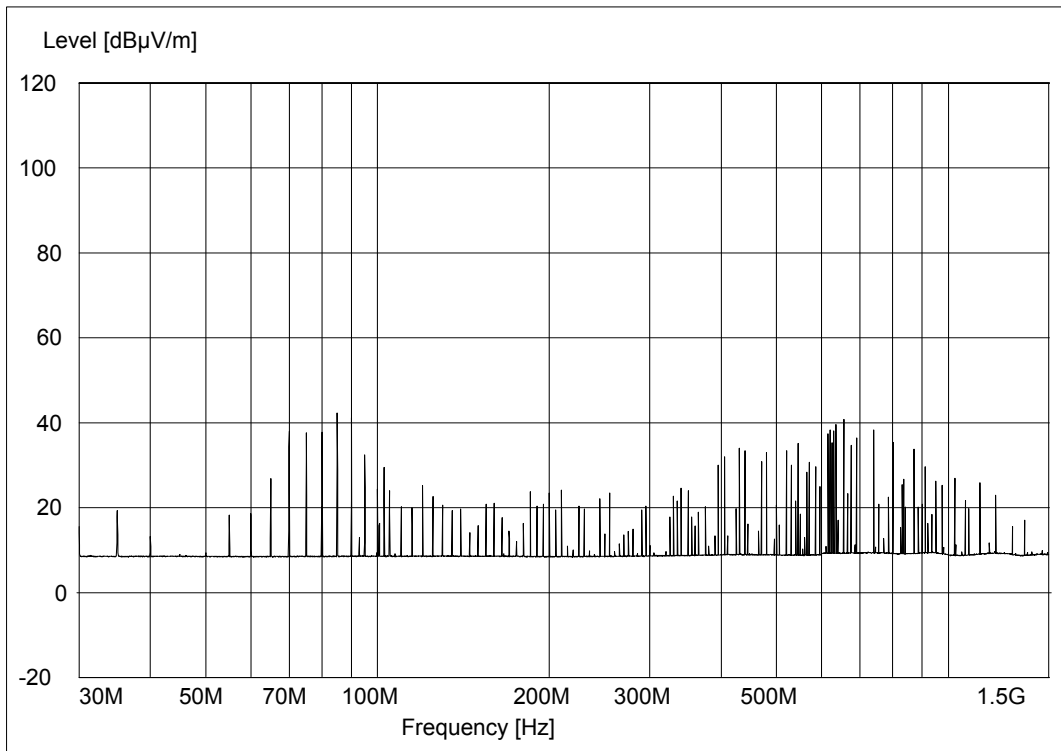


Figure 4.3 2D Planar Output – Node (2,1)

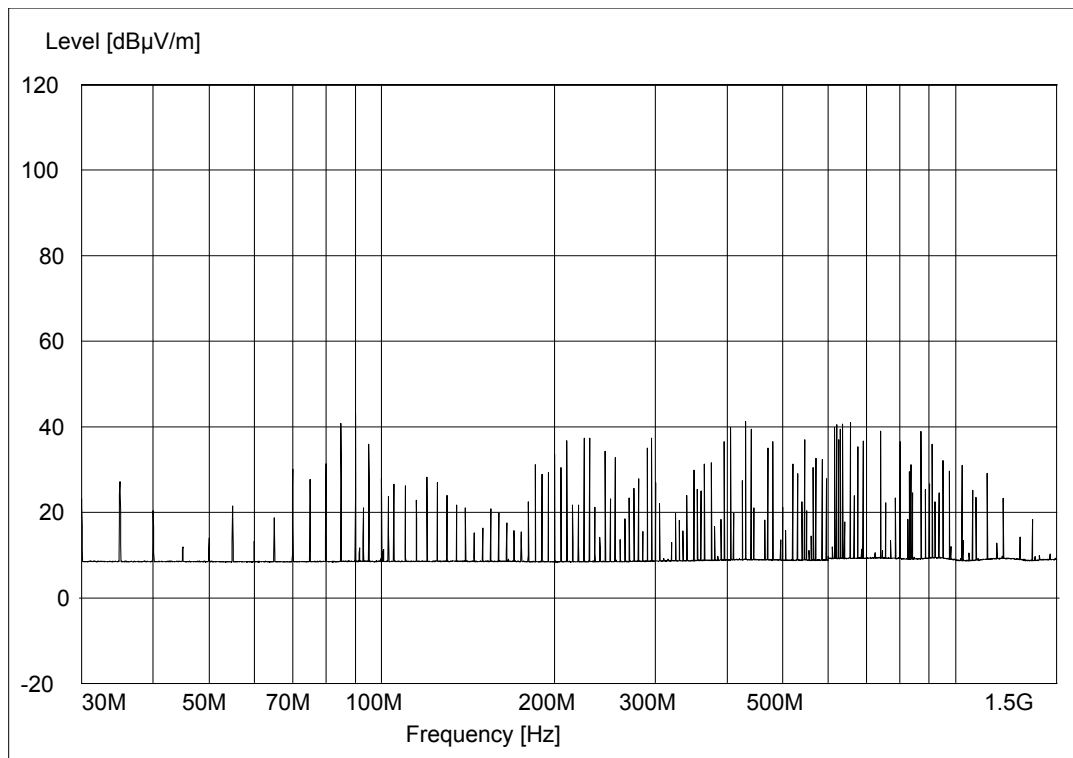


Figure 4.3 2D Planar Output – Node (2,2)

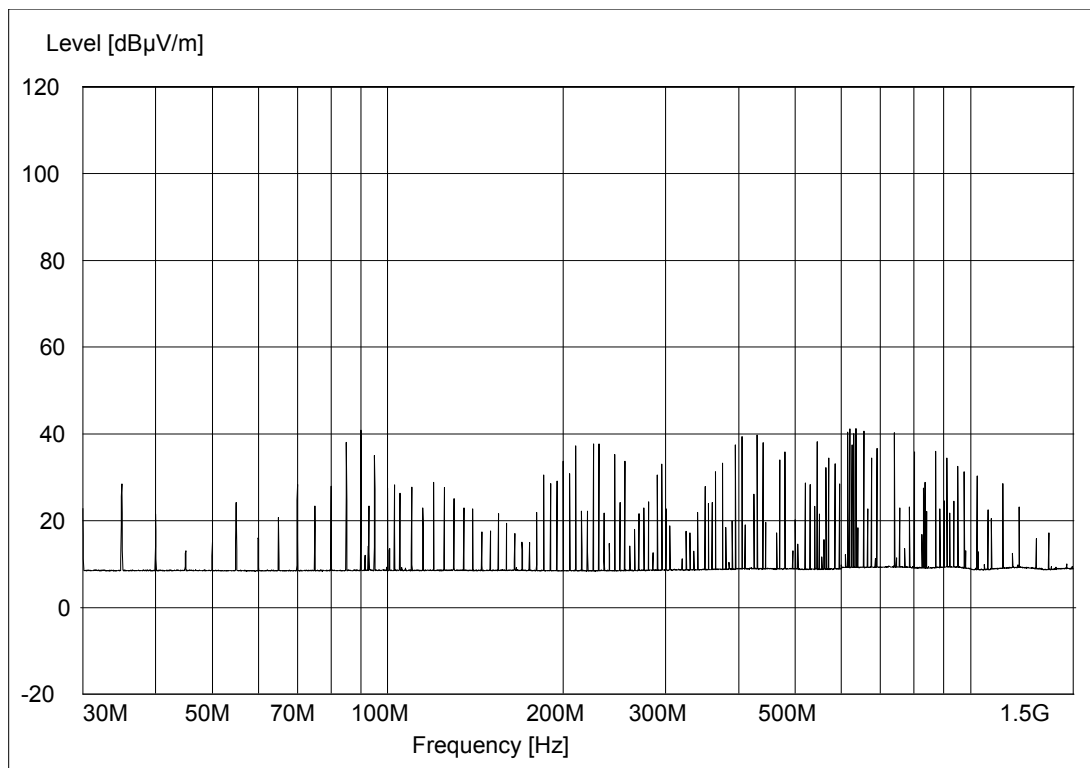


Figure 4.3 2D Planar Output – Node (2,3)

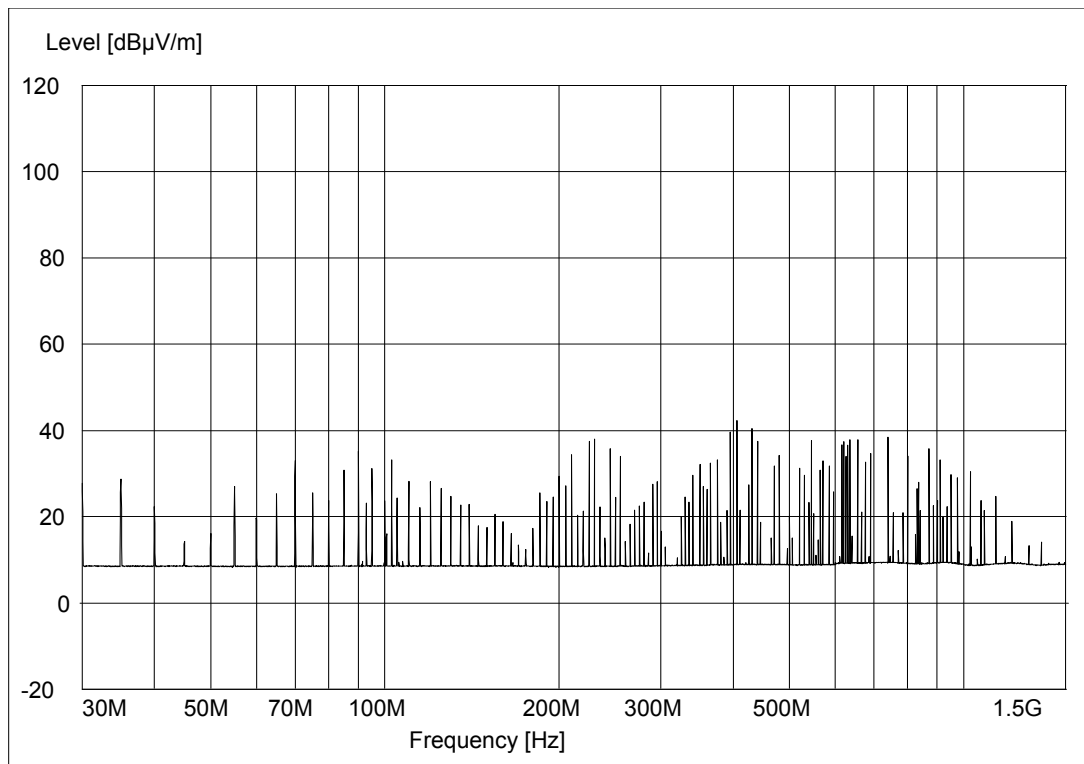


Figure 4.3 2D Planar Output – Node (2,4)

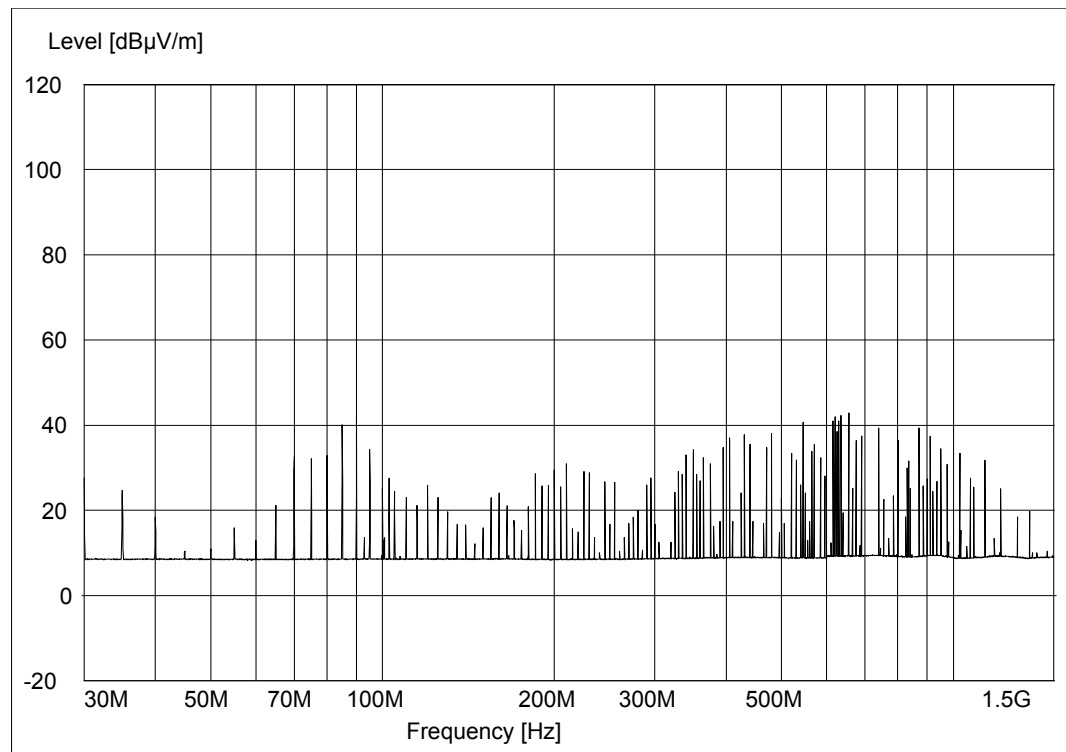


Figure 4.3 2D Planar Output – Node (3,0)

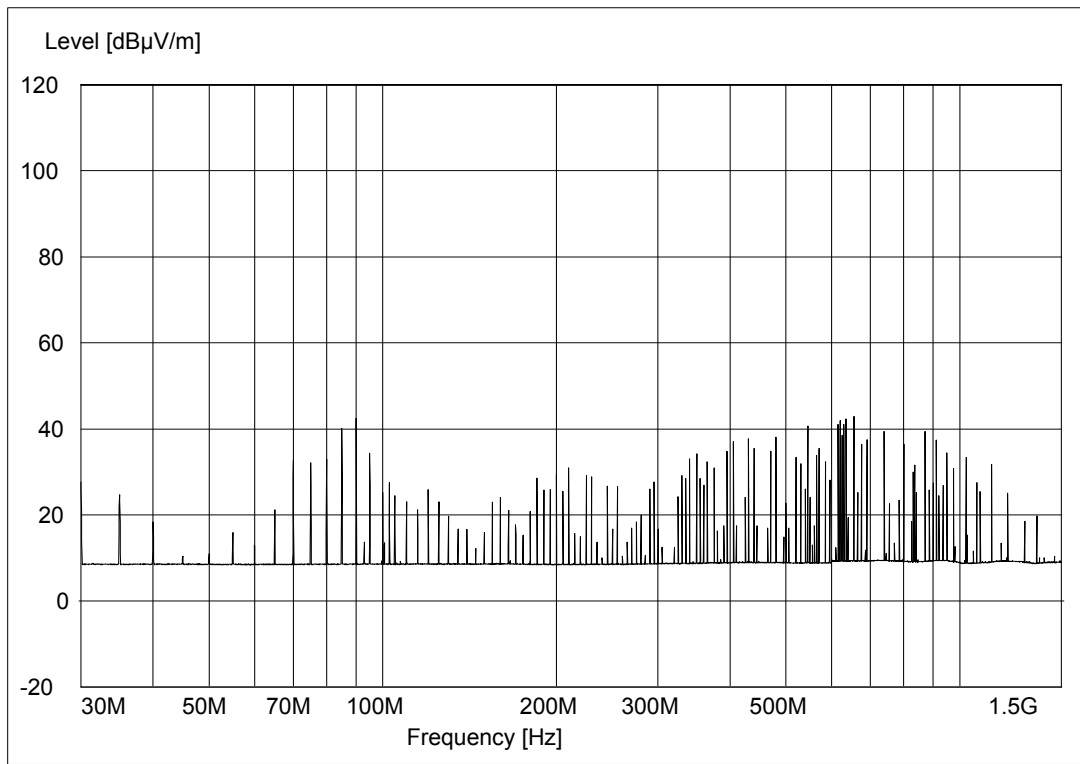


Figure 4.3 2D Planar Output – Node (3,1)

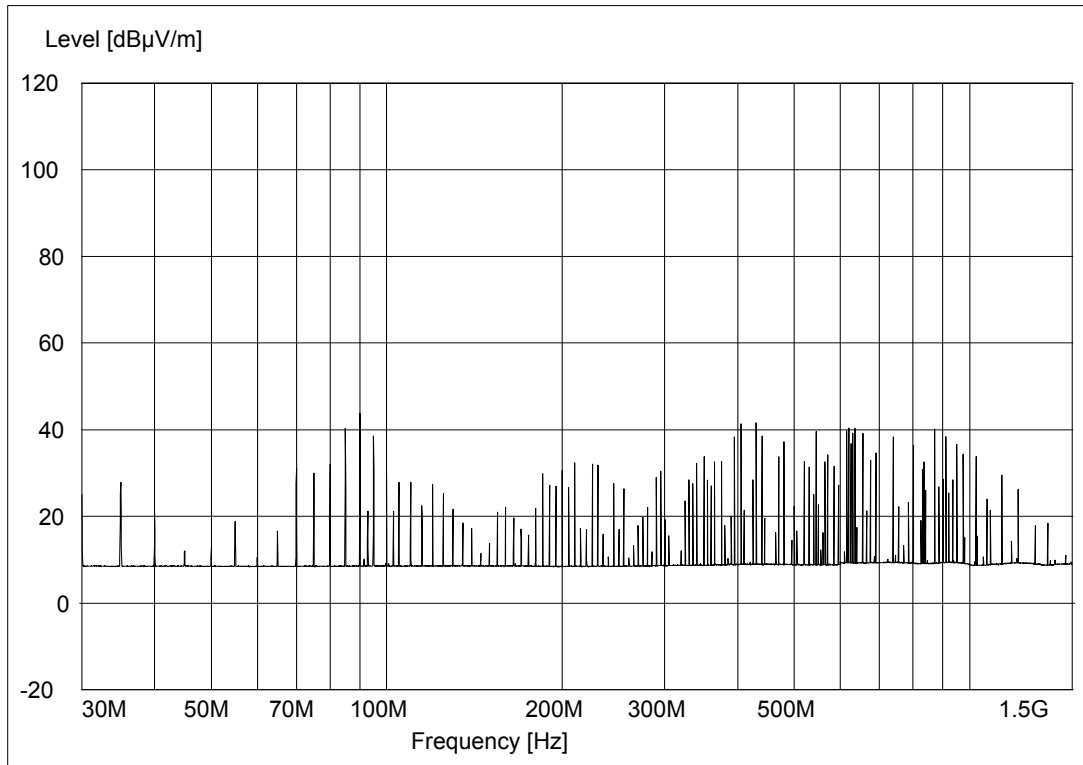


Figure 4.3 2D Planar Output – Node (3,2)

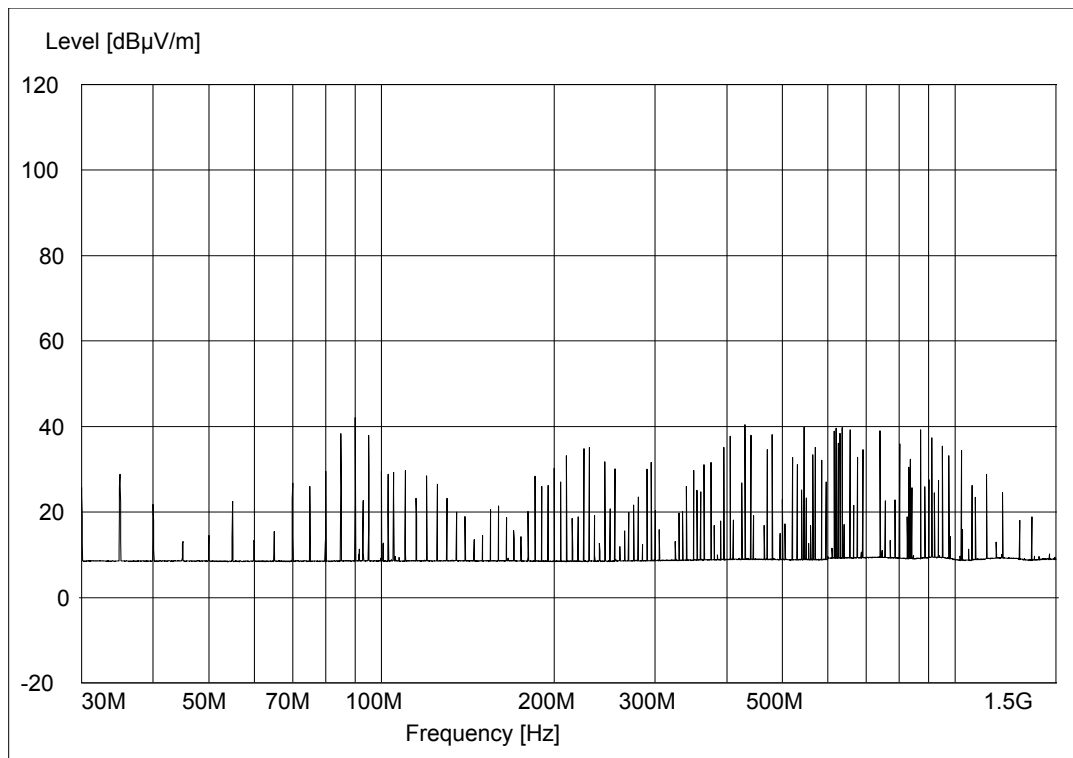


Figure 4.3 2D Planar Output – Node (3,3)

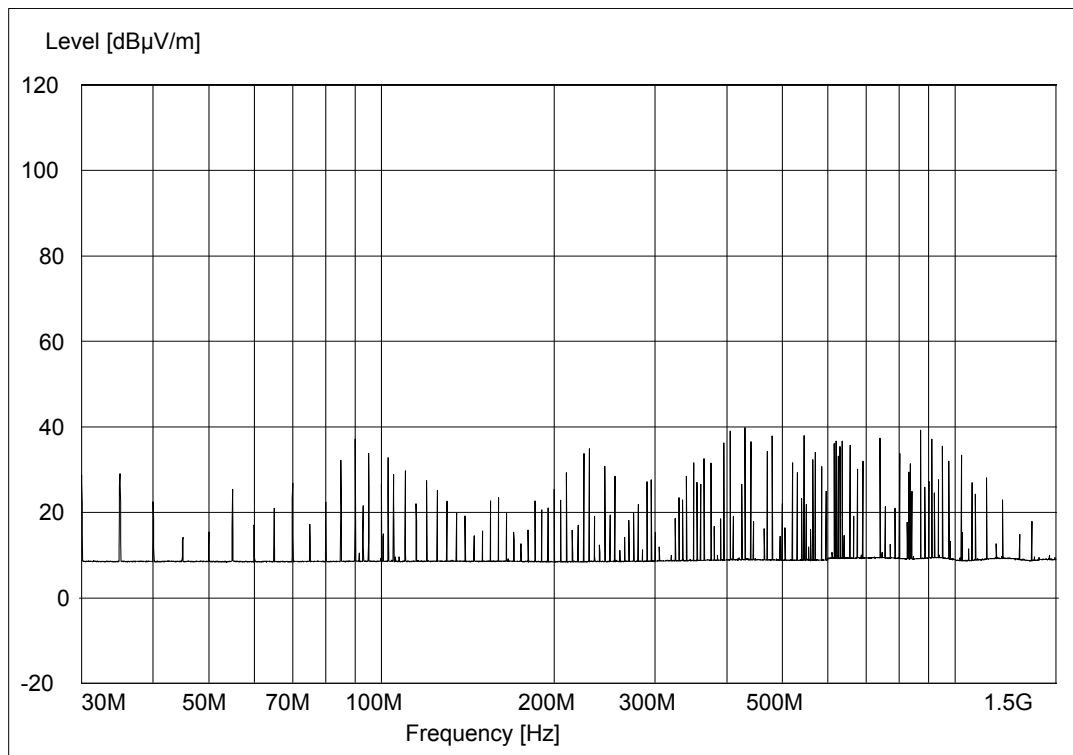


Figure 4.3 2D Planar Output – Node (3,4)

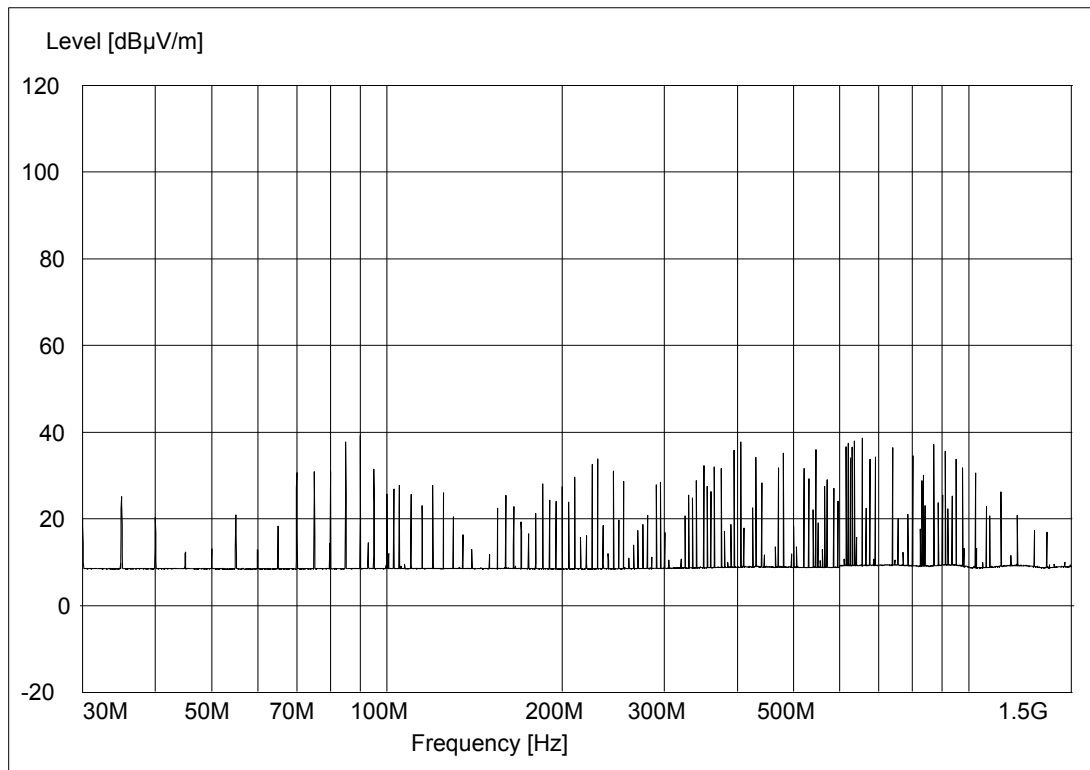


Figure 4.3 2D Planar Output – Node (4,0)

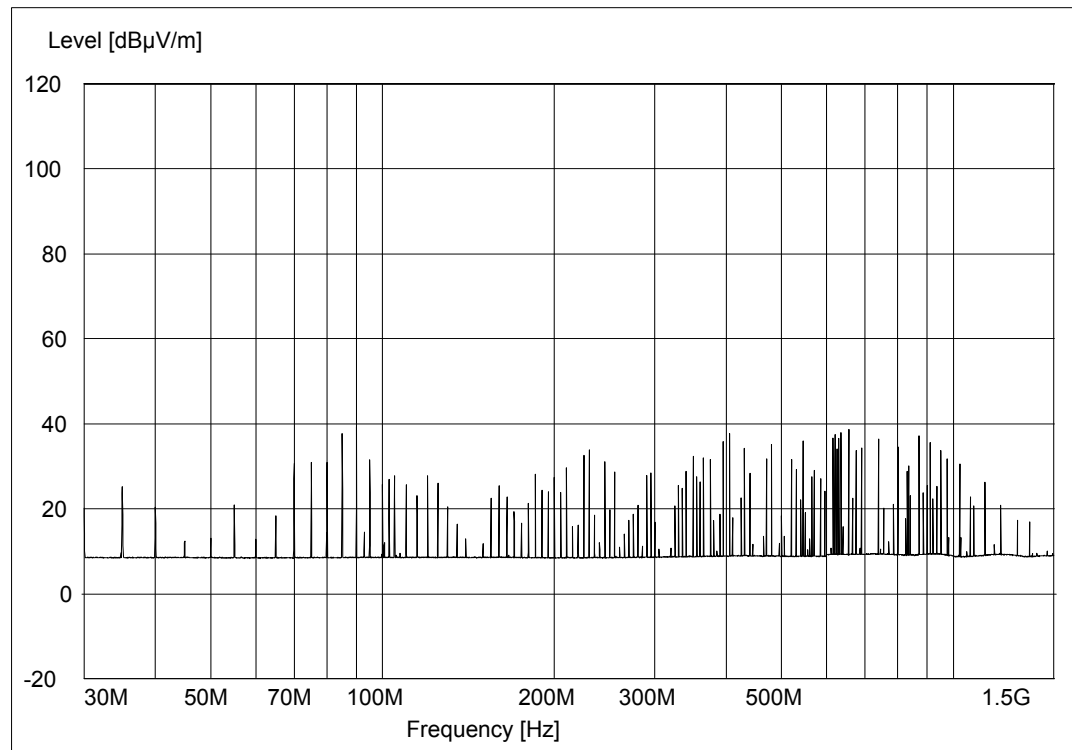


Figure 4.3 2D Planar Output – Node (4,1)

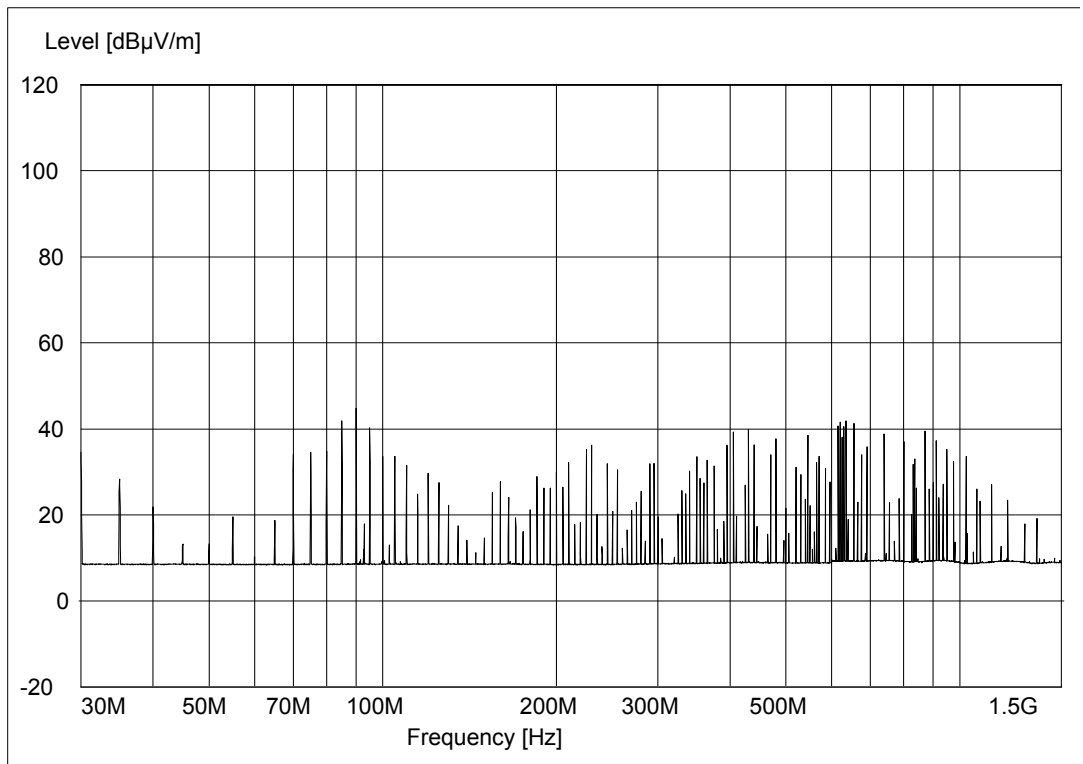


Figure 4.3 2D Planar Output – Node (4,2)

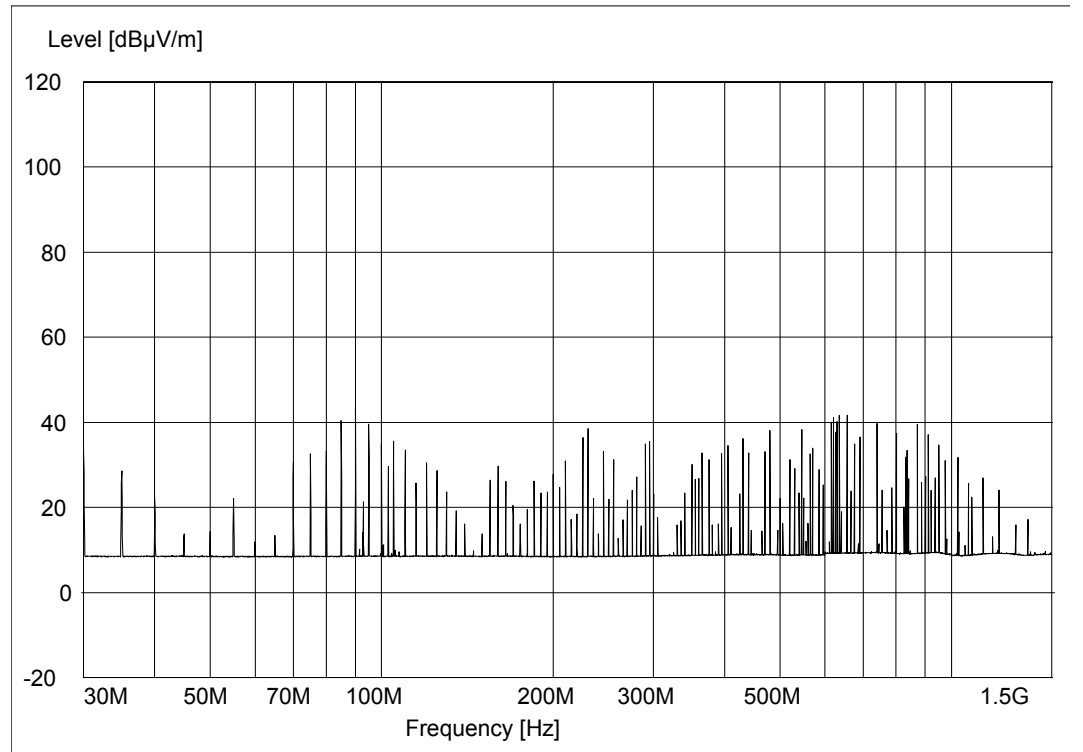


Figure 4.3 2D Planar Output – Node (4,3)

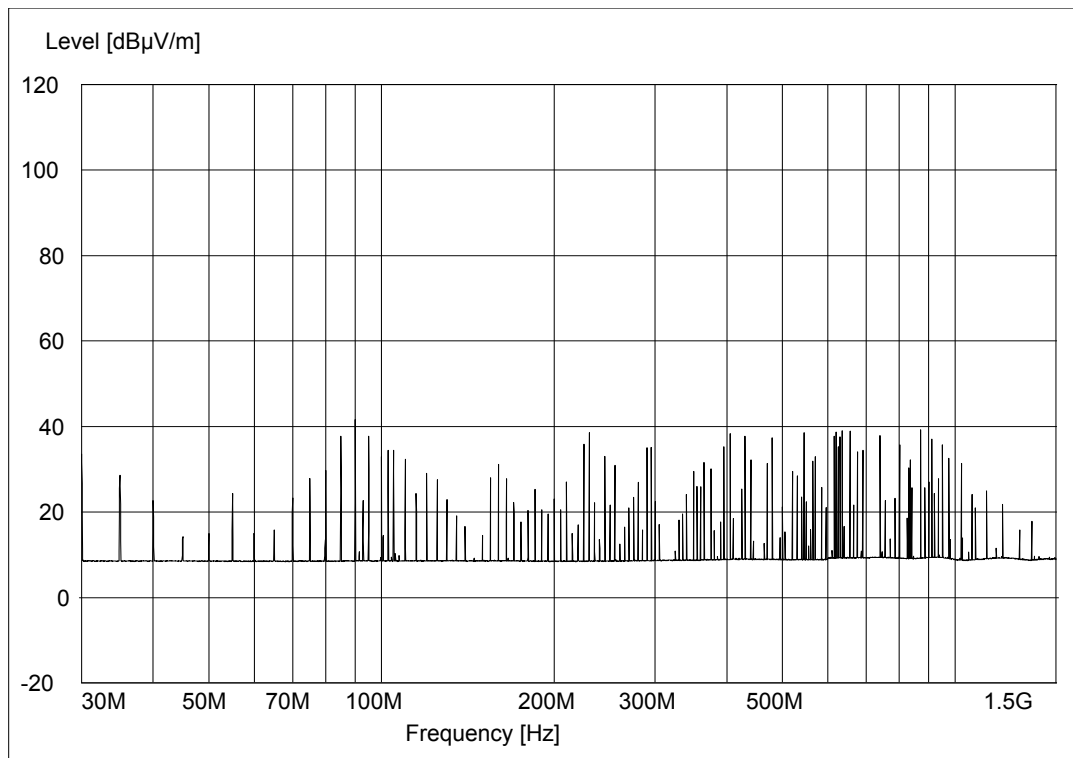


Figure 4.3 2D Planar Output – Node (4,4)